

# UNCLASSIFIED

AD NUMBER
AD048279
NEW LIMITATION CHANGE
TO Approved for public release, distribution unlimited
FROM Distribution: Further dissemination only as directed by WADD, Air Research and Development Command, USAF, WPAFB, OH 45433; June 1954 or higher DoD authority.
AUTHORITY
AFAL ltr, 27 Dec 1979

THIS PAGE IS UNCLASSIFIED

THIS REPORT HAS BEEN DELIMITED  
AND CLEARED FOR PUBLIC RELEASE  
UNDER DOD DIRECTIVE 5200.20 AND  
NO RESTRICTIONS ARE IMPOSED UPON  
ITS USE AND DISCLOSURE.

DISTRIBUTION STATEMENT A

APPROVED FOR PUBLIC RELEASE;  
DISTRIBUTION UNLIMITED.

# Armed Services Technical Information Agency

This Document  
Reproduced From  
Best Available Copy

# 48279

NOTE: WHEN GOVERNMENT OR OTHER DRAWINGS, SPECIFICATIONS OR OTHER DATA ARE USED FOR ANY PURPOSE OTHER THAN IN CONNECTION WITH A DEFINITELY RELATED GOVERNMENT PROCUREMENT OPERATION, THE U. S. GOVERNMENT THEREBY INCURS NO RESPONSIBILITY, NOR ANY OBLIGATION WHATSOEVER; AND THE FACT THAT THE GOVERNMENT MAY HAVE FORMULATED, FURNISHED, OR IN ANY WAY SUPPLIED THE DRAWINGS, SPECIFICATIONS, OR OTHER DATA IS NOT TO BE REGARDED BY ANY PERSON OR CORPORATION, OR OTHERWISE AS IN ANY MANNER LICENSING THE HOLDER OR ANY OTHER PERSON OR CORPORATION, OR CONFERRING ANY RIGHTS OR PERMISSION TO MANUFACTURE, REPRODUCE, OR SELL ANY PATENTED INVENTION THAT MAY IN ANY WAY BE RELATED THERETO.

Reproduced by  
**DOCUMENT SERVICE CENTER**  
KNOTT BUILDING, DAYTON, 2, OHIO

# UNCLASSIFIED

## **REPRODUCTION QUALITY NOTICE**

**This document is the best quality available. The copy furnished to DTIC contained pages that may have the following quality problems:**

- **Pages smaller or larger than normal.**
- **Pages with background color or light colored printing.**
- **Pages with small type or poor printing; and or**
- **Pages with continuous tone material or color photographs.**

**Due to various output media available these conditions may or may not cause poor legibility in the microfiche or hardcopy output you receive.**

☐ **If this block is checked, the copy furnished to DTIC contained pages with color printing, that when reproduced in Black and White, may change detail of the original copy.**



WADC TECHNICAL REPORT 54-71

## INVESTIGATIONS OF PHENIUM

C. T. SIMS, C. M. CRAIGHEAD, P. I. JAFFEE,  
D. N. GIDEON, E. N. WYLER, F. C. TODD,  
D. M. ROSENBAUM, E. M. SHERWOOD AND I. E. CAMPBELL

BATTELLE MEMORIAL INSTITUTE

JUNE 1954

WRIGHT AIR DEVELOPMENT CENTER

WADC TECHNICAL REPORT 54-371

## INVESTIGATIONS OF RHENIUM

C. T. Sims, C. M. Craighead, R. I. Jaffco,  
D. N. Gideon, E. N. Wyler, F. C. Todd,  
D. M. Rosenbaum, E. M. Sherwood, and I. E. Campbell

Battelle Memorial Institute

June 1954

Aeronautical Research Laboratory  
Contract No. AF 33(616)-232  
Task No. 70646

Wright Air Development Center  
Air Research and Development Command  
United States Air Force  
Wright-Patterson Air Force Base, Ohio

## FOREWORD

This report serves as a summary of the first 2 years' experimental work and is issued in lieu of the Eighth Quarterly Progress Report.

This report was prepared by Battelle Memorial Institute under USAF Contract No. AF 33(616)-232. The contract was initiated under Task Number 70646 and administered under the direction of the Aeronautical Research Laboratory, Directorate of Research, Wright Air Development Center. At various times during the project, Lt. George Johnson, Captain John Mosher, and Lt. John P. Hirth served as Project Engineers.

Work at Battelle on the preparation of rhenium-metal powder, electroplating rhenium, and the vapor pressure of rhenium was done by D. M. Rosenbaum, Principal Chemist, E. M. Sherwood, Assistant Division Chief, and I. E. Campbell, Chief of the Division of Inorganic Chemistry and Chemical Engineering. The work on the physical and mechanical properties and physical metallurgy was done primarily by C. T. Sims, Principal Metallurgist, C. M. Craighead, Technical Consultant, and R. I. Jaffee, Chief of the Division of Nonferrous Physical Metallurgy. Studies of the electrical, electronic, and other physical properties were made by D. N. Gideon, Principal Physicist, E. N. Wyler, Assistant Division Chief, and F. C. Todd, Chief of the Division of Electronic Physics.

The potassium perrhenate, from which rhenium metal was processed, consolidated, and fabricated, was supplied to this project free of charge through the kindness of the Kennecott Copper Corporation and its representatives, Drs. H. P. Croft and L. G. Jenness.

### ABSTRACT

Methods for the preparation of fine rhenium powder from potassium perrhenate and ammonium perrhenate are discussed in detail. Consolidation of this powder by pressing and sintering into a sound master bar is included. The metal was fabricated into rod, wire, sheet, and foil by cold-working and annealing procedures developed after hot working proved impractical. The metal was also made available in arc-melted and crystal-bar forms, and electroplating procedures were developed.

Various physical, mechanical, and electronic properties were determined on the available stock. The melting point was 3180 C; the density 21.0 g/cm<sup>3</sup>; the electrical resistivity 19 to 21 microhm-centimeters; the vapor pressure slightly more than that of tantalum; the spectral emissivity 0.36 to 0.42; and the thermal expansion  $6.8 \times 10^{-6}$  per cm for 0 to 1500 C.

Rhenium has a Young's modulus of about  $67 \times 10^6$  psi, is ductile at room temperature, and, when annealed, has a tensile strength of about 170,000 psi at room temperature. It work hardens greatly and has high elevated-temperature strength, but low ductility. Recrystallization occurs around 1300 to 1500 C.

A guard-ring diode was constructed and the thermionic emission characteristics of rhenium determined; the work function is 4.80 ev and the Richardson constant 52 amp/cm<sup>2</sup>/K<sup>2</sup>. Additions of thorium to rhenium did not produce enhanced emission, as with tungsten. Emission constants determined on cathodes impregnated with barium aluminate are believed to be incorrect because of poisoning.

Rhenium has been found to have a far greater resistance to the deleterious water cycle than tungsten. Electrical-contact tests showed that, under the test conditions, rhenium was superior to tungsten and osmium-rhenium.

The oxidation resistance is good at room temperature, but a volatile oxide forms above 500 C. Porosity appears in osmium filaments above 2300 C, but was eliminated when rigid impurity control was invoked.

A high level of cooperation has been maintained with industrial, educational, and Governmental organizations to forward the use of rhenium. Approximately forty organizations have been contacted, and half of these have been given rhenium samples gratis in exchange for information on the uses to which they put the metal.

### PUBLICATION REVIEW

This report has been reviewed and is approved.

FOR THE COMMANDER:

*Leslie E. Williams*  
LESLIE E. WILLIAMS  
Colonel, USAF  
Chief, Research Laboratory  
Directorate of Research

# TABLE OF CONTENTS

	Page
FOREWORD . . . . .	ii
ABSTRACT . . . . .	iii
PUBLICATION REVIEW . . . . .	iii
INTRODUCTION . . . . .	1
METAL PREPARATION . . . . .	2
Introduction . . . . .	2
Source Material . . . . .	2
Rhenium Metal Powder From High-Purity Potassium Perrhenate . . . . .	2
Rhenium Metal Powder From Ammonium Perrhenate . . . . .	4
Potassium Perrhenate as Starting Material . . . . .	4
Rhenium Scrap as a Starting Material . . . . .	6
Rhenium Crystal Bar . . . . .	6
CONSOLIDATION AND FABRICATION . . . . .	9
Pure Rhenium . . . . .	9
Crystal-Bar Rhenium . . . . .	9
Hot Swaging . . . . .	9
Cold Swaging . . . . .	10
Arc-Melted Rhenium . . . . .	10
Cold Pressing . . . . .	10
Hot and Cold Rolling . . . . .	11
Hot Clad Swaging and Cold Swaging . . . . .	11
Powder-Metallurgy-Type Rhenium . . . . .	15
Particle Size . . . . .	16
Pressing . . . . .	16
Presintering . . . . .	16
Electric Sintering . . . . .	16
Hot Working . . . . .	20
Cold Working: General . . . . .	21
Cold Forging . . . . .	22
Cold Rolling; I. Preparation of Rod . . . . .	22
Cold Rolling; II. Preparation of Sheet and Strip . . . . .	22
Cold Swaging . . . . .	25
Cold Turk's Head Drawing . . . . .	25
Cold Wire Drawing . . . . .	26
Cold Rod Rolling . . . . .	26
Rhenium Alloys . . . . .	27
Arc-Melted Rhenium-Thorium Alloys . . . . .	27
Thoriated Sintered Rhenium . . . . .	27
Arc-Melted Rhenium With Deoxidizing Elements Added . . . . .	27
PHYSICAL PROPERTIES . . . . .	29
Lattice Constants . . . . .	29
Density . . . . .	30
Melting Point . . . . .	33
Vapor Pressure of Solid Rhenium . . . . .	33
Description of the Test Method . . . . .	35
Test Specimens . . . . .	35
Test Equipment . . . . .	36
Procedure . . . . .	38
Data . . . . .	38
Discussion of Results . . . . .	39
Estimation of the Boiling Point and Liquid Vapor Pressure of Rhenium . . . . .	39
Boiling Point . . . . .	39
Vapor Pressure of Liquid Rhenium . . . . .	41
Electrical Resistivity . . . . .	45
Room-Temperature Resistivity (I) and the Effect of Cold Work on Resistivity . . . . .	45
Room-Temperature Resistivity (II) and the Temperature Dependency of Resistivity . . . . .	47

**TABLE OF CONTENTS**  
(Continued)

	<u>Page</u>
Room-Temperature Resistivities: Summary . . . . .	49
Spectral Emissivity . . . . .	49
The Prescott Method . . . . .	49
Theory . . . . .	49
Measurements . . . . .	50
The Bored-Hole Method . . . . .	52
Combined Results . . . . .	52
Thermal Expansion . . . . .	56
<b>MECHANICAL PROPERTIES . . . . .</b>	<b>56</b>
Pure Rhenium . . . . .	57
Modulus of Elasticity . . . . .	57
Tensile Strength and Ductility . . . . .	60
Room-Temperature Tensile Tests . . . . .	60
Elevated-Temperature Tensile Tests . . . . .	62
Annealed Hardnesses . . . . .	70
Work Hardening and Recrystallization . . . . .	70
Grain Size and Grain Growth . . . . .	74
Thoriated Rhenium . . . . .	78
Tensile Strength and Ductility . . . . .	78
Work Hardening and Recrystallization . . . . .	78
<b>ELECTRONIC PROPERTIES . . . . .</b>	<b>83</b>
Thermionic Emission of Pure Rhenium . . . . .	83
Introduction . . . . .	83
Design of the Guard-Ring Diode . . . . .	84
Preparation of the Rhenium Cathodes . . . . .	84
Processing of the Guard-Ring Diode . . . . .	86
Determination of the Thermionic-Emission Constants . . . . .	86
The Effects of Impurities on Thermionic Emission . . . . .	87
Thermionic Emission of Thoriated Rhenium . . . . .	91
Introduction . . . . .	91
Fabrication of Cathode for Guard-Ring Diode . . . . .	93
Processing of Guard-Ring Diode . . . . .	93
Determination of the Thermionic-Emission Constants . . . . .	93
Thermionic Emission of Impregnated Cathodes . . . . .	94
Cathodes Impregnated With Barium-Strontium Carbonates . . . . .	94
Cathodes Impregnated With Barium Aluminate . . . . .	95
Secondary-Electron-Emission Coefficient . . . . .	96
The Water-Cycle Effect . . . . .	101
Qualitative Observation . . . . .	101
Relative Water-Cycle Losses of Rhenium and Tungsten . . . . .	103
The Water-Cycle Effect on Rhenium at High Water-Vapor Pressures . . . . .	106
Rhenium Contacts for Relay Service . . . . .	106
<b>MISCELLANEOUS PROPERTIES . . . . .</b>	<b>114</b>
Maximum Theoretical Oxygen Solubility . . . . .	114
Oxidation Resistance . . . . .	115
Rhenium Coatings . . . . .	117
Purity, Porosity, and Temperature Relationships . . . . .	118
Controlled Porosity and Fracture Tests . . . . .	120
The Effects of Purity on Porosity and Burn-Outs . . . . .	122
Gaseous Impurities . . . . .	124
Nongaseous Impurities . . . . .	124
Metallographic Techniques . . . . .	128
<b>DISTRIBUTION OF INFORMATION AND MATERIALS . . . . .</b>	<b>129</b>
Organizations Contacted . . . . .	129

**TABLE OF CONTENTS**  
(Continued)

	<u>Page</u>
Research on Rhenium by Various Industrial and Educational Organizations . . . . .	132
Electrical-Contact Tests . . . . .	132
Electronic Properties . . . . .	132
Metallizing Applications . . . . .	132
SUMMARY . . . . .	133
FUTURE WORK . . . . .	135
REFERENCES . . . . .	136

**LIST OF ILLUSTRATIONS**

Figure 1. Flowsheet for Conversion of Potassium Perrhenate to Ammonium Perrhenate and the Reduction of Ammonium Perrhenate to Rhenium Metal . . . . .	5
Figure 2. Crystal Bar: Apex of the V . . . . .	7
Figure 3. Photomicrograph Montage of Transverse Section of Rhenium Crystal Bar . . . . .	8
Figure 4. Rhenium Consolidated by Three Different Methods . . . . .	12
Figure 5. Arc-Melted Rhenium After Cold and Hot Rolling and After Hot Forging . . . . .	13
Figure 6. Photomicrographs of Three Heat-Treated Rhenium Buttons . . . . .	14
Figure 7. Effect of Sintering in Hydrogen at 1500 C for 2 Hours on Rhenium Metal Powder Prepared From Potassium Perrhenate (above) and Ammonium Perrhenate (below) . . . . .	17
Figure 8. Rhenium Metal Powder Reduced From Ammonium Perrhenate; Particle Size 1 to 25 Microns . . . . .	17
Figure 9. Stages in the Sintering of Rhenium Powder . . . . .	18
Figure 10. Microstructure of Sintered Rhenium Bar at 92.2 Per Cent of Theoretical Density; Transverse Section . . . . .	19
Figure 11. Steps in the Preparation of Rhenium Rod . . . . .	24
Figure 12. Photomicrograph of Rhenium-2 Per Cent Thorium Alloy, Solution Annealed and Quenched, Showing a Second Phase at Grain Boundaries and in the Grains . . . . .	28
Figure 13. Structure of Rhenium Containing 1 Per Cent Thorium as Thorin . . . . .	28
Figure 14. Longitudinal Microstructure of a Typical Rhenium Test Wire . . . . .	36
Figure 15. Vapor-Pressure Apparatus . . . . .	37
Figure 16. The Vapor Pressure of Rhenium and Other Refractory Metals as a Function of Reciprocal Temperature . . . . .	40
Figure 17. Estimated Vapor Pressure of Liquid Rhenium as a Function of 1/T . . . . .	44
Figure 18. Room-Temperature Resistivity and the Effect of Cold Work on the Resistivity of Rhenium . . . . .	46
Figure 19. Rhenium Resistivity Curves at Room and Elevated Temperatures . . . . .	48
Figure 20. Spectral Emisivity of Rhenium by Present Method . . . . .	51
Figure 21. Spectral Emisivity of Sintered Rhenium at 0.655 Micron . . . . .	53
Figure 22. Black-Body Versus Brightness Temperature for Sintered Rhenium Bars . . . . .	54

**LIST OF ILLUSTRATIONS**  
(Continued)

	<u>Page</u>
Figure 23. Combined Data Illustrating the Spectral Emissivity of Rhenium Metal at 0.655 Micron . . . . .	55
Figure 24. Relationship Between the Position of Certain Metals in the Periodic System and Their Tension Modulus of Elasticity . . . . .	59
Figure 25. True Stress-Strain Diagram for Three Pure Rhenium Specimens . . . . .	63
Figure 26. Average True Stress-Strain Diagram for Rhenium and Other Metals . . . . .	64
Figure 27. Apparatus for Elevated-Temperature Tensile Testing of Rhenium Under Controlled Atmosphere . . . . .	66
Figure 28. Ultimate Tensile Strength of Annealed and Cold-Worked 0.050 to 0.065-Inch-Diameter Rhenium Wire at Elevated Temperatures . . . . .	67
Figure 29. Comparison of the Elevated-Temperature Tensile Properties of Wrought Rhenium (15% Reduced), Molybdenum, and Tungsten . . . . .	69
Figure 30. Hardness and Grain Structures of Hot-Wire-Deposited, Arc-Melted, and Powder-Metallurgy Types of Rhenium, All in the Annealed Condition . . . . .	71
Figure 31. Microstructures of Annealed, Cold-Worked, and Recrystallized Rhenium . . . . .	72
Figure 32. Cold-Work-Hardening Characteristics of Rhenium and Nickel . . . . .	73
Figure 33. The Effect of 1-Hour Annealing Treatments on the Hardness of Cold-Worked Rhenium . . . . .	76
Figure 34. The Effect of 1-Hour Annealing Treatments on the Grain Size of Cold-Worked Rhenium . . . . .	77
Figure 35. Microstructures of Annealed, Cold-Worked, and Recrystallized Thoriated Rhenium . . . . .	80
Figure 36. The Effect of 1-Hour Heat Treatments at Various Temperatures on the Hardness of Cold-Worked Thoriated Rhenium . . . . .	81
Figure 37. Guard-Ring Diode Used for Thermionic-Emission Measurements on Pure Rhenium . . . . .	85
Figure 38. Schottky Plot for Drawn-Wire Rhenium Cathode . . . . .	88
Figure 39. Schottky Plot for Ground-Wire Rhenium Cathode . . . . .	89
Figure 40. Average Richardson Plot for Rhenium Cathodes . . . . .	90
Figure 41. Activation Plot for Pure Rhenium Filaments . . . . .	92
Figure 42. Richardson Plot of Pulse Emission Data for Impregnated Cathode: 20 Per Cent Barium Aluminate, 80 Per Cent Rhenium . . . . .	97
Figure 43. Richardson Plot of D-C Emission Data for Impregnated Cathode: 20 Per Cent Barium Aluminate, 80 Per Cent Rhenium . . . . .	98
Figure 44. Block Diagram of Secondary-Emission Apparatus . . . . .	99
Figure 45. Secondary-Emission Coefficient for Rhenium Metal . . . . .	102
Figure 46. Relative Water-Cycle-Resistance Tube . . . . .	104
Figure 47. Rate of Weight Loss by Water-Cycle Mechanism From Rhenium Filament at 1500 C Brightness Temperature . . . . .	107
Figure 48. Condition of Rhenium Contacts Following Breaker-Point Tests . . . . .	110
Figure 49. Condition of Tungsten Contacts Following Breaker-Point Tests . . . . .	111



LIST OF ILLUSTRATIONS  
(Continued)

	<u>Page</u>
Figure 50. Condition of Platinum-Ruthenium Contacts Following Breaker-Point Tests . . . . .	112
Figure 51. The Influence of Temperature on the Air Oxidation of Arc-Melted Rhenium . . . . .	116
Figure 52. Macrographs of the External Appearance of Rhenium Specimens Failed in High-Temperature Tests . . . . .	119
Figure 53. Porosity in Rhenium Vapor-Pressure Specimen Which Failed in Test . . . . .	121
Figure 54. Porosity and Burn-Out Ends of Rhenium Heated in Vacuum and Hydrogen . . . . .	123
Figure 55. Porosity in Rhenium Metal Heated to 2900 C. . . . .	128

LIST OF TABLES

Table 1. Chemical Analyses of Materials Used and Prepared During the Course of This Study . . . . .	3
Table 2. Rhenium Crystal Bars . . . . .	9
Table 3. Analytical History of Three Heat-Treated Rhenium Buttons . . . . .	15
Table 4. Procedure for the Preparation of Sintered Rhenium Bar From Rhenium Powder . . . . .	20
Table 5. Procedure for the Preparation of Rhenium Wire From Sintered Bar . . . . .	23
Table 6. Lattice Constants of Rhenium . . . . .	30
Table 7. Density Determinations on Rhenium . . . . .	31
Table 8. The Density of Rhenium Compared With the Densities of Other Elements . . . . .	32
Table 9. The Melting Point of Rhenium . . . . .	34
Table 10. The Melting Points of Rhenium and Several Other Elements . . . . .	34
Table 11. Experimental Vapor-Pressure Data for Rhenium . . . . .	38
Table 12. $H_0^0$ of Sublimation for Rhenium. . . . .	42
Table 13. The Vapor Pressure of Liquid Rhenium . . . . .	43
Table 14. Resistivity of Annealed Rhenium at 20 C by Determination (I) . . . . .	47
Table 15. Linear Thermal Expansion for Pure Rhenium . . . . .	57
Table 16. Moduli of Elasticity for Three Annealed Rhenium Specimens . . . . .	58
Table 17. Moduli of Elasticity of Rhenium and Several Other Metals . . . . .	58
Table 18. Tensile and Elongation Data for Pure Annealed Rhenium . . . . .	61
Table 19. Room- and Elevated-Temperature Strengths of Annealed and Cold-Worked Rhenium Wire . . . . .	68
Table 20. Hardness Values for Rhenium After Work Hardening by Swaging and Recrystallizing by Reheating . . . . .	75
Table 21. Tensile and Elongation Data for Annealed Thoriated Rhenium . . . . .	79
Table 22. Hardness Values for Thoriated Rhenium After Work Hardening by Swaging and Recrystallizing by Annealing. . . . .	82
Table 23. Temperatures at Which Softening Occurs in Pure and Thoriated Rhenium . . . . .	83

LIST OF TABLES  
(Continued)

	<u>Page</u>
Table 24. Comparison of Water-Cycle Losses of Rhenium and Tungsten . . . . .	105
Table 25. Resistance of Contacts, Experiment 1 . . . . .	109
Table 26. Resistance of Contacts, Experiment 2 . . . . .	113
Table 27. Oxidation of Rhenium in Air . . . . .	117
Table 28. The Effect of Heating Rhenium in High Vacuum and Hydrogen . . . . .	122
Table 29. Gas Content of Rhenium as Determined by Vacuum-Fusion Analysis . . . . .	125
Table 30. Metallic Impurities Present During the Processing of Rhenium . . . . .	125
Table 31. Boiling Points of Metallic Impurities and of Certain of Their Oxides . . . . .	127

# INVESTIGATIONS OF RHENIUM

## INTRODUCTION

The metal rhenium never has been the subject of a full-scale investigation to determine its physical and mechanical properties with the immediate objective of translating these properties into commercial usefulness, even though it possesses a favorable position in the periodic system between such high-temperature metals as tantalum and tungsten and the precious metals, such as iridium and platinum. This indicates that rhenium might possess rather good properties and, indeed, prior to this investigation, its melting point was known to be above 3150 C (second only to tungsten).

The knowledge that rhenium, although generally very scarce, was probably available in commercial quantities in North America has come from relatively recent findings by the Kennecott Copper Company and The Miami Copper Company. These factors, combined with the ever-growing need for materials to perform more efficiently under more strenuous conditions, led to this investigation of the basic properties of rhenium.

Since considerable information is already available about the chemistry of rhenium, the current work has involved investigations into the physical, mechanical, electronic, metallurgical, and electrical properties. This was done only after an extensive survey of the literature, however, which was published shortly after the inception of this research program.

At first, it was necessary to develop methods for the preparation of massive rhenium to provide sound testing material. After many attempts, it was realized that rhenium could not be hot worked readily. Sintered powder-metallurgy-type rhenium, however, was successfully fabricated by cold working and annealing, so that rhenium rod, wire, sheet, and strip have been prepared.

Information uncovered to date by properties tests has revealed that rhenium is a very dense high-melting metal with a vapor pressure close to that of tantalum. It possesses high room-temperature and elevated-temperature tensile strength. Although ductile at room temperature when annealed, it work hardens very greatly. These latter properties led to basic studies of rhenium's potentialities as an electrical contact material; the results of these studies are very promising.

In addition, rhenium has shown high resistance to the deleterious "water cycle", a phenomenon that plagues tungsten when it is operated as a high-temperature filament. This property, combined with rhenium's room-temperature ductility and high strength, bodes well for the feasibility of using rhenium as an electron-tube component. Further, recent findings

may lead to the use of rhenium as a constituent of impregnated cathodes. Several other uses have been suggested and are contemplated for the metal.

Throughout the recent studies, close contact has been maintained with industrial, educational, and Governmental institutions, so that the potential of rhenium can be realized to the fullest. An almost continuous demand for samples of the metal, combined with the recent encouraging experimental findings, indicates that rhenium may soon "come of age" and be made available commercially.

## METAL PREPARATION

### Introduction

The main objective of this phase of the work was the preparation of high-purity rhenium metal in powder form suitable for subsequent fabrication into massive metal by the powder-metallurgy techniques described in the next section of this report. Since only a limited amount of rhenium was available, a scrap-recovery program was instituted which permitted the conversion of used or impure rhenium back into the form of high-purity powder for subsequent studies.

Rhenium was also prepared in massive form by a hot-wire reduction technique, which involved consolidation of metal in the form of U-shaped "crystal bars" weighing about 1/2 pound each.

### Source Material

The starting material for the preparation of rhenium powder is high-purity potassium perrhenate. A total of 12 pounds of potassium perrhenate was supplied gratis by the Kennecott Copper Corporation. An analysis of this starting material is given in Table 1.

### Rhenium-Metal Powder From High-Purity Potassium Perrhenate

The starting material for the preparation of rhenium powder is high-purity potassium perrhenate mentioned above. About 3 pounds of this potassium perrhenate is placed in a 4-inch stainless steel tube and reduced to a mixture of rhenium metal and rhenium dioxide by hydrogen at 500 C. Reduction was considered complete when condensation of moisture from the

TABLE 1. CHEMICAL ANALYSES OF MATERIALS USED AND PREPARED DURING THE COURSE OF THIS STUDY

Element <sup>(a)</sup>	Analysis, wt %									
	Rhenium-Metal Powder									
	Potassium Perbhenate Starting Material, Sample 1	NH <sub>4</sub> ReO <sub>4</sub> From KReO <sub>4</sub> , Sample 3	NH <sub>4</sub> ReO <sub>4</sub> From Scrap, Sample 11	From KReO <sub>4</sub> , Sample 7	From Ball-Milled NH <sub>4</sub> ReO <sub>4</sub> From Scrap, Sample 12	From Hand-Ground NH <sub>4</sub> ReO <sub>4</sub> , Sample 17	Massive Rhenium Metal Crystal Bar, Sample 8	Powder Metallurgy Sample 15		
Aluminum	0.008 %	N. F.	0.004 %	0.001 %	0.094 %	0.005 %	0.020 %	0.040 %		
Calcium	0.04	0.002 %	N. F.	0.005	0.017	0.005	0.020	0.018		
Chromium	N. F. (b)	N. F.	N. F.	0.002	N. F.	N. F.	Not reported	N. F.		
Copper	0.0004	0.0002	0.0003	0.0007	0.0021	0.0015	0.0010	0.0002		
Iron	0.02	0.004	0.003	0.03	0.024	0.015	0.06	0.040		
Lead	0.02	0.02	N. F.	N. F.	N. F.	N. F.	N. F.	0.008		
Magnesium	N. F.	0.002	0.005	N. F.	0.038	0.012	0.035	0.025		
Manganese	0.002	N. F.	N. F.	0.007	0.0020	0.005	0.007	N. F.		
Molybdenum	N. F.	N. F.	N. F.	0.03	N. F.	N. F.	N. F.	N. F.		
Nickel	N. F.	N. F.	N. F.	0.002	N. F.	N. F.	N. F.	N. F.		
Potassium	Major	N. F.	N. F.	0.39	N. F.	N. F.	N. F.	N. F.		
Rhenium	Major	Major	Major	Major	Major	Major	Major	Major		
Silicon	0.005	0.004	0.005	0.007	0.023	0.039	0.030	0.020		
Sodium	0.15	N. F.	N. F.	N. F.	N. F.	N. F.	N. F.	N. F.		
Tin	N. F.	N. F.	N. F.	0.002	N. F.	N. F.	0.002	N. F.		
Oxygen	--	--	--	--	--	--	(9 ppm)	(6 ppm)		
Hydrogen	--	--	--	--	--	--	(1.4 ppm)	(0.6 ppm)		
Nitrogen	--	--	--	--	--	--	(<8 ppm)	(<5 ppm)		

(a) Elements checked but not found were arsenic, barium, beryllium, bismuth, boron, cadmium, cobalt, columbium, gallium, germanium, gold, platinum, silver, strontium, tellurium, titanium, tungsten, vanadium, zinc, and zirconium.

(b) N. F. = Not found.

exit gas was no longer observed. The reduction products were washed by decantation with hot water until essentially free of alkali. The leached rhenium - rhenium dioxide mixture was reduced to metal at 1000 C in hydrogen. The metal was leached with dilute hydrochloric acid and then washed by decantation with hot distilled water until neutral. The rhenium powder was treated with hydrogen at 1000 C again. The process was carried out with recovery of about 93 per cent of the available rhenium. Approximately 1.6 pounds of powder was prepared by this method. A typical analysis of this powder is given in Table 1.

It was impossible to remove all traces of residual potassium from the powder; therefore, ammonium perrhenate was prepared from potassium perrhenate and used as source material for the preparation of rhenium powder. In the reduction of ammonium perrhenate, the ammonium hydroxide, formed as a reduction product, was volatile and did not remain behind to contaminate the powder.

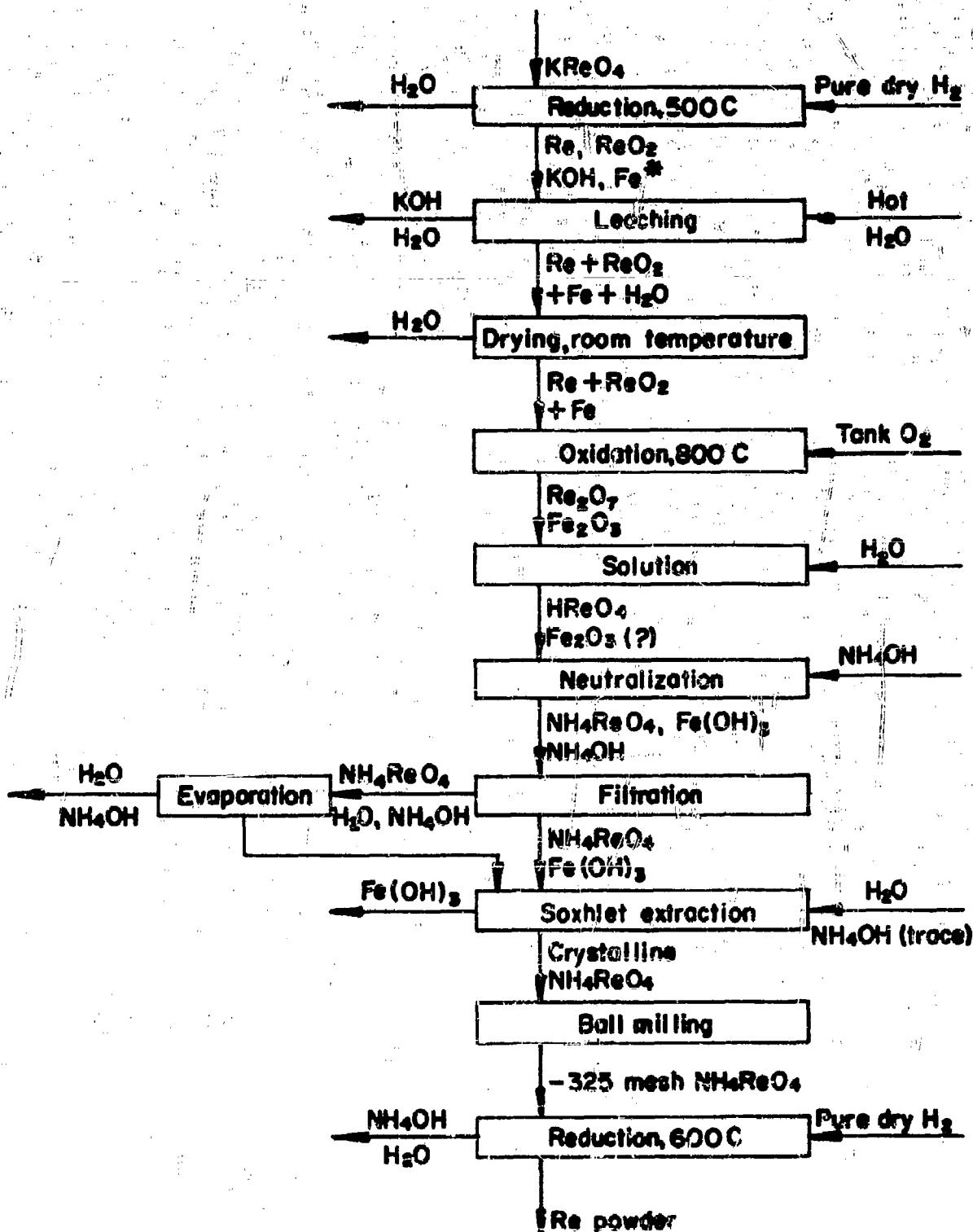
### Rhenium-Metal Powder From Ammonium Perrhenate

#### Potassium Perrhenate as Starting Material

Starting with high-purity potassium perrhenate, a rhenium - rhenium dioxide mixture was prepared by one hydrogen reduction and one leaching, as described above (see Flowsheet, Figure 1). This powder was then placed in a Vycor tube and heated to 800 C in a helium atmosphere. Tank oxygen was permitted to flow through the tube, resulting in the formation of the volatile rhenium heptoxide, which condensed in a cooler portion of the tube. The heptoxide was washed out of the tube with distilled water and then this aqueous solution was filtered to remove any acid-insoluble impurities. Then the perrhenic acid solution was neutralized with concentrated ammonium hydroxide, precipitating moderately soluble crystalline ammonium perrhenate. Iron, picked up from the stainless steel reductor, was co-precipitated as ferric hydroxide with the ammonium perrhenate. This ferric hydroxide was separated from the ammonium perrhenate by using a Soxhlet Extractor with very dilute ammonium hydroxide as the solvent. The insoluble ferric hydroxide remained in the thimble, while the moderately soluble ammonium perrhenate went into solution. This purified ammonium perrhenate (see typical analysis in Table 1) was recovered from the aqueous solution by evaporation.

Previous experimentation (see section on consolidation and fabrication) had indicated that minus 325-mesh rhenium powder was suitable for powder-metallurgy studies. Minus 325-mesh ammonium perrhenate was prepared by dry grinding high-purity material for 1 hour in a Canadian rubber-lined ball mill using Burundum\* balls. Approximately two-thirds of the charge

\* Approximately 81%  $Al_2O_3$ ; balance  $CaO$ ,  $SiO_2$ , and  $MgO$ .



\* Stainless steel reduction vessel is source of this iron

FIGURE 1. FLOWSHEET FOR CONVERSION OF POTASSIUM PERRHENATE TO AMMONIUM PERRHENATE AND THE REDUCTION OF AMMONIUM PERRHENATE TO RHENIUM METAL

had the required particle size; the other fraction was repurified in a Soxhlet Extractor as described above. Approximately 4 pounds of metal powder was prepared by this method at an over-all efficiency of about 90 per cent. Considerable amounts of impurities (see Table 1 for typical analysis) were picked up in this ball-milling operation. At first, this impurity content did not appear to affect the physical and mechanical properties noticeably. Further investigations indicated, however, that metal powder prepared from high-purity ammonium perrhenate, which was reduced to a particle size of -325 mesh by grinding in an agate mortar (for analysis see Table 1), possessed a melting point approximately 80 C higher than that of the ball-milled material. Various methods for the preparation of high-purity minus 325-mesh ammonium perrhenate are now under investigation.

#### Rhenium Scrap as a Starting Material

An important phase in any metal-preparation program is scrap recovery. This scrap rhenium included all test specimens, many rhenium alloys (particularly with thorium), material that had failed during fabrication, and the unfabricable ends of sintered bars.

Rhenium scrap was converted to ammonium perrhenate in the manner described above. The first step in this procedure was the oxidation of the metal at 800 C, followed by solution of the heptoxide, and neutralization of the perrhenic acid by ammonium hydroxide to form ammonium perrhenate (see Table 1 for typical analysis). Then this perrhenate was purified and reduced to rhenium powder. Approximately 7.5 pounds of metal powder was prepared from rhenium scrap at a recovery efficiency of about 95 per cent.

#### Rhenium Crystal Bar

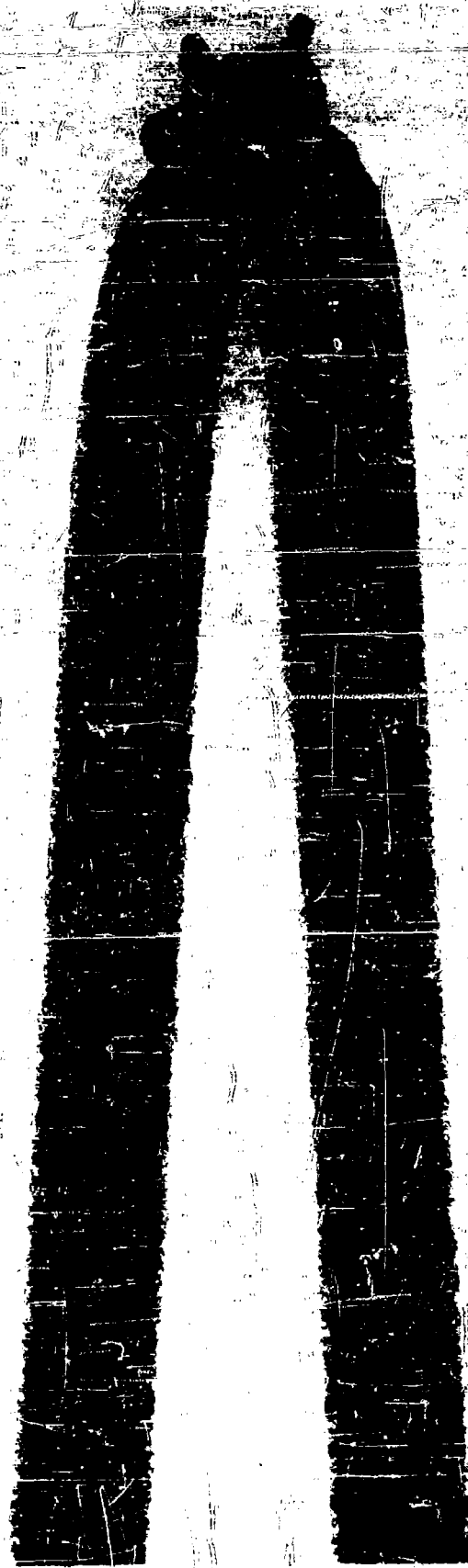
Three V-shaped crystal bars of rhenium metal were prepared by a hot-wire reduction technique developed for the Kennecott Copper Corporation.

Table 2 is a summary of some descriptive characteristics of the crystal bars.

The general appearance of one of the crystal bars as compared with other types of consolidates is illustrated in the next section of the report. In Figure 2, a magnification of the hairpin V, the polycrystalline nature of the deposited metal is evident.

Figure 3 is a photomicrograph montage of the transverse section of a crystal bar. The pronounced concentrations of voids at least two radial distances from the tungsten core wire made fabrication extremely difficult.





4X

95707

FIGURE 2. CRYSTAL BAR: APEX OF THE V

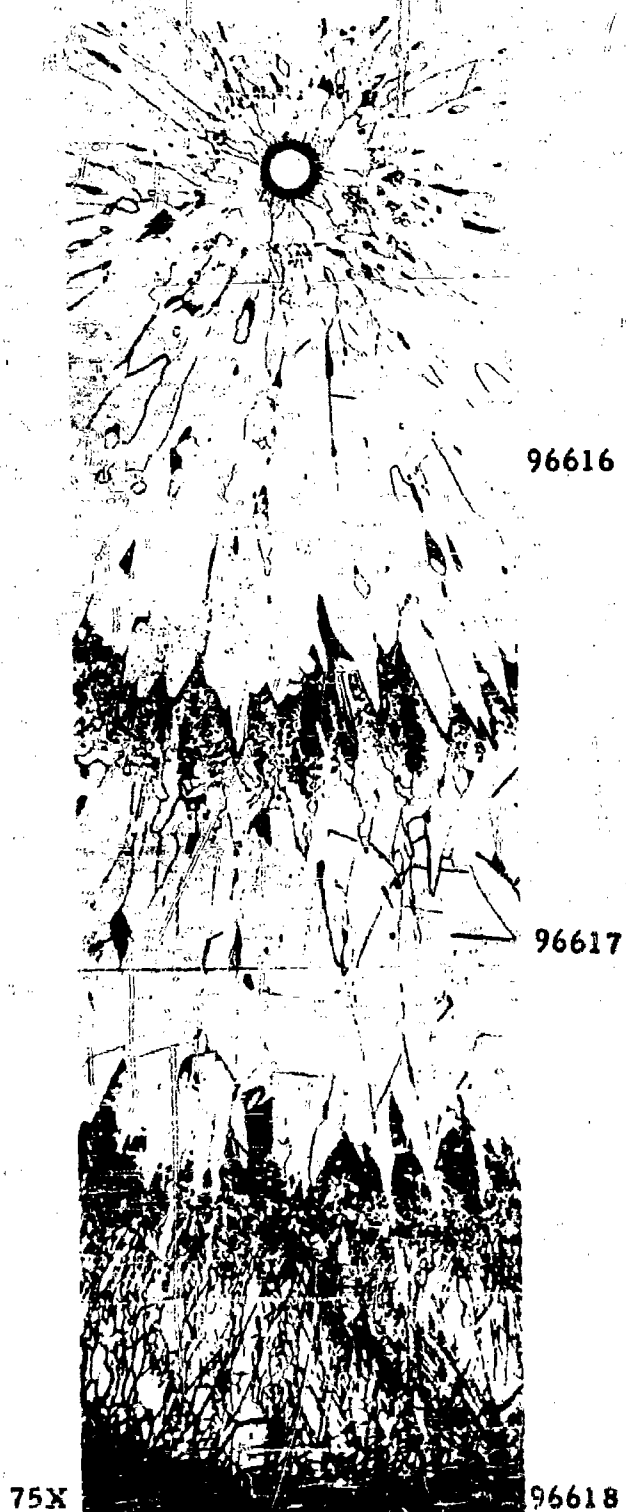


**FIGURE 3. PHOTOMICROGRAPH MONTAGE OF TRANSVERSE SECTION OF RHENIUM CRYSTAL BAR**

**Electrolytic Oxalic Acid Etch**

TABLE 2. RHENIUM CRYSTAL BARS

Bar	Weight, grams	Diameter, inch	Appearance
1	223.8	0.199	Dark-gray to black diffuse illumination (Figures 2 and 4a). "Surface" comprised many fine, needle-shaped radial crystals, individually producing good specular reflection
2	193.3	0.185	Ditto
3	196.3	0.192	"

Analysis of a typical crystal bar is given in Table 1.

### CONSOLIDATION AND FABRICATION

#### Pure Rhenium

Rhenium was consolidated by three different methods for use in fabrication studies. These methods yielded three types of rhenium: (1) crystal-bar rhenium prepared by the decomposition of a rhenium halide on a hot tungsten wire; (2) arc-melted rhenium prepared from cut crystal bar or granules of partially sintered bar stock; and (3) sintered rhenium compacts, prepared by pressing and sintering rhenium using accepted powder-metallurgy techniques. In general, attempts to fabricate the first two types of consolidated metal gave poor results, but fabrication of powder-metallurgy-type rhenium progressed satisfactorily to wire and sheet. The three types of metal in the consolidated condition are shown in Figure 4. A more detailed discussion of this work follows.

#### Crystal-Bar Rhenium

Hot Swaging. Following the general procedures recommended by Smithells<sup>(1)\*</sup> for tungsten, this was the first fabrication technique attempted. References are listed at the end of the report.

In this procedure, the swaging temperature was lowered slowly from 1500 C to 1400 C during nine passes, each pass at 10 per cent reduction in area. The specimen was heated to swaging temperature in hydrogen. The bar commenced cracking on the third pass and had broken up completely by the ninth pass. The rod was covered with cracks and voids, and metallographic inspection showed what appeared to be many oxide centers within the metal. It was obvious that internal oxidation caused most of the poor hot workability.

Accordingly, two separate crystal-bar specimens, ground to a smooth surface finish, were encapsulated in mild steel and evacuated to eliminate oxygen from the ambient atmosphere during swaging. The capsules were swaged at 1400 C with 10 per cent reduction in cross-sectional area per pass. One specimen broke up during swaging after a few passes and the other, although reducing well, behaved strangely. Subsequent inspection of both showed that the rhenium had broken up into small pieces, scattered more or less uniformly in the iron matrix along the centers of the rods. It was then apparent that hot swaging of crystal bar, encapsulated or not, was impractical.

Cold Swaging. In this experiment, one pass at 10 per cent reduction was given, followed by an anneal at 2500 C. On the second cold pass, the bar cracked up.

It had become quite evident that crystal bar was virtually unworkable, largely for the following reasons:

- (1) The as-deposited surface was rough and spiny, causing many stress raisers (see Figure 2).
- (2) Internally, the crystal bar appeared to possess rings of voids where various deposition cycles commenced or ended (see Figure 3).
- (3) The grains were quite large, tending toward poor internal cohesion during working operations (see Figure 3).

#### Arc-Melted Rhenium

Arc melting, as a method of consolidation, was accomplished by melting together small chunks of crystal bar or partially sintered pressings. The melting was carried out under argon on a water-cooled copper hearth, the arc being directed to the button with a movable tungsten electrode. In this manner, 5 to 50-gram rhenium buttons possessing few voids were prepared.

Cold Pressing. A 15-gram arc-melted button was cold pressed to 40 per cent reduction in height before cracking, indicating that rhenium possessed a certain amount of room-temperature ductility, despite the

failure of hot- and cold-working operations on crystal-bar metal. This also indicated that cold-working or hot-working operations might be more successful if carried out on starting material that was more nearly sound and compact than the crystal bar.

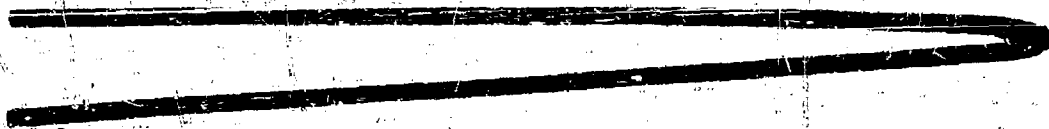
Hot and Cold Rolling. The arc-melted rhenium exhibited the same ductility as mentioned above when cold rolled. It was found possible to roll out 50-mil sheet from arc-cast buttons if intermediate anneals of 1 to 2 hours at 1400 to 1700 C were given to keep the surface hardness low. Reduction was about 20 per cent between each anneal, and sheets of the type illustrated in Figure 5a were obtained. Conversely, numerous hot-rolling attempts at temperatures ranging from 800 to 1500 C resulted in failure by an intergranular type of separation, as illustrated by Figure 5b.

Concurrently, hot break-down forging of the large button illustrated in Figure 4 was carried out at 1500 C. Results were even worse than those observed with hot rolling. Two blows of the forging hammer produced the separated, exfoliated condition shown in Figure 5c.

Other concurrent experiments on the hot working of sintered rhenium (as reported below) were also a failure. Thus, it was apparent that rhenium could not be hot worked in air, its consolidated form notwithstanding, so an analytical study was conducted on a series of arc-melted buttons to determine the cause of rhenium's apparent hot shortness.

One as-melted button was analyzed for oxygen, hydrogen, and nitrogen by the vacuum-fusion method; this was considered a blank. Another was annealed in hydrogen at 1500 C for 30 minutes, and then hydrogen quenched and analyzed. The third was heated in hydrogen to 1500 C for ten periods of 3 minutes each, being taken from the furnace for an air quench between each heating period; analysis followed. This simulated hot-working conditions without physically distorting the specimen. The metallographic structure of each specimen is shown in Figure 6 and the analytical results are given in Table 3. As can be seen, the hydrogen annealing treatment with hydrogen cooling reduced the gas content in almost all cases, but caused the appearance of a dark phase at the grain boundaries. The simulated hot-working treatment caused a large increase in gas content and the appearance of considerable dark phase at the grain boundaries. It is probable that rhenium, which oxidizes readily in air at elevated temperatures, forms an oxide phase at the grain boundaries. Since  $\text{Re}_2\text{O}_7$ , rhenium heptoxide, melts at 297 C and boils at 363 C, it is probable that this oxide is in vapor form during hot working and causes hot shortness.

Hot Clad Swaging and Cold Swaging. The hot clad swaging was conducted in exactly the same manner as described above for crystal bar. Results were inconclusive, but work was abandoned because successful methods had been developed meanwhile for working sintered rhenium.



95708

a. Hot-Wire-Deposited Rhenium (Crystal Bar)



2X

97388

b. Arc-Melted 45-Gram Rhenium Button

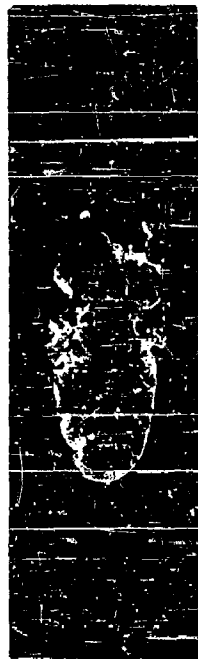


1X

N4097

c. Rhenium Powder, Pressed and Sintered to 5-Inch Bar

FIGURE 4. RHENIUM CONSOLIDATED BY THREE DIFFERENT METHODS



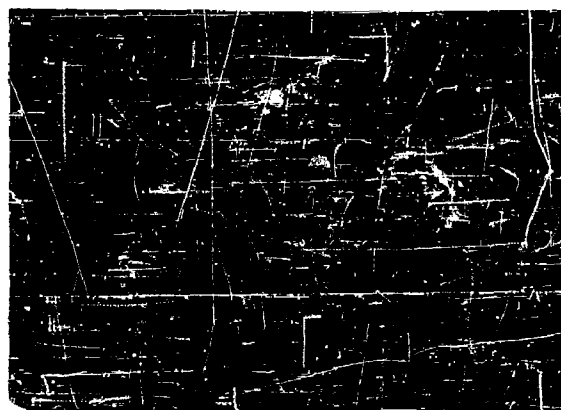
1X 99248

a. Reduced by Cold Rolling



1X 99248

b. Reduced by Hot Rolling  
at 1500 C



2X

97397

c. After Hot Forging at 1500 C

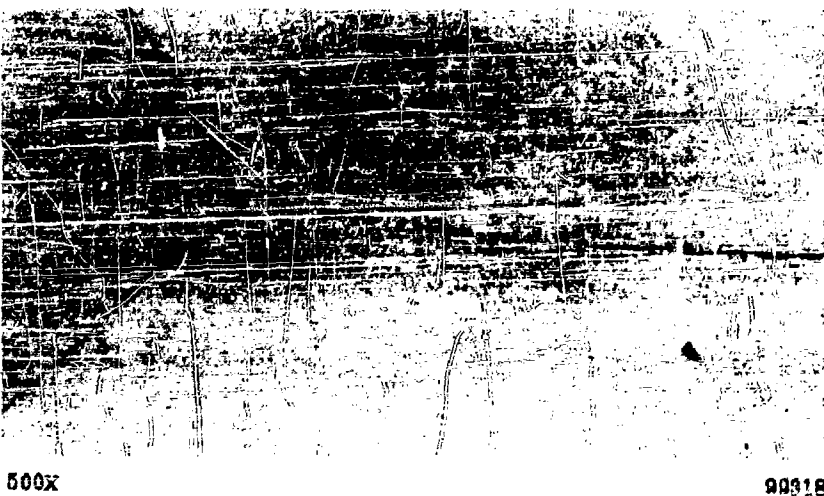
FIGURE 5. ARC-MELTED RHENIUM AFTER COLD AND HOT ROLLING AND AFTER HOT FORGING



a. As-Received Arc-Melted Button



b. Heated in Hydrogen at 1500 C for 30 Minutes; Hydrogen Muffle Cooled



c. Heated in Hydrogen at 1500 C for 10 Periods of 30 Minutes Each;  
Air Quenched Between Cycles

FIGURE 8. PHOTOMICROGRAPHS OF THREE HEAT-TREATED RHENIUM BUTTONS



TABLE 3. ANALYTICAL HISTORY OF THREE HEAT-TREATED RHENIUM BUTTONS

Condition of Button	Vacuum-Fusion Analysis, ppm			Reference Figure
	O <sub>2</sub>	H <sub>2</sub>	N <sub>2</sub>	
As arc melted	10	1.0	< 2	6a
Heated in hydrogen at 1500 C for 30 minutes; hydrogen muffle cooled	3	0.2	< 4	6b
Heated in hydrogen at 1500 C for 10 periods of 3 minutes each; air quenched between cycles	76	12.0	13	6c

Cold swaging was more successful, however. A finger-shaped arc-melted button was cast, and then cold forged and cold rolled to a round cross section. Intermediate anneals of 1 to 3 hours at 1700 C were given. The button was then loosely encased in one end of a length of copper tubing and cold swaged. Annealing, re-encasement, and more swaging followed. Eventually the button was long enough to swage without being supported by the copper tubing, and 80-mil rod was prepared by alternately swaging at 20 per cent reduction in cross-sectional area per pass and annealing at 1700 C for about 2 hours. The rod so prepared possessed some cracks and surface flaws, but proved that arc-melted metal could be worked into fine-gage rod by cold working if sufficient care was taken.

As was previously mentioned, simpler cold-working techniques had been developed meanwhile for pressed and sintered rhenium. Metal preparation from arc-melted consolidates was abandoned entirely in favor of the methods described below.

#### Powder-Metallurgy-Type Rhenium

Rhenium currently used for experimental purposes on this project is prepared entirely by powder-metallurgy procedures, as the products of this consolidation method can be fabricated more easily and are more versatile than rhenium prepared by the methods described above. The starting material is rhenium-metal powder reduced from ammonium pererrhenate. Chemical procedures for the preparation of this metal were

Initially, attempts were made to press and sinter rhenium-metal powder reduced from potassium perrhenate, an attack which proved fruitless. Proper pressing was achieved, but insufficient densification occurred during numerous and varying sintering attempts. Accordingly, ammonium perrhenate was prepared and rhenium-metal powder reduced from it as described previously. Similar  $1/4 \times 1/4 \times 6$ -inch pressings were made from each type of powder, and both sintered together at 1500 C for 2 hours. The results are shown in Figure 7, and indicate that the presence of  $K_2O$ , a major impurity in the potassium perrhenate-parent metal, inhibits proper densification.

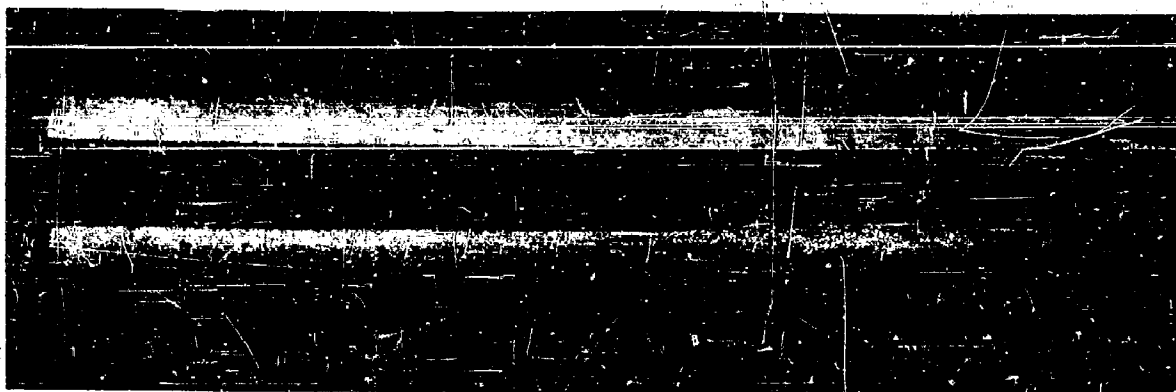
Following this experiment, all metal was prepared from ammonium perrhenate and consolidated and fabricated by the following procedures.

**Particle Size.** This factor is of prime importance, as is the case in all powder-metallurgy processes. It was found by trial and error that proper densification could not be obtained unless virtually all the powder passed a 325-mesh screen. Visual examination of this powder (Figure 8) showed that the particle size probably ranged between 1 and 25 microns.

**Pressing.** This operation was accomplished in a hardened steel die, so designed as to give a  $1/4$  by  $1/4$  by 6-inch pressing. This long shape is required in order to sinter the bar by self-resistance heating. In general, 60 to 65 grams of rhenium powder are required for this size. The die is lubricated with a solution of stearic acid in ether, applied to the walls with a swab prior to pressing. The pressing pressure is 30 tons per square inch, and, since the rhenium powder is quite bulky, the pressing ratio is 6 to 1. The as-pressed bars are extremely fragile and must be handled with care. Their density is usually about 40 per cent of the theoretical value, 21 grams per cubic centimeter. A bar in the as-pressed condition is shown in Figure 9a.

**Presintering.** This process is designed to provide sufficient strength for handling prior to high-temperature sintering, and is accomplished by heating the pressed bar to 1200 C for 2 hours in a vacuum of about 0.01 micron. This causes a slight densification and a great increase in strength. The density increases to about 50 per cent of theoretical, and the bar appears as in Figure 9b. The vacuum presinter evidently has some purification action; hydrogen presinter were used originally, but it was found that a vacuum presinter improved subsequent densification by electric sintering.

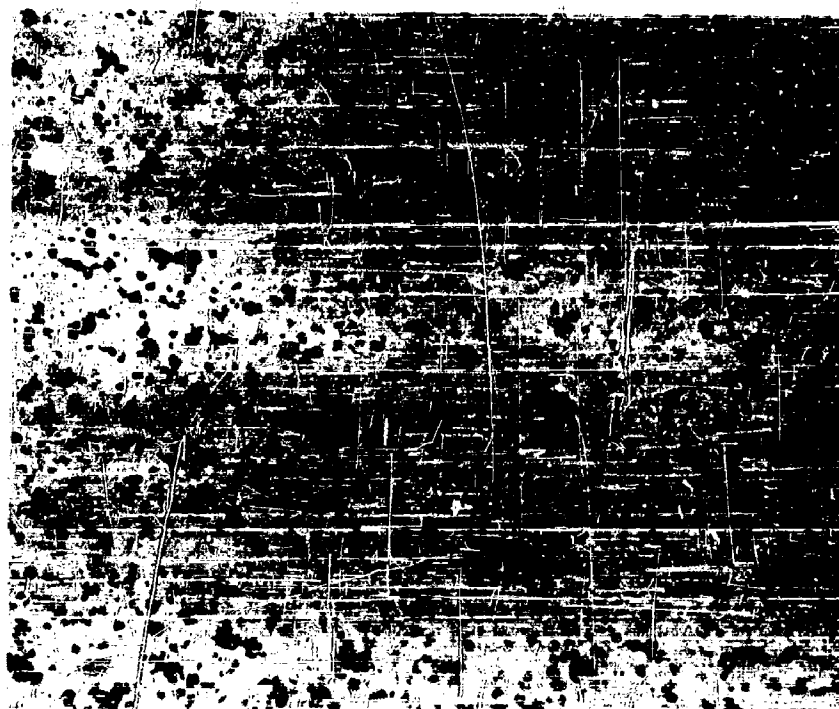
**Electric Sintering.** Following presintering, the bar is electrically heated by self-resistance in a sintering "bottle" similar to those used in industry, where the presintered bar is suspended vertically between two water-cooled molybdenum clips and heated by self-resistance. The lower of the two clips is suspended in a pool of mercury, so that electrical contact is maintained as the bar shrinks in length. The entire operation is conducted under dry flowing hydrogen. Current is applied slowly to the bar until it



1X

98533

**FIGURE 7. EFFECT OF SINTERING IN HYDROGEN AT 1500 C FOR 2 HOURS ON RHENIUM-METAL POWDER PREPARED FROM POTASSIUM PERRHENATE (ABOVE) AND AMMONIUM PERRHENATE (BELOW)**



100X

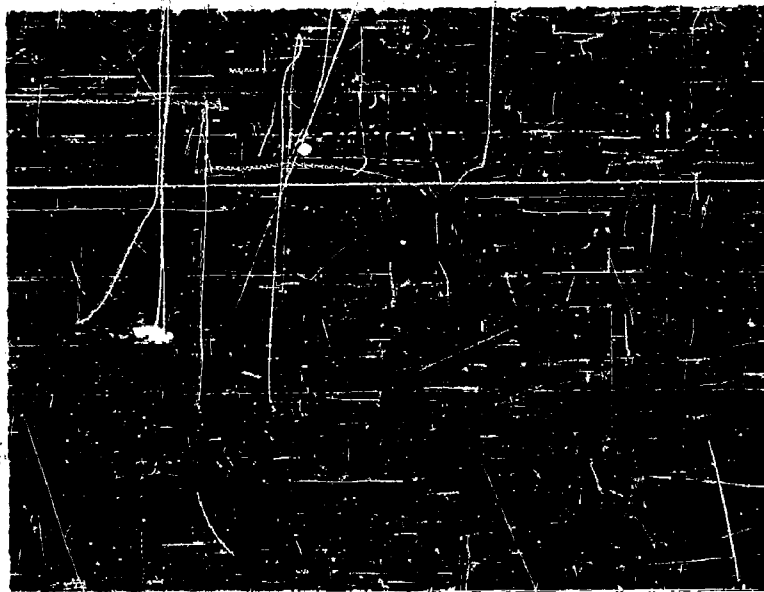
N1732

**FIGURE 8. RHENIUM-METAL POWDER REDUCED FROM AMMONIUM PERRHENATE; PARTICLE SIZE 1 TO 25 MICRONS**



- A. As-Pressed Bar, 38 to 40 Per Cent of Theoretical Density
- B. Presintered Bar, 45 to 50 Per Cent of Theoretical Density
- C. Sintered Bar, 87 to 93 Per Cent of Theoretical Density

FIGURE 9. STAGES IN THE SINTERING OF RHENIUM POWDER



100X

N2520

**FIGURE 10. MICROSTRUCTURE OF SINTERED RHENIUM BAR  
AT 92.2 PER CENT OF THEORETICAL DENSITY;  
TRANSVERSE SECTION**

reaches a true temperature of 2700 C. It is maintained at this temperature for about 1 hour. For a 1/4 by 1/4 x 6-inch bar, this requires about 8 volts and 1200 amperes. Following sintering, the bar is about 90 per cent of theoretical density and has the outward appearance shown in Figure 9c. Its microstructure is shown in Figure 10.

Vacuum sintering was attempted several times to test its effect on subsequent fabrication operations, but difficulty was encountered because of mechanical problems, and the effort was abandoned. A summation of the powder-consolidation procedures is given in Table 4.

TABLE 4. PROCEDURE FOR THE PREPARATION OF SINTERED RHENIUM BAR FROM RHENIUM POWDER

Operation	Time, hours	Temperature, C	Percentage of Theoretical Density, Achieved	Reference Figure	Remarks
Pressing	--	--	40	9a	30 T/in. <sup>2</sup> . Lubricate die with stearic acid
Presintering	2	1200	50	9b	In vacuum
Sintering	1	2700	90	9c	In hydrogen

Hot Working. Generally, all hot-working attempts on pressed and sintered bar were unsuccessful. These attempts consisted primarily of hot rolling, hot swaging, and hot wire drawing of a previously cold-swaged rod.

Hot swaging was tried at this laboratory and also at the Cleveland Wire Works of The General Electric Company. Hot swaging at Battelle was attempted at 1400 C on a square sintered bar. The bar developed cracks during the third pass of a 10 per cent reduction series, and breakage occurred on the tenth pass. Dies of different barrel lengths were investigated, but no better results were obtained. Concurrently, sintered rhenium was taken to the Cleveland Wire Works, with the request that it be "swaged as if it were tungsten". It completely broke up during the first pass at 1550 C.

Hot swaging was also attempted after rounding and partial reduction of a sintered bar by cold swaging. Fair success was attained for several passes at 10 per cent reduction, but cracking eventually appeared and die wear was very heavy. Clad and evacuated swaging operations on sintered bar also resulted in failure; despite the cladding, the specimen was crushed by the swaging operation. The hot-swaging program was abandoned subsequently.

Numerous attempts at hot rolling from temperatures in the range 1400 C to 1700 C, and by reductions ranging from 10 to 40 per cent per pass, generally resulted in failure by cracking. One attempt was successful, however, and it is planned to expand this work in the future. In this one case, a specimen previously reduced 75 per cent by cold rolling and possessing a few edge cracks was reduced an additional 60 per cent at 1475 C to 0.026-inch thickness. No further edge or surface cracking occurred, although hardening from 300 VHN initially to about 500 VHN took place. This indicates that hot rolling at these temperatures requires some intermediate annealing. If care were to be exercised, hot rolling might be possible after initial fabrication by cold working.

Hot-wire drawing of rhenium rod reduced to 60-mil diameter by cold swaging was investigated through the courtesy of the Cleveland Wire Works. Breakage usually occurred on the second or third pass, each at about 10 per cent reduction in cross-sectional area. However, several successful passes were made at 10 per cent reduction by drawing very slowly (8 to 9 feet per minute) using a Karo-graphite lubricant. The wire was heated to cherry red for the drafts. It was decided that the lubrication was poor in all cases, and that copper-plated wire might draw well. This was attempted, but was unsuccessful.

Cold Working: General. The various types of cold working are described separately in detail below, as cold working has proved quite successful. From the experiments and operations described, procedures for the preparation of wire and sheet have been evolved. For simplicity, the cold-working operations necessary for wire preparation are summarized in Table 5. Several basic requirements, which apply to virtually all of the cold-working operations, follow:

- (1) As-sintered bar should be lightly surface worked by either hand forging or rolling to build up a fine-grained structure to prevent surface cracking.
- (2) Reduction is usually from 10 to 20 per cent in cross-sectional area per pass.
- (3) Each cold-working pass must be preceded by an anneal, usually in hydrogen, at 1600 to 1750 C for 1 to 3 hours.

- (4) Following the anneal, the surface hardness must not exceed about 300 VHN for forged, swaged, or drawn material and about 350 VHN for rolled material.

Typical microstructures resulting from cold fabrication of sintered rhenium may be seen in the section on recrystallization later in this report.

Cold Forging. No heavy machine forging has been done cold on sintered rhenium, but the initial operation following sintering of a bar in preparation for swaging is a cold hand-forging operation. The bar is lightly hand hammered (or peened) along the corners of the bar. This flattens the corners slightly and tends to build up a fine, strong, grain structure with high resistance to cracking at the zones of high secondary tensile stress during fabrication, namely the corners.

Cold Rolling; I. Preparation of Rod. The cold rolling of rhenium has fallen into two phases in the present work. The first phase was the use of cold rolling as a tool in the preparation of swaged rod, as is being related in this section. The other phase was the direct cold rolling of rhenium to sheet and strip, which is reported later.

In the preparation of rod, cold rolling is used in three operations. First, if the bar is not square following sintering, the bar is cold rolled very lightly to square it. This is usually a matter of 1 or 2 per cent reduction and is not reported in Table 5.

The second cold-rolling operation is a very important step. Following the peening operation, the bar is cold rolled on the small flats resulting from the peening until it resembles an octagon in cross section, as shown in Figure 11c. Reduction is of the order of 5 to 8 per cent per pass and usually is repeated twice. Intermediate anneals are given; 1/2 hour at 1700 C is usually sufficient.

Following this, it is usually necessary to cold roll on the original square flats to decrease creping caused by the octagonizing. This step is summarized in Table 5.

Cold Rolling; II. Preparation of Sheet and Strip. Since success was achieved in the fabrication of rod by cold-working methods, cold rolling was investigated as a means of preparing thin sheet and strip.

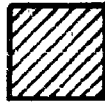
Sintered rhenium bar is lightly peened along the edges and corners to build up a fine-grained structure. Next, the bar is cold rolled lightly several times, about 1 or 2 per cent reduction per pass, and then heavy rolling commences. In general, the procedure is to reduce between 5 and 10 per cent per pass and then anneal for 2 hours at 1700 C. Postanneal hardnesses do not seem to fall so low as during swaging operations, where the same amount of reduction is involved. It is sometimes difficult to lower the hardness under 350 VHN, even after repeated annealing. Nevertheless, cold



TABLE 5. PROCEDURE FOR THE PREPARATION OF RHENIUM WIRE FROM SINTERED BAR

Operation	Reduction per Operation, per cent	Number of Operations	Anneals	Remarks
Cold peening	4 (on length of diagonals)	2-3	Intermediate; 1/2 hour at 1700 C	Flattens corners of original - square bar (see Figure 11b)
Cold rolling	5-8 (on length of diagonals)	3	Intermediate; 1/2 hour at 1700 C	Octagonalizes bar (see Figure 11c)
Cold rolling	1 (on original square faces)	1	None	Smoothens bar faces creped by edge rolling
Cold swaging	10-20 (of cross- sectional area)	As many as desired	Intermediate; 2 hours at 1700 C	Postanneal hardness < 300 VHN (see Figure 11d)
Cold Turk's head drawing	10 (of cross- sectional area)	As many as desired	Intermediate; 2 hours at 1700 C	Postanneal hardness < 300 VHN
Cold drawing(a)	10 (of cross- sectional area)	As many as desired	Intermediate; 2 hours at 1700 C	Postanneal hardness < 300 VHN

(a) This operation may follow swaging directly; if very fine wire is desired, the Turk's head operation should be included.



(a) As-Sintered Rhenium Cross Section



(b) As-Edge-Forged Rhenium Cross Section



(c) As-Octagonized Rhenium Cross Section



(d) As-Swaged Rhenium Cross Section

FIGURE 11. STEPS IN THE PREPARATION OF RHENIUM ROD

A-8417

working after annealing to about 350 VHN has been found quite satisfactory if the operation is rolling only. This is not true for swaged material, as is noted below.

Obviously, the reduction to thin sheet of sintered bar  $1/4 \times 1/4$  inch in cross section by 10 per cent reductions with long intermediate anneals is very time consuming. The procedure has been shortened considerably by adopting a policy of pressing bars with a  $1/8 \times 1/2$ -inch cross section, which can be processed in the same manner as the square bars if additional care (due to additional fragility) is observed. In this case, the  $1/8$ -inch edges are cold peened before full-scale rolling commences. After reduction to about 10-mil thickness, this strip has a width of about  $5/8$  inch.

Another innovation that has been introduced is cross rolling. Short (2-inch) lengths of partially cold-rolled bar were cross rolled to make sheet. Reduction is slower, but several passes without annealing may be taken until a total reduction of 10 per cent is attained. This is followed by annealing.

At the present time, a small stock of 3-, 5-, and 10-mil strip or foil has been built up by these cold-rolling procedures. Edge cracking is quite infrequent, and the as-rolled surface is bright and shiny. Much of the material is being used for experimental work. It is planned to prepare a small amount of 1-mil foil, and then cease cold-rolling studies.

Cold Swaging. Following the octagonization of a square sintered bar by the process described under Cold Rolling; I., cold swaging is introduced. This operation follows the same over-all methods as described above for other cold-working operations, namely, cold working with intermediate annealing. Reduction, however, is usually 20 per cent per pass. The annealing, as shown in Table 5, is 2 hours at 1700 C. Postanneal hardnesses always fall to 300 VHN and are often around 270 VHN.

With the available equipment, swaging is possible down to diameters of about 65 mils. At that juncture, wire drawing would be expected to be the next operation if finer diameter stock is desired. However, due to difficulties in wire drawing that seem to be almost inherent with rhenium, wire drawing is done only if wire of 50 to 65-mil diameter is desired. If wire of finer dimensions is needed, Turk's head drawing enters, as indicated in the next section.

Cold Turk's Head Drawing. First, the as-swaged metal is "scalped", which removes 1 or 2 mils of its surface by grinding with a large aluminum oxide wheel. This eliminates tiny surface fissures that occasionally appear as a result of swaging. The wire is then drawn through a Turk's head draw plate, a series of four small rolls so arranged as to give square wire. This operation, with intermediate annealing, is carried out at 10 per cent reduction in cross-sectional area per pass. The rhenium reduces easily and maintains an excellent surface because of the rolling type of reduction. Finning of the wire corners between the rolls may occur, but can be eliminated

by reversing drawing direction for each pass. Wire ranging in thickness from 10 to 15 mils has been prepared in this manner, and can be drawn to round wire subsequently if desired.

Cold Wire Drawing. Wire drawing may be done directly following swaging, but, since repeated drafts seem to produce a poor wire surface, it is not recommended that the wire drawing be extensive. For instance, 65-mil swaged rod, scalped and drawn with the best lubrication methods yet developed for rhenium, has an excellent surface when drawn to 50 mils, a good surface when drawn to 40 mils, but a poor surface at 30 mils and below. If 10-mil wire is desired, the swaged material is Turk's head drawn from 65 mils to about 30 mils, and then round-wire drawing to 10 mils commences. If equipment for swaging to 20 or 30 mils were available, the Turk's head operation probably would be unnecessary. A more detailed description of the wire-drawing work follows.

Wire drawing is accomplished by reductions of 10 per cent in cross-sectional area per pass with intermediate anneals of 2 hours at 1700 C, as described in Table 5.

The specific procedure so far developed is to "scalp" a swaged rod as previously described and lightly polish the rod with abrasive paper to remove the grinding marks from scalping. A point is then ground on the wire with an aluminum oxide grinding wheel, lubricant is applied to the wire, and drawing is done in a linear draw bench at about 10 feet per minute.

Despite continuous experimentation, rhenium wire with a surface free of imperfections has not yet been prepared if more than three or four drafts are given. These imperfections appear first as longitudinal gouged or pitted areas, next as longitudinal fissures, and then as small transverse cracks. Evidently the die friction is very high, probably a result of rhenium's high resistance to deformation and its rapid hardening by cold working. Approximately 20 lubricants have been investigated, including liquid-type materials, solids, and combinations of each. In general, the best results were obtained by using a lithium stearate-base grease-like material containing tallow, and Houghton's Cyl Tal No. 81, a heavy oil. Hard coatings produced very poor surfaces, and baked-on coatings were absolutely worthless. All of this drawing was done in Carboloy dies. Below 10-mil diameter, however, diamond dies are used. Drawing through diamond dies appears to be easier than through Carboloy. The smallest diameter wire prepared to date is 7 mils.

Cold Rod Rolling. Another method of reduction of sintered bar that has been investigated is rod rolling. Short sections of sintered rhenium in the as-sintered, as-peened, as-octagonized, and as-swaged conditions were all reduced from about 0.20 inch square or round to 0.09 inch square with considerable success. Reduction was at the rate of 15 per cent in cross-sectional area per pass, with the usual intermediate anneals. Little edge cracking developed on any of the specimens, and the experiment indicated

that sintered bar could be cold rod rolled directly, with no preparatory steps such as are necessary for swaging. However, swaging at 20 per cent reduction per pass produces a smaller diameter product faster for the purposes of this work.

### Rhenium Alloys

No alloy program has been undertaken with the expressed idea of studying the alloys, per se. However, at several points in the program, the fabrication of certain alloys was studied as a result of material requirements for other work, usually electronic studies.

### Arc-Melted Rhenium-Thorium Alloys

It was first thought that rhenium-thorium alloys were necessary for thermionic-emission studies, with the thorium present as metal. Accordingly, arc-melted rhenium buttons containing 0.5, 1, and 2 per cent thorium were prepared, the buttons to be fabricated or to be cut and ground to cylindrical test specimens. Breakage occurred consistently during grinding, and fabrication was impossible. The thorium metal definitely caused embrittlement. The structure is shown in Figure 12.

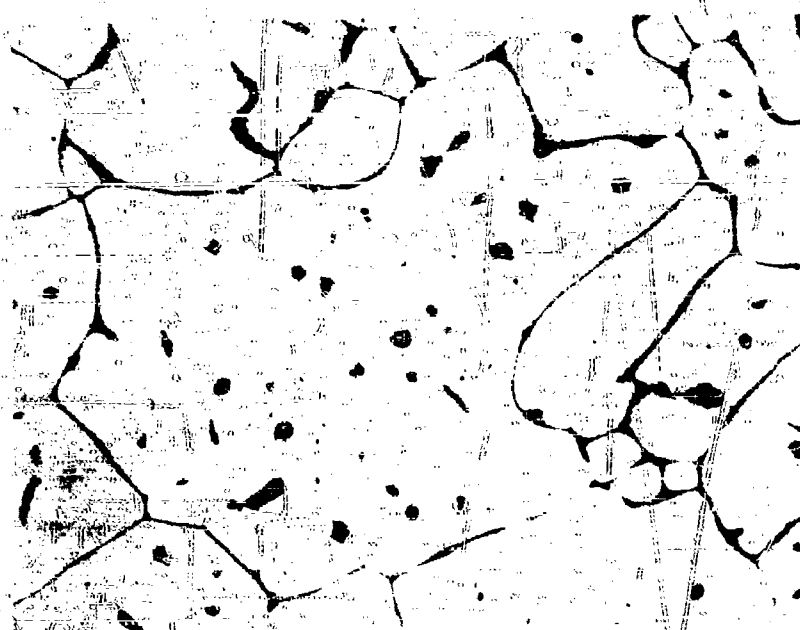
### Thoriated Sintered Rhenium

Although thoriated rhenium is not an alloy in the strict sense of the word, it will be discussed in this context.

Following the failure of efforts to fabricate rhenium-thorium alloys, it was found that rhenium containing thorium in the form of thoria (thorium oxide,  $\text{ThO}_2$ ) would be quite acceptable for thermionic-emission studies. Accordingly, thoria was blended with rhenium powder in amounts of 0.5, 1, 2, and 5 per cent, calculated on the basis of thorium content by weight. The bars were pressed, sintered, and fabricated. The thorium, when present as 0.5, 1, and 2 per cent as thoria, allowed fabrication to proceed unhindered. However, 5 per cent thorium as thoria caused embrittlement, and breakage occurred during swaging. A typical thoriated structure is illustrated in Figure 13.

### Arc-Melted Rhenium With Deoxidizing Elements Added

During attempts at hot working of rhenium, it was thought that, if certain deoxidizing elements could be added to tie up oxygen internally, the hot shortness native to rhenium might be alleviated. Five elements, aluminum, titanium, zirconium, uranium, and thorium, were added in 1 per cent



250X

N3505

**FIGURE 12. PHOTOMICROGRAPH OF RHENIUM-2 PER CENT THORIUM ALLOY, SOLUTION ANNEALED AND QUENCHED, SHOWING A SECOND PHASE AT GRAIN BOUNDARIES AND IN THE GRAINS**



500X

N4343

**FIGURE 13. STRUCTURE OF RHENIUM CONTAINING 1 PER CENT THORIUM AS THORIA**

quantities each. All of the alloys developed rather excessive cracking. Only the titanium alloy showed any improvement over rhenium, and it did not show sufficient improvement to warrant further investigation.

## PHYSICAL PROPERTIES

Up to the inception of this research project, information on the physical properties of rhenium was very sketchy. A number of determinations had been made, but very few of these had been verified by other workers. It was felt that a thorough investigation into these properties was warranted, so as to provide a firm basis for further less basic investigations.

### Lattice Constants

Several determinations of the lattice constants of this hexagonal-close-packed metal have been made. The most accurate group of values appears to have been the result of investigations by Stenzel and Weertz<sup>(2)</sup>, but Agte, et. al.<sup>(3)</sup>, Goldschmidt<sup>(4)</sup>, and Moeller<sup>(5)</sup> also have published data.

Three sets of values, all determined by X-ray diffraction methods, have been obtained in the present work. One of these patterns was made from purified powder reduced from ammonium perrhenate, and two, a major and minor pattern, were obtained from crystal-bar rhenium. These are all recorded in Table 6, which includes the results found by Stenzel and Weertz and by the other investigators for comparison purposes.

Powder-pattern results from the present work and the values given by Stenzel and Weertz agree exactly. The minor phase from crystal bar also agrees well with these two values. The crystal-bar major pattern does not match the other values, which may be a result of the presence of impurities during deposition of a certain section of the crystal bar. This value is indicative of a contracted lattice, and must be, therefore, a result of substitutional impurities. Although interstitial impurities can only expand a lattice, substitutional impurities may cause either contraction or expansion.

The powder-pattern value from the present work is preferred, and it agrees well with the several other values. In general, calculations from these constants give density values slightly higher than reported previously, and tend to point up the high density values determined experimentally and reported below.

TABLE 6. LATTICE CONSTANTS OF RHENIUM

$a_0$ , A	$c_0$ , A	$c/a$	Investigator	Remarks
2.760(a)	4.458(a)	1.615	Present work	Purified powder
2.753(a)	4.445(a)	1.615	Present work	Crystal bar (major)
2.760(b)	4.460(b)	1.616	Present work	Crystal bar (minor)
2.760(c)	4.458(c)	1.615	Stenzel and Weertz <sup>(4)</sup>	--
2.771(c)	4.479(c)	1.616	Agte, et al. (3)	0.3% Mo
2.761(c)	4.459(c)	1.615	Moeller <sup>(5)</sup>	0.5% K <sub>2</sub> O
2.758(c)	4.457(c)	1.616	Goldschmidt <sup>(6)</sup>	0.3% Mo

(a) Accurate to  $\pm 0.001$  A.(b) Accurate to  $\pm 0.005$  A.

(c) Converted from the literature to true angstrom units.

### Density

Agte, et al. (3), had calculated the density of rhenium from the accepted atomic weight, 186.31, and the lattice constants they determined (see Table 6). This value, 20.53 g/cm<sup>3</sup>, is the one most often cited; in addition, Agte found an experimental density of 20.9 g/cm<sup>3</sup>, indicating his lattice constants were probably high. One other literature value for the density exists, that of Goldschmidt<sup>(6)</sup>, who calculated 21.40  $\pm$  0.06 g/cm<sup>3</sup>. This was based on an atomic weight now known to be incorrect.

Several direct density measurements were conducted in the present work. The first of these was made on unworked crystal bar, and the others were conducted on seemingly sound sections of swaged crystal bar and hot-rolled strip. As can be seen in Table 7, none of these values exceeded 21.0 g/cm<sup>3</sup>. Finally, measurements were made on fabricated rod approximately 6.6 inches long and 0.150 inch in diameter. The rod had been fabricated by swaging from 1/4-inch sintered bar, using the cold-working procedures now considered standard. It was then annealed repeatedly. Metallographic examination verified that the rod was completely sound. The method used was water displacement; two values, 21.02 and 21.03 g/cm<sup>3</sup> were obtained.



TABLE 7. DENSITY DETERMINATIONS ON RHENIUM

Density, g/cm <sup>3</sup>	Type of Rhenium	Determination Method	Investigator
21.02 ± 0.01 21.03 ± 0.01	Sintered and swaged rod	Water displacement	Present work
20.82 ± 0.01	Swaged crystal bar	Water displacement	Ditto
20.9 ± 0.1	Unworked crystal bar	Water displacement	"
20.75 ± 0.01	Hot-worked sintered sheet	Water displacement	"
20.9	Probably crystal bar	Probably water dis- placement	Agte, et al. (3)
<hr/>			
21.04 ± 0.01	Crystal bar	From lattice con- stants	Present work
20.53	Probably crystal bar	From lattice con- stants	Agte, et al. (3)
<hr/>			
21.02	Sintered and swaged rod, reduced 22.0 per cent by cold work	Water displacement	Present work

To date, these are the highest values recorded, and, since most impurities could only lower the density, they are probably more nearly correct. Thus,  $21.02 \pm 0.01 \text{ g/cm}^3$  is the preferred value for pure rhenium and is compared with the values for other elements in Table 8.

Calculation of the theoretical density from the new lattice constants and the accepted atomic weight was accomplished by use of the equation:

$$d = \frac{knM}{V},$$

where

$d$  = density, grams per cubic centimeter  
 $k$  = 1.66020, a constant<sup>(7)</sup> (mass of the hydrogen atom  $\times 10^{24}$ )  
 $n$  = 8, number of atoms per unit cell  
 $M$  = 186.31, the atomic weight (after Agte<sup>(3)</sup>)  
 $V$  = volume of the unit cell, calculated from the lattice constants:

$$a_0 = 2.760 \pm 0.001 \text{ A},$$

$$c_0 = 4.458 \pm 0.001 \text{ A},$$

by the equation

$$V = 3\sqrt{3/2} a_0^2 c_0.$$

This calculation gave  $21.04 \text{ g/cm}^3$ , in excellent agreement with the experimental value of  $21.02 \pm 0.01 \text{ g/cm}^3$ . These figures establish rhenium as the fourth most dense element (see Table 8).

TABLE 8. THE DENSITY OF RHENIUM COMPARED WITH THE DENSITIES OF OTHER ELEMENTS<sup>(8)</sup>

Element	Density, $\text{g/cm}^3$
Osmium	22.6
Iridium	22.5
Platinum	21.5
Rhenium	21.0
Gold	19.3
Tungsten	19.3
Uranium	18.7

In addition, a density determination was obtained on swaged rod 22.0 per cent reduced by cold work to determine whether cold working affected the density. Two values were obtained, 20.99 and 21.04 g/cm<sup>3</sup>, the average of which is 21.02 g/cm<sup>3</sup>, the same density as established for annealed metal. The conclusion is that cold working does not affect the density of rhenium.

### Melting Point

Two investigators had determined the melting point of rhenium previously, and each agreed quite well with the other. The investigators, Agte, et al. (3), and Jaeger and Rosenbohm (8), found 3170 ± 60 C and 3160 C, respectively.

In the present investigation, first results using the bored-hole method in sintered bars indicated that the melting point was not so high as these investigators claimed. An average value of 3010 ± 90 C was found from four determinations.

However, recent work on high-temperature porosity has focused attention on the impurity content of the powder-metallurgy-type rhenium, a factor which often affects melting points deeply. When highly purified rhenium, containing less than 0.09 per cent impurities, was available and its melting point determined, the early results were found to be in error. The determination by the bored-hole method gave a new melting point of 3180 ± 20 C, as averaged from two separate determinations, 3184 C and 3175 C. Since good corrections were available for absorption in the sight-hole glass and the filter used, and since the optical pyrometer has been calibrated recently, the new value of 3180 ± 20 C is to be preferred. Along with the results of previous investigators, this value confirms that rhenium is the second highest melting metal and the third highest melting element.

The melting points determined in the present work are summarized in Table 9 and compared therein with the work of the early investigators. In Table 10, the melting point of rhenium is compared with those of other high-melting elements.

### Vapor Pressure of Solid Rhenium

In order to evaluate fully the potential importance of rhenium as a material for electronic applications, it is necessary to have information on the vapor pressure. No specific data are available in the literature relating to the vapor pressure of rhenium as a function of temperature.

TABLE 9. THE MELTING POINT OF RHENIUM

Temperature, C	Temperature, F	Investigator
3170 ± 60	5740 ± 110	Agte, et al. (3)
3160	5720	Jaeger and Rosenbohm(9)
3010 ± 100	5450 ± 200	Present work, 0.2 per cent impurities
3180 ± 20	5760 ± 40	Present work, <0.09 per cent impurities

TABLE 10. THE MELTING POINTS OF RHENIUM  
AND SEVERAL OTHER ELEMENTS(9)

Element	Melting Point, C
Carbon (graphite)	3700 ± 100
Tungsten	3410 ± 20
Rhenium	3180 ± 20
Tantalum	2996 ± 50
Molybdenum	2625 ± 50

To obtain the required information, the Langmuir weight-loss method, which has been used previously at Battelle in determining the vapor pressure of such metals as titanium<sup>(10)</sup>, was employed. The validity of the data was checked by thermodynamic calculations, and the boiling point of the metal was estimated.

### Description of the Test Method

The Langmuir weight-loss method<sup>(11)</sup> involves heating a wire of the desired material in a good vacuum ( $10^{-5}$  mm of mercury or less) at a constant temperature for a measured time interval and determining the loss in weight as a result of evaporation of metal from the wire. Relation 1 and 2, following, are then used to compute the vapor pressure:

$$\log p_{\text{atm}} = \log m - 1/2 \log M + 1/2 \log T - 1.647, \quad (1)$$

where  $p_{\text{atm}}$  = vapor pressure, atmospheres

$M$  = gram-molecular weight of the vapor

$T$  = temperature, degrees Kelvin

$m$  = rate of evaporation, g/cm<sup>2</sup>/sec.

Further:

$$m = \left( \frac{\rho}{\pi} \right)^{1/2} \cdot \left( \frac{W_0^{1/2} - W^{1/2}}{t} \right), \quad (2)$$

where  $\rho$  = computed density at temperature of run, g/cm<sup>3</sup>

$W_0$  = initial weight per unit length of wire, g/cm

$W$  = final weight per unit length of wire, g/cm

$t$  = time of run, seconds.

### Test Specimens

The specimens used in the experimental work were in the form of wires about 0.050 inch in diameter by 6 inches long. These wires were made by cold pressing, sintering, and cold working as described in the section on consolidation and fabrication.

\* Strictly,  $\alpha \cdot p_{\text{atm}} = m \cdot \text{const} \cdot T^{1/2} \cdot M^{-1/2}$ , the Knudsen equation. As is customary when dealing with metals,  $\alpha$ , the accommodation coefficient, is assumed equal to unity. (12)

Figure 14 is a photomicrograph of a longitudinal section of a typical wire specimen in its condition prior to test.

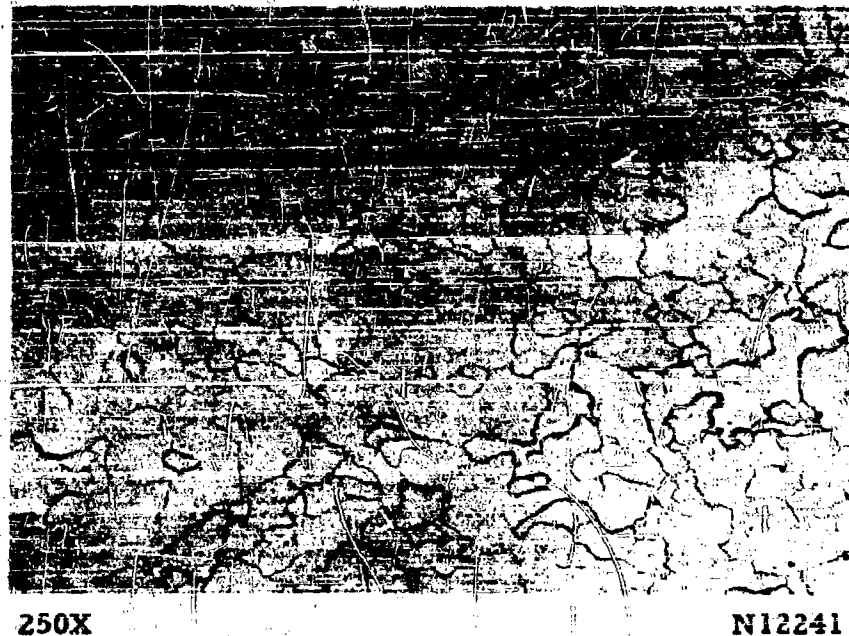
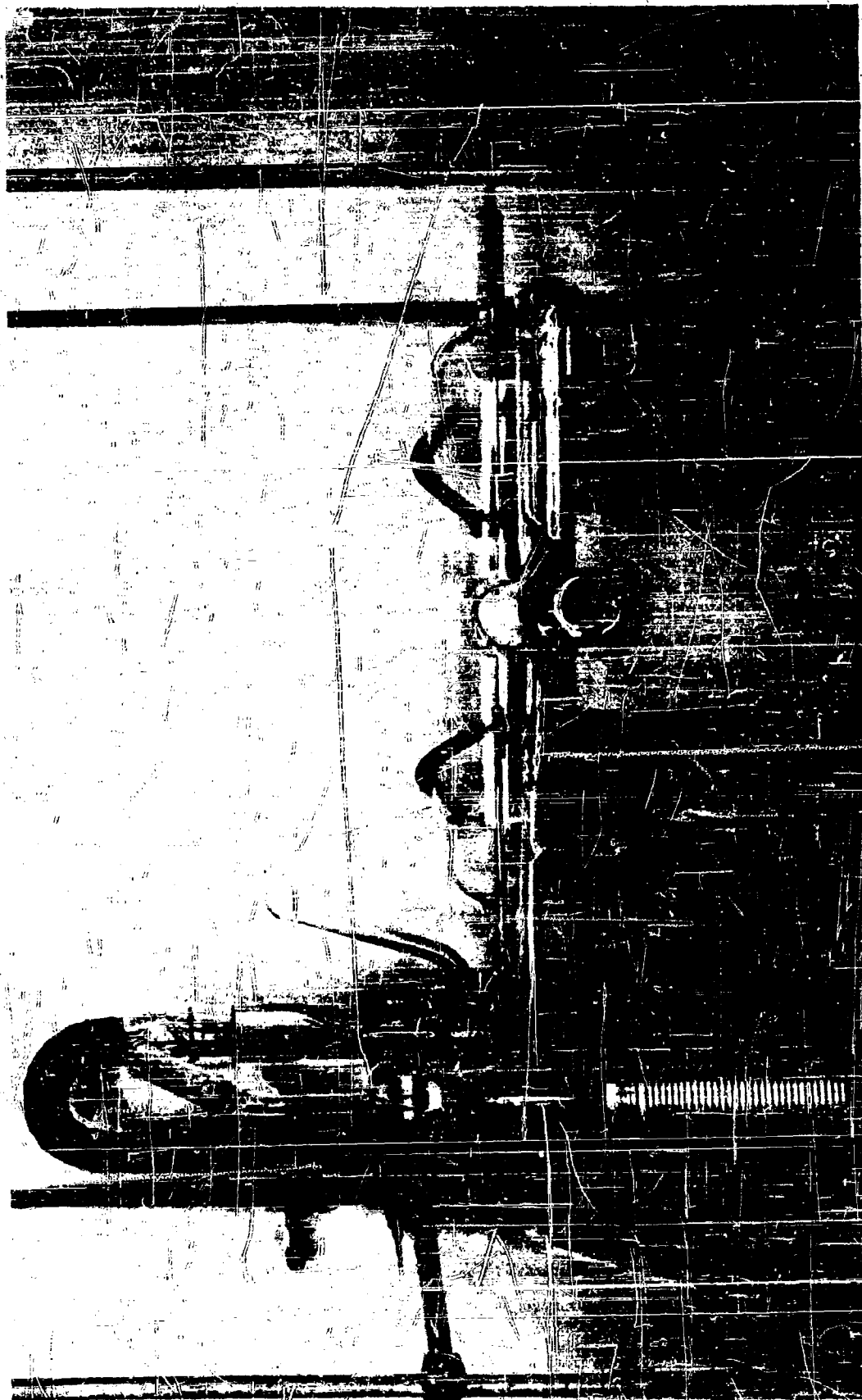


FIGURE 14. LONGITUDINAL MICROSTRUCTURE  
OF A TYPICAL RHENIUM TEST WIRE

#### Test Equipment

The test specimen was supported in a horizontal position by two split molybdenum clamping blocks, each 0.5 inch in diameter by 1.5 inches long. Each of these blocks was provided with a tapped hole so that it could be screwed onto the 0.25-inch-diameter tungsten supporting electrodes. This assembly was mounted in a 100-mm Pyrex bulb with the ends of the tungsten electrodes protruding from the bulb and sealed to it by uranium glass (Figure 15).

A 45-mm Pyrex tube, with an optically flat Pyrex plate sealed in its free end, was joined at right angles to the bulb, and perpendicular to the test specimen at its center. The temperature of the wire was determined by means of a standardized optical pyrometer sighted through the flat Pyrex plate. A magnetically operated glass shutter was placed in the line of sight between the test wire and the optical window to prevent condensation of evaporated rhenium on the window. The shutter was maintained in this position except when temperature determinations were being made.



N6094

FIGURE 15. VAPOR-PRESSURE APPARATUS

Figure 15 illustrates the complete vacuum system (except for the mechanical fore pump), which includes an ionization gage, a liquid-nitrogen trap, and a three-stage mercury diffusion pump.

In all test runs, the vacuum was less than  $10^{-5}$  mm of mercury.

### Procedure

With the specimen in place, the system was evacuated to about  $10^{-5}$  mm of mercury and then filled with high-purity helium as a purge. Next, the system was re-evacuated to  $10^{-5}$  mm of mercury, or lower, and the rhenium wire was heated electrically with stabilized a-c power to the desired temperature as rapidly as possible. The wire temperature was maintained constant by adjusting the applied voltage so that the product of the cube root of the current and the voltage did not vary. The test runs were terminated when it was judged that sufficient metal had been evaporated from the surface of the wire to permit accurate weight-loss determination.

### Data

Table 11 lists the experimental results. Calculated high-temperature densities ranging from 19.73 to 19.93 g/cm<sup>3</sup> were used in computations based on Equations 1 and 2. One run was made at each of the temperatures reported.

TABLE 11. EXPERIMENTAL VAPOR-PRESSURE DATA FOR RHENIUM

Corrected Temperature		Duration of Run, seconds	Rate of Evaporation, m, g/cm <sup>2</sup> /sec	Vapor Pressure	
C	K			Atmosphere	mm Hg
2221	2494	259,200	$1.54 \times 10^{-8}$	$1.24 \times 10^{-9}$	$9.39 \times 10^{-7}$
2250	2523	151,200	$3.23 \times 10^{-8}$	$2.61 \times 10^{-9}$	$1.98 \times 10^{-6}$
2332	2605	30,600	$7.35 \times 10^{-8}$	$6.04 \times 10^{-9}$	$4.59 \times 10^{-6}$
2475	2748	54,000	$6.96 \times 10^{-7}$	$5.56 \times 10^{-8}$	$4.23 \times 10^{-5}$
2480	2753	23,400	$4.67 \times 10^{-7}$	$3.93 \times 10^{-8}$	$2.99 \times 10^{-5}$
2606	2879	7,200	$2.77 \times 10^{-6}$	$2.38 \times 10^{-7}$	$1.81 \times 10^{-4}$
2726	2999	1,560	$8.41 \times 10^{-6}$	$7.37 \times 10^{-7}$	$5.60 \times 10^{-4}$



An empirical expression for the vapor pressure of rhenium was calculated from the experimental determinations, using the method of least squares. For the temperature range covered, Equation 3 is a valid representation of the vapor pressure of rhenium:

$$\log_{10} P_{\text{mm}} = 10.4038 - \frac{40865}{T}, \quad (3)$$

where

$P_{\text{mm}}$  = vapor pressure, millimeters of mercury

$T$  = temperature, degrees Kelvin.

The vapor pressure of rhenium so determined is about ten times greater than that of tungsten and is about 1-1/2 times that of tantalum. This is illustrated in Figure 16.

### Discussion of Results

There are several sources of possible error in the experimentally determined vapor pressure of rhenium.

For example, the wire specimen was assumed to be at a constant temperature except for about 1/4 inch on each end. However, there was a slight temperature gradient from the center of the wire to locations 1/4 inch from each end. Since the temperature was measured at the center of the wire, the average true temperatures may have been slightly below the values indicated. Thus, the measured vapor pressures should be associated with lower temperatures and, hence, would be slightly low at the stated temperatures.

### Estimation of the Boiling Point and Liquid Vapor Pressure of Rhenium

#### Boiling Point

Extrapolation of Equation 3 to  $p_{\text{mm}} = 760$  gives only a very crude estimate of the boiling point of rhenium, i. e., 5430 K. To obtain a better estimate, a thermodynamic treatment is employed in which the following important thermodynamic relationship is satisfied:

$$R \ln P_{\text{atm}} - \left( \frac{F^{\circ} - H_0^{\circ}}{T} \right)_{c,l} - \left( \frac{F^{\circ} - H_0^{\circ}}{T} \right)_g - \frac{\Delta H_0^{\circ}}{T}, \quad (4)$$

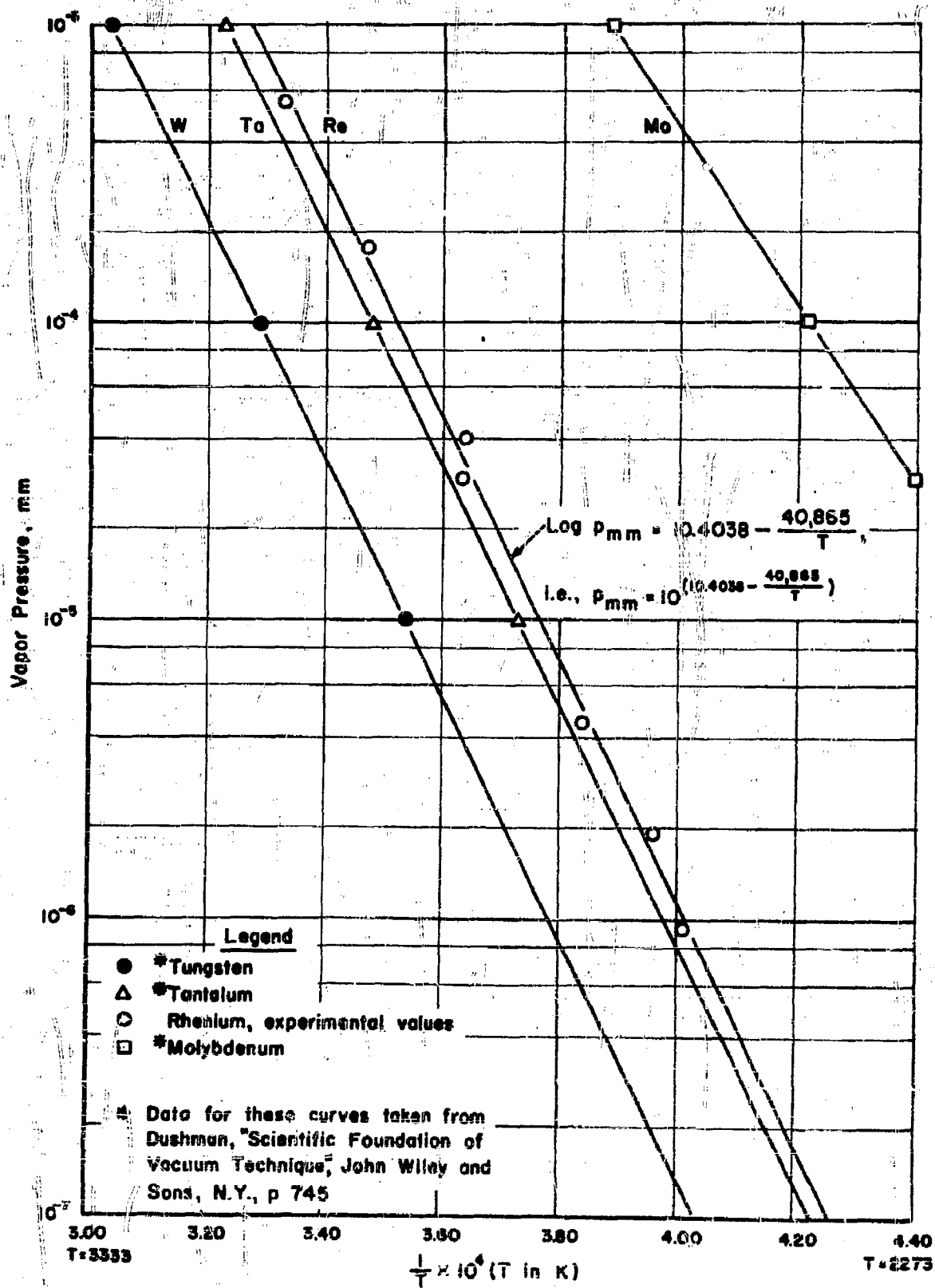


FIGURE 16. THE VAPOR PRESSURE OF RHENIUM AND OTHER REFRACTORY METALS AS A FUNCTION OF RECIPROCAL TEMPERATURE  
 WADC TR 54-371  
 40  
 A-2697

where

$R$  = the universal gas constant, 1.987 cal/mole

$P_{\text{atm}}$  = vapor pressure, atmospheres

$\left(\frac{F^0 - H_0^0}{T}\right)_{c,l}$  = the free-energy function for liquids and crystalline solids, i. e., the "condensed" phases of matter

$\left(\frac{F^0 - H_0^0}{T}\right)_g$  = the free-energy function for the vapor

$\Delta H_0^0 = (H^0 - H_0^0)$ , in which  $H^0$  is the heat of sublimation at temperature  $T$  and  $H_0^0$  is the heat of sublimation at absolute zero, in calories per mole.

The free-energy functions for solids and for liquid  $\left(\frac{F^0 - H_0^0}{T}\right)_{c,l}$  can be evaluated when the thermal variation of  $C_p$ , the heat capacity, is known and appropriate account is taken of phase changes. The free-energy function for the vapor,  $\left(\frac{F^0 - H_0^0}{T}\right)_g$ , can be determined from spectroscopic data(13).

Equation 4 is used first to assess the quantitative accuracy of the experimental data of Table 11, i. e.,  $\Delta H_0^0$  is computed for each of the experimental temperatures, using the corresponding measured values of the vapor pressure. Table 12 lists the results of these computations. Although the standard deviation from the mean is 1015 calories, somewhat higher than might be desired, no over-all trend upward or downward is indicated, so that large systematic errors apparently have been avoided. The value 187,000 calories has been taken as  $\Delta H_0^0$  of sublimation for rhenium.

If  $P_{\text{atm}}$  is set equal to 1 in Equation 4, then its logarithm is zero, and, by a method of successive approximation,  $T_B, P.$ , the boiling point of rhenium, can be estimated. The value so obtained is 5900 K, or about 5630 C.

#### Vapor Pressure of Liquid Rhenium

Once a reasonable value for  $\Delta H_0^0$  has been obtained, Equation 4 can be used to compute the vapor pressure of liquid rhenium at various temperatures above the melting point. These computed values are, in reality, estimates, since no data are available for the heat capacity of liquid rhenium. Brewer<sup>(14)</sup> has estimated the entropy of fusion of rhenium as 2.3

TABLE 12.  $H^\circ$  OF SUBLIMATION FOR RHENIUM

T, deg K	$-\left(\frac{F^\circ - H^\circ}{T}\right)_g$	$-\left(\frac{F^\circ - H^\circ}{T}\right)_{c,l}$	Vapor Pressure, atm	$\Delta H^\circ$ , calories
2494	50.735	16.172	$1.24 \times 10^{-9}$	187,826
2523	50.793	16.254	$2.61 \times 10^{-9}$	186,218
2605	50.953	16.481	$6.04 \times 10^{-9}$	188,013
2748	51.222	16.865	$5.56 \times 10^{-8}$	185,622
2753	51.231	16.878	$3.93 \times 10^{-8}$	187,848
2879	51.458	17.203	$2.38 \times 10^{-7}$	185,860
2999	51.670	17.505	$7.37 \times 10^{-7}$	186,601
				Avg = 186,855 $\pm$ 1015 cal

entropy units, and this value was used in the computation of  $\left(\frac{F^o - H_o^o}{T}\right)_{c,l}$  above the melting point of rhenium ( $3170 \pm 60$  C). The heat capacity of liquid rhenium was assumed to be 10.8 cal/mole/C. To implement the calculations,

$$\Delta\left(\frac{F^o - H_o^o}{T}\right) = \left(\frac{F^o - H_o^o}{T}\right) - \left(\frac{F^o - H_o^o}{T}\right)_{c,l}$$

was expanded as a quadratic function of T above the melting point, i. e.,

$$\Delta\left(\frac{F^o - H_o^o}{T}\right) = -40.582 + 25.807 \times 10^{-4} T - 1.824 \times 10^{-7} T^2. \quad (5)$$

Using Equations 4 and 5, the values of Table 13 and Figure 17 were computed.

TABLE 13. THE VAPOR PRESSURE OF LIQUID RHENIUM

T, deg K	$\Delta\left(\frac{F^o - H_o^o}{T}\right)$	Vapor Pressure of Liquid Re, atm
3370(a)	-33.953	$2.01 \times 10^{-5}$
3500	-33.784	$5.09 \times 10^{-5}$
4000	-33.177	$1.08 \times 10^{-3}$
4500	-32.663	$1.14 \times 10^{-2}$
5000	-32.238	$7.44 \times 10^{-2}$
5500	-31.906	0.349
5900	-31.702	1.000

(a) The temperature used for the melting point of rhenium was 3100 C.

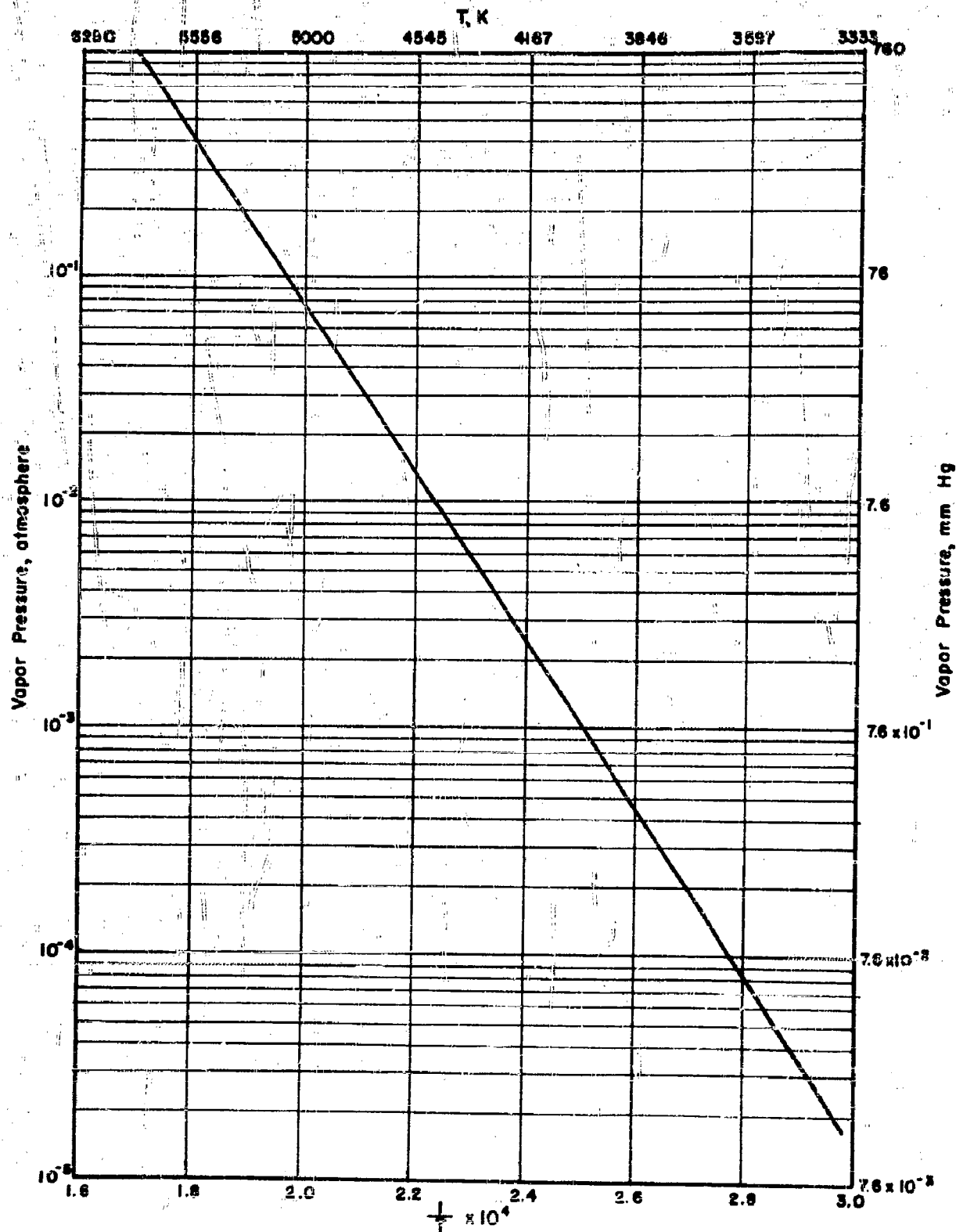


FIGURE 17. ESTIMATED VAPOR PRESSURE OF LIQUID RHENIUM AS A FUNCTION OF  $1/T$

## Electrical Resistivity

The literature lists two values for the electrical resistivity of rhenium. One of these, reported by Agte, et al. (3), is 21.1 ( $\pm 15$  per cent) microhm-centimeters, and the other, 18.9 microhm-centimeters (at 0 C) was found by Meissner and Voigt(15).

In the present work, the electrical resistivity of rhenium has been determined by two separate investigations at room temperature and by a single investigation at elevated temperatures. The effect of cold work on the resistivity has been determined also. Wide variations at room temperature were found, so the investigations are reported separately below, with a summary section following the discussion of each.

### Room-Temperature Resistivity (I) and the Effect of Cold Work on Resistivity

Approximately 40 resistivity determinations were made on rhenium of purity comparable to that listed in Table 1, Sample 12. The wire ranged from 8 to 18 inches long, 30 to 60 mils in diameter, and was in both the annealed and the cold-worked conditions. A Kelvin bridge located in a constant-temperature room was used to make the measurements. The resistivity was calculated by the equation:

$$\rho = \frac{RA}{\ell},$$

where

$\rho$  = resistivity, ohm-centimeters

R = resistance, ohms

A = cross-sectional area, cm<sup>2</sup>

$\ell$  = length, cm.

The results are plotted in Figure 18 as a function of cold work for each specimen measured. Considerable scatter is evident among both the annealed and the cold-worked values, although it is readily evident that the resistivity increases with increased cold work. These measurements were made at an average temperature of 25 C.

The room-temperature values have been averaged and reported in Table 14 as corrected to 20 C. For comparison, the values found by Agte and co-workers and by Meissner and Voigt are included.

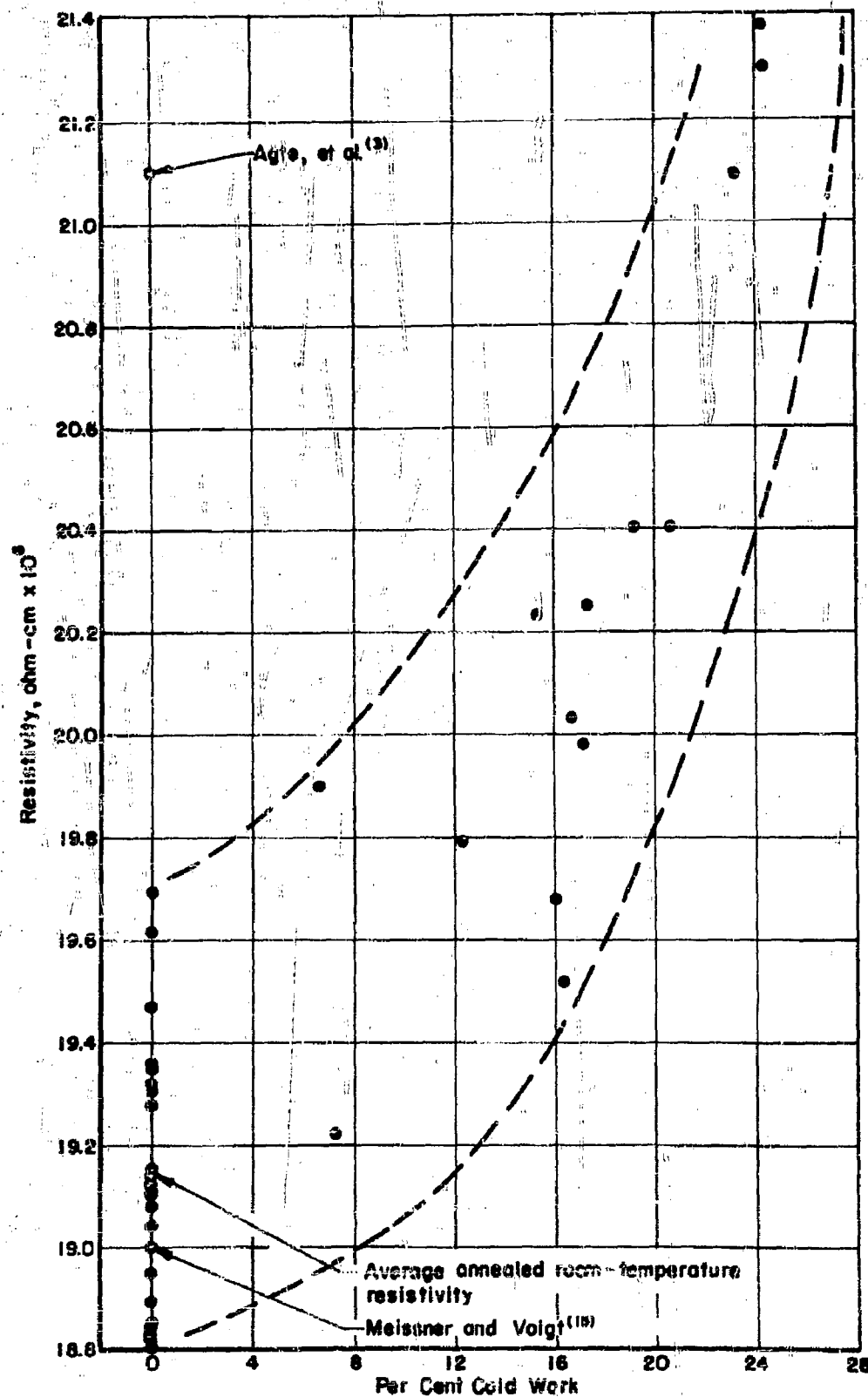


FIGURE 18. ROOM-TEMPERATURE RESISTIVITY AND THE EFFECT OF COLD WORK ON THE RESISTIVITY OF RHENIUM

A-8418



TABLE 14. RESISTIVITY OF ANNEALED RHENIUM AT 20 C  
BY DETERMINATION (I)

Resistivity, $\rho$ , ohm-cm $\times 10^6$	Investigator and Condition
18.79	Present work, lowest value
$19.14 \pm 0.25$	Present work, average value
$21.1 (\pm 15\%)$	Agte and co-workers <sup>(3)</sup>
19.0	Meissner and Voigt <sup>(15)</sup>

The results from Determination (I) indicate that Agte's values are somewhat too high, but the best data from the present work agree rather closely with the findings of Meissner and Voigt.

#### Room-Temperature Resistivity (II) and the Temperature Dependency of Resistivity

The resistivity of a sample of rhenium wire, which was drawn to a diameter of 0.0146 inch, was determined over a temperature range from room temperature to about 2500 K. Probes were attached to the wire to measure the voltage drop over a measured length of the center portion of the resistivity specimen. This test portion of the specimen was chosen far from the current leads in order to minimize errors arising from end-cooling effects. The specimen was placed in an evacuated and gettered glass tube to assure minimum contamination of the sample. The pressure in the test chamber was estimated to be less than  $10^{-8}$  mm of mercury. The measurements at room temperature were made in a constant-temperature room. The temperature of the specimen at higher temperatures was determined with an optical pyrometer, and was corrected for the spectral emissivity of rhenium. The resistivity measurements were made in steps for several temperature cycles from room temperature to the highest temperature and back to room temperature.

A total of 135 resistivity determinations, which are represented by the points in Figure 19, establish a curve for the dependency of resistivity on temperature. The resistivity of rhenium at a temperature of  $32.7 \pm 0.55$  C was found to be  $21.63 \pm 0.03$  microhm-centimeters, an average of 13 measurements of resistivity and temperature. When corrected to 20 C, which is normally taken as room temperature, the resistivity is 21.59 microhm-centimeters. The resistivity at other temperatures can be read directly from the temperature-resistivity curve.

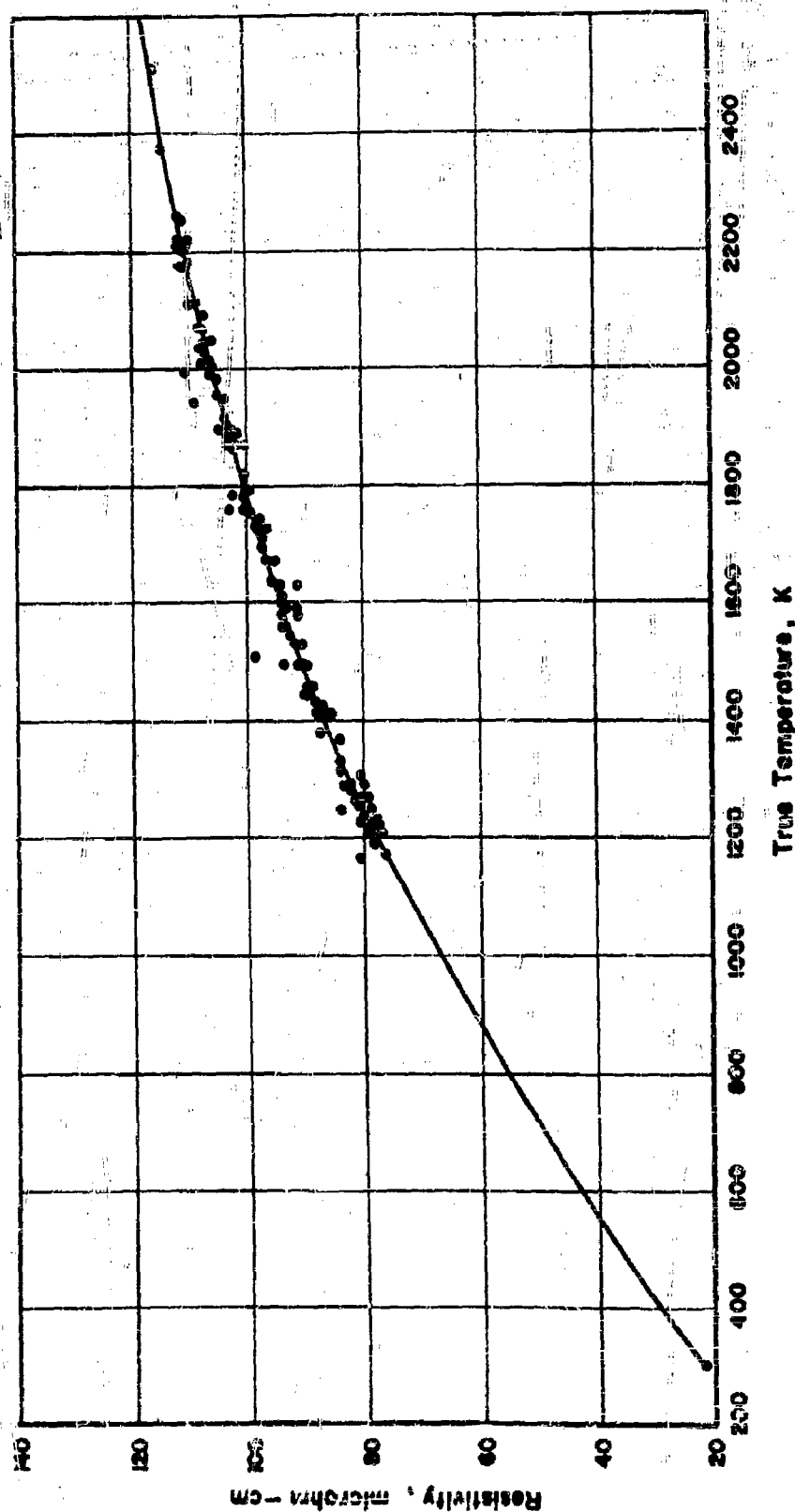


FIGURE 19. RHENIUM-RESISTIVITY CURVE AT ROOM AND ELEVATED TEMPERATURES

A-9696

The room-temperature value, 21.59 microhm-centimeters, agrees quite well with the value reported by Agte (see Table 14), but not with that reported by Meissner and Voigt.

#### Room-Temperature Resistivities: Summary

Two determinations of the room-temperature resistivity have been completed. They disagree by about 12 per cent, far too great a disagreement to allow averaging. All attempts to explain the difference have been fruitless; for instance, porosity might have caused the high value for Determination (II), but microinspection showed no porosity. Furthermore, all of these measurements were conducted on rhenium containing 0.15 to 0.20 per cent impurity, as opposed to the recently processed very high-purity metal of about 0.08 per cent impurity containing very little aluminum, magnesium, and calcium.

Accordingly, as soon as fine wire of the new high-purity material is available, a single section will be tested for resistivity values by the two methods described above; a single correct value for room-temperature resistivity will be obtained thus. In addition, a determination of the resistivity in the temperature range from 20 to 1200 C will be attempted.

#### Spectral Emissivity

Two methods were used to determine the spectral emissivity of rhenium: (1) the Prescott method<sup>(16)</sup> for low and intermediate temperatures; and (2) the bored-hole method<sup>(17)</sup> for very high temperatures.

#### The Prescott Method

Theory. In the Prescott method, the specimen is placed in an evacuated glass bulb inside a light-tight cylinder lined with a material of high reflectivity, so that the light in the cylinder reaches equilibrium with the emitter. White cotton velvet magnesium oxide is satisfactory for this application. The white velvet backwall of the enclosing cylinder was illuminated in the first measurements by six 32-candlepower automotive headlight bulbs, and in later measurements by a carbon arc. The emissivity of the specimen can be calculated from Wien's radiation law with accuracy sufficient for most purposes. The quantities measured are the optical temperature of the specimen, with and without illumination, and the optical temperature of the back-wall illuminated by the specimen and the auxiliary lamps. Then the spectral emissivity can be calculated from the formula:

$$e = 1 - \text{antilog}_{10} \left( \frac{-c \log_{10} e}{\lambda} \frac{T-S}{TS} \right) \\ - \text{antilog}_{10} \left( \frac{-c \log_{10} e}{\lambda} \frac{T-D}{TD} \right),$$

where

$c = 14330$  micron-degrees

$\lambda$  = wavelength, in microns, of light passed by pyrometer filter

$T$  = backwall brightness temperature

$S$  = brightness temperature of heated and illuminated specimen

$D$  = brightness temperature of heated specimen.

When spectral emissivities are determined by this method, there is an upper temperature limit imposed by the highest brightness temperature of the backwall of the lined, cylindrical enclosure. When the brightness temperature of the specimen approaches the brightness temperature of the backwall, the error becomes large and the method fails. One obvious solution to this problem is to increase the backwall illumination until sufficient illumination is present to give an accurate difference between these two temperatures.

**Measurements.** In the first experiment, the rhenium specimen was a polished, hollow cylinder, 0.134 inch in diameter and 0.4 inch in length, which had been ground from a solid rod of crystal-bar rhenium. The measurements were obtained in a dynamic vacuum system with a Distillation Products three-stage oil diffusion pump, a Welch Duo-Seal mechanical pump, and a liquid-nitrogen cold trap. The illumination was furnished by six 32-candlepower automotive lamps. The spectral emissivities that were obtained from measurements with this equipment are presented in Figure 20. The room-temperature point is an average value calculated from 19 determinations of the spectral emissivity. The probable error of the mean for this value is  $\pm 0.009$ .

For the second experiment, a new envelope was designed to obtain accurate measurements by the Prescott method at temperatures above 1000 C. A 0.015-mil rhenium wire was used for the measurements above 1000 C. Probe wires were attached to this specimen for the purpose of measuring the potential drop across a known length of the wire. With this arrangement, the resistivity and the emissivity could be measured at the same time. The tube containing the rhenium specimen was sealed off from the vacuum system, so that the Prescott apparatus could be moved to an arc light to gain more intense backwall illumination. In the measurements, a

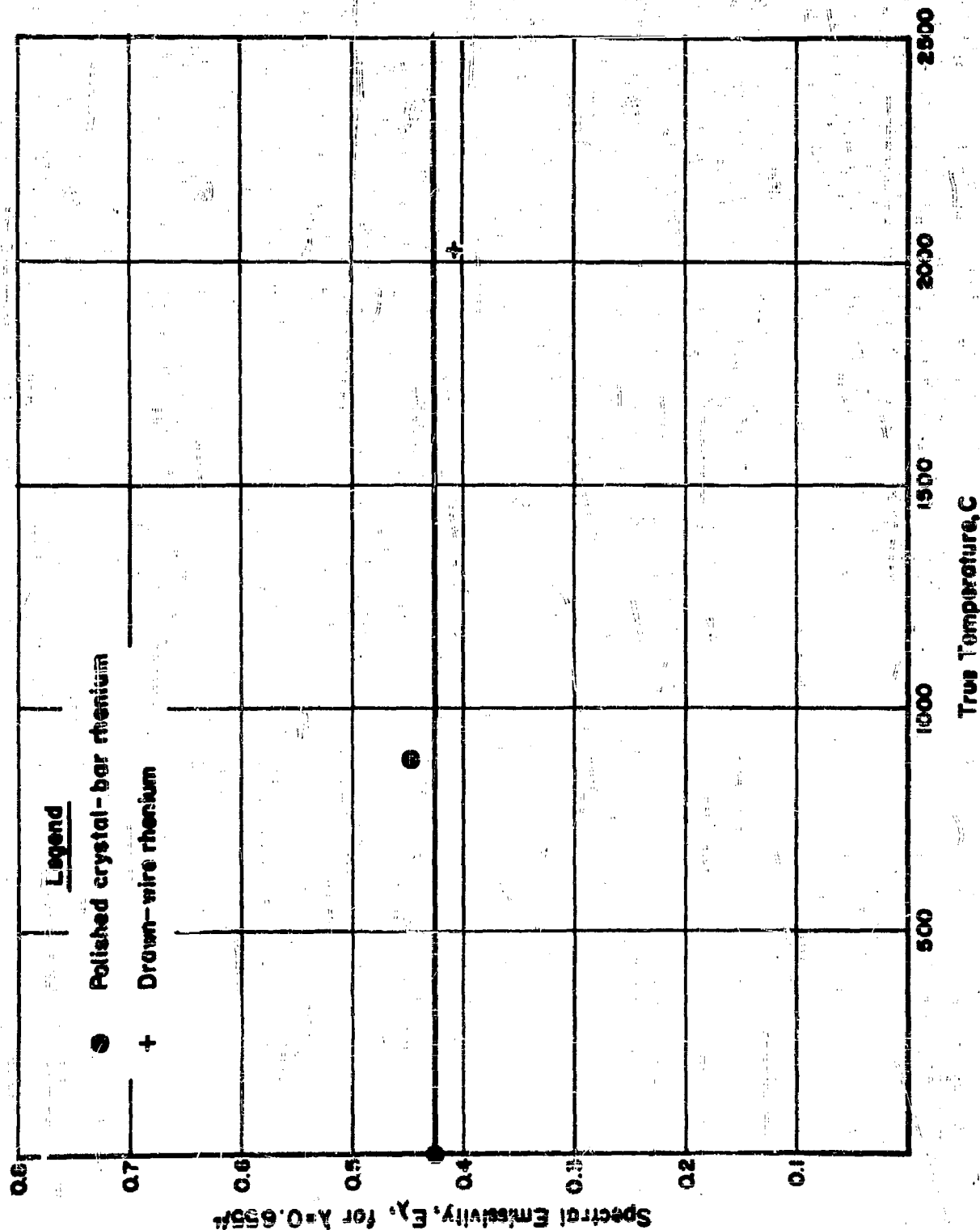


FIGURE 20. SPECTRAL EMISSIVITY OF RHENIUM BY PRESCOTT METHOD

A-11720

monochromator received some of the light from the arc, and the light intensity near 0.655 micron was monitored and was the same for each reading. With this apparatus the emissivity was found to be 0.416 at a temperature of 2030 C.

### The Bored-Hole Method

During sintering and melting-point studies, the spectral emissivity of rhenium from about 1300 C to 3000 C was determined. This was accomplished simply by recording the black-body hole temperature in a heated bar and also recording the corresponding brightness (surface) temperature of the bar under equilibrium conditions. The emissivity was calculated for each point by means of the relationship<sup>(18)</sup>:

$$\frac{1}{T} - \frac{1}{T'} = \frac{\lambda}{C} \ln E_{\lambda} ,$$

where

$T$  = black-body temperature, K,

$T'$  = brightness temperature, K (surface temperature)

$\lambda$  = 0.655, the wavelength

$C$  = 14,362, a constant

$E_{\lambda}$  = spectral emissivity.

A plot of the variation of spectral emissivity,  $E_{\lambda}$ , with black-body temperature is shown in Figure 21. Included on the plot are the emissivity constants found by Levi and Espersen<sup>(19)</sup>, who found 0.366 at an unspecified but elevated temperature. This value checks well with the present high-temperature values, and is plotted at 2800 C for information purposes. In addition, Becker and Moers<sup>(20)</sup> reported a value of  $E_{\lambda} = 0.42$ , which agrees well with the recent data at about 1400 C, although these authors also specified no temperature.

Following calculation of the emissivity for each experimental point, data were taken from the average curve of  $E_{\lambda}$  versus  $T$  (Figure 21) and plotted as  $T'$  versus  $T$  to give a curve of black-body temperature versus brightness temperature. This is shown in Figure 22, and is more practical for everyday usage.

### Combined Results

$E_{\lambda}$  versus the true temperature has been plotted in Figure 23 for the data from both the Prescott and the bored-hole determinations. Even though the bored-hole method fails at lower temperatures (about 1200 C) in the

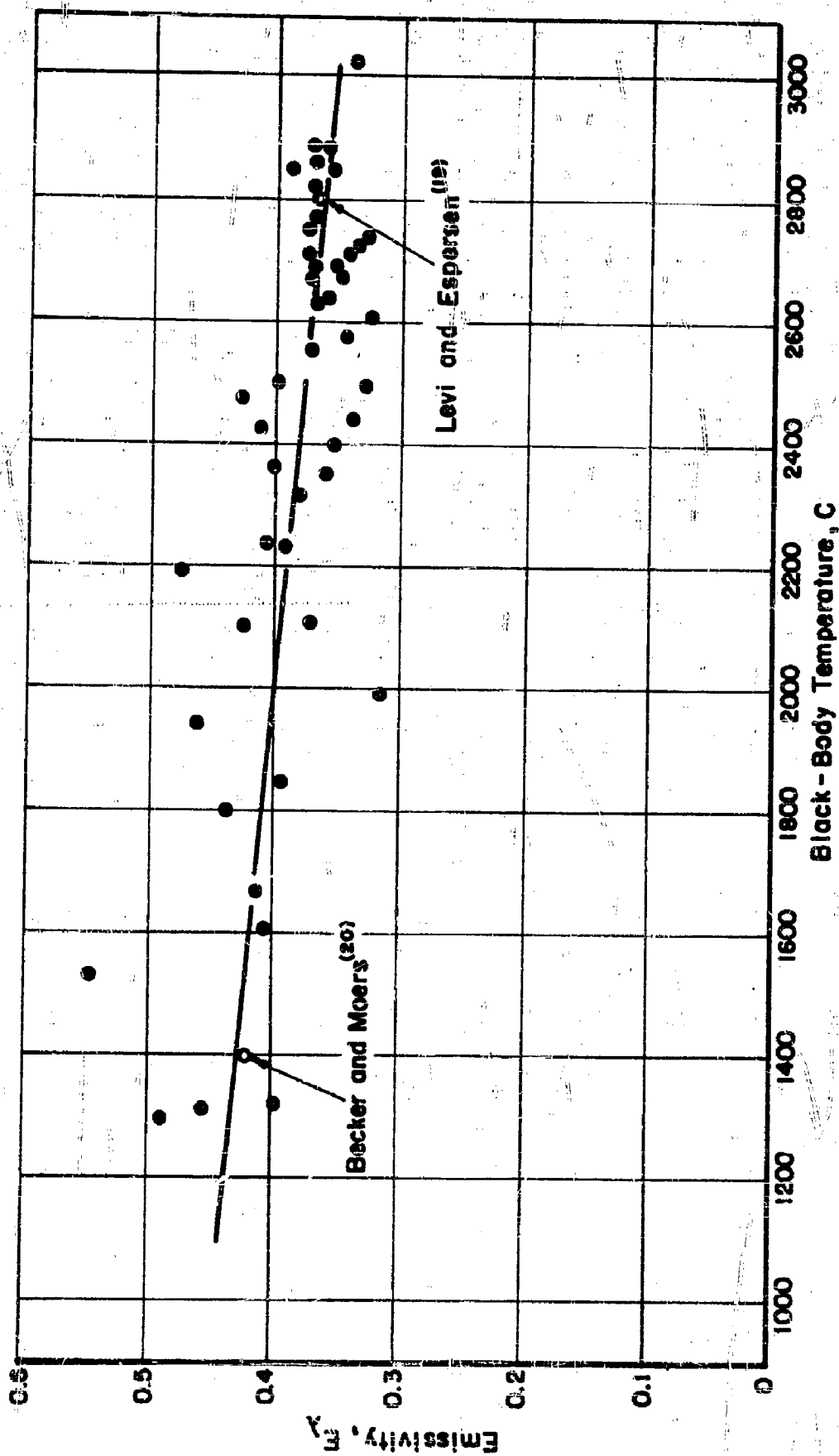


FIGURE 21. SPECTRAL EMISSIVITY OF SINTERED RHENIUM AT 0.655 MICRON

A-8419

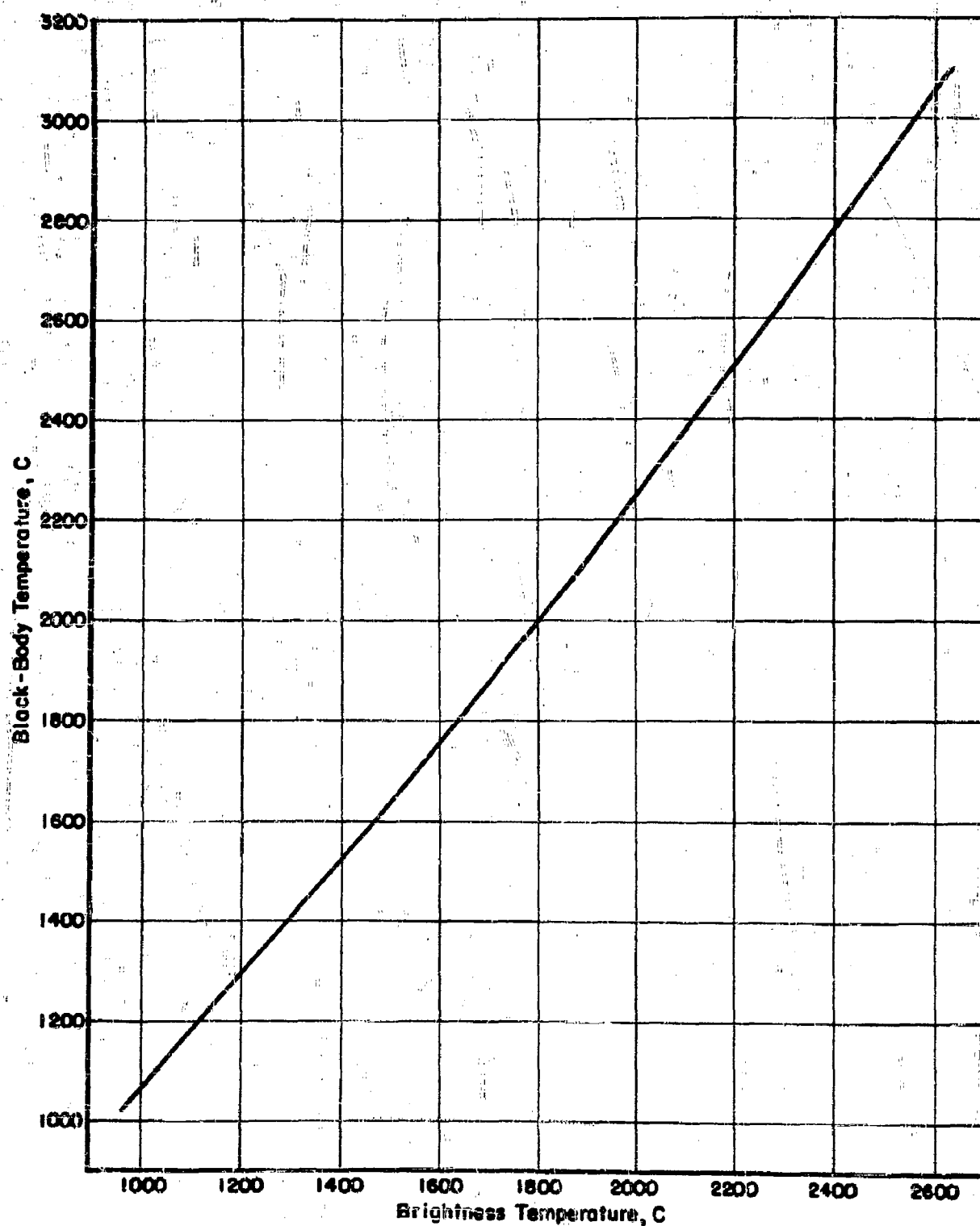


FIGURE 22. BLACK-BODY VERSUS BRIGHTNESS TEMPERATURE FOR SINTERED RHENIUM BARS

A-8420



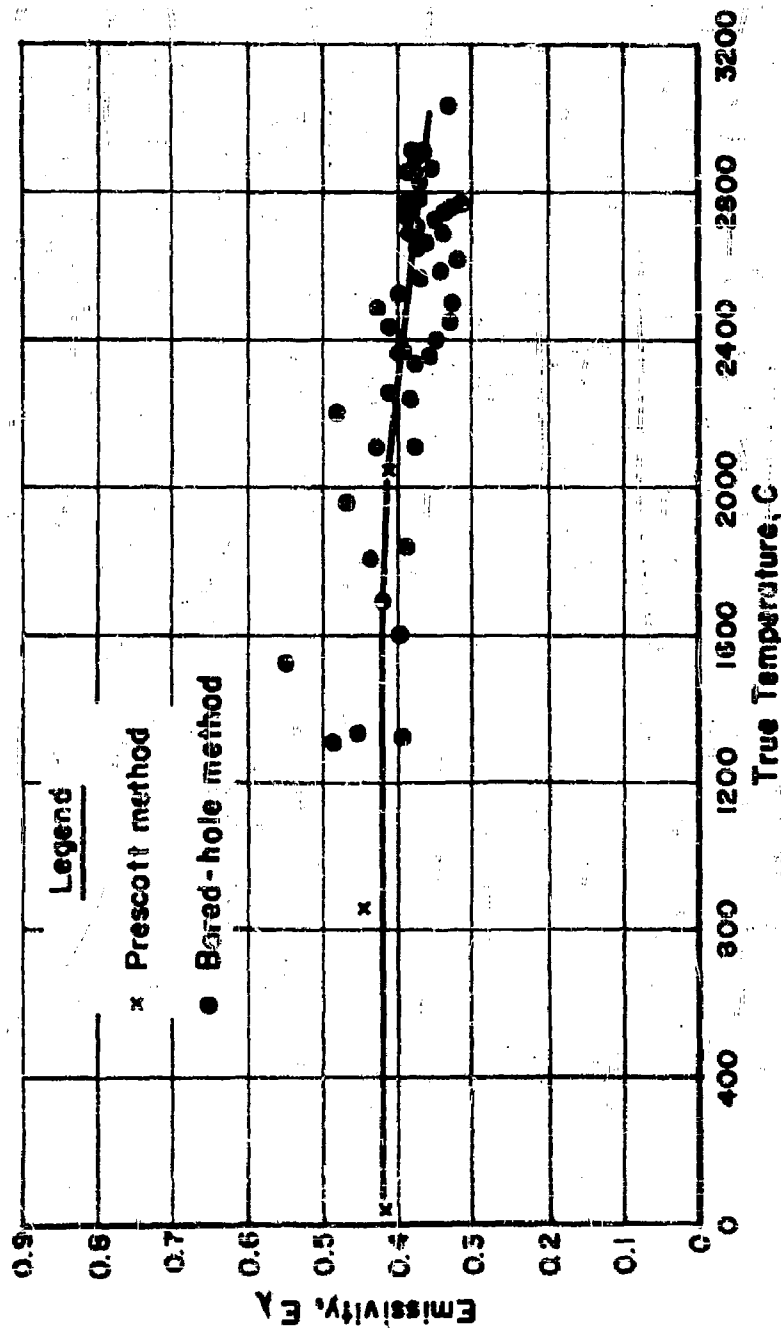


FIGURE 23. COMBINED DATA ILLUSTRATING THE SPECTRAL EMISSIVITY OF RHENIUM METAL AT 0.655 MICRON

A-11721

range where it applies, the Prescott method can be relied upon around these temperatures. Thus, the combined plot covers the complete temperature range from room temperature to 3000 C with a fair degree of reliability. The results indicate a slight drop of the emissivity with increasing temperature from about 0.42 at room temperature to about 0.36 at 3000 C. This is in opposition to the results obtained by Stephens<sup>(21)</sup>, which indicated a slight increase in emissivity is to be expected with an increase in temperature.

### Thermal Expansion

One determination of the thermal expansion of rhenium by X-ray methods was made by Agte, et al.<sup>(3)</sup>. The values were determined from data taken at room temperature and at 1917 C, and are as follows:

$$\beta [001] = 12.45 \times 10^{-6} \text{ per C} \pm 3\%$$

$$\beta [100] = 4.67 \times 10^{-6} \text{ per C} \pm 8\%$$

The c-axis expansion was 2.6 times the a-axis expansion; the authors claimed no variation with temperature.

The linear-thermal-expansion coefficients have been determined recently for a 150-mil rod 3 inches long. The measurements, taken on a recording dilatometer over a temperature range from 20 to 1000 C, show a slight increase in expansivity with temperature. The results are presented in Table 15, and compared therein with those for tungsten<sup>(1)</sup> for the 20 to 500 C range.

### MECHANICAL PROPERTIES

The literature shows virtually no data on the mechanical properties of rhenium. This is despite the fact that rhenium's position in the periodic system and a few pieces of extant data indicate that its mechanical properties might be quite interesting. Recent measurements have shown that rhenium is amazingly strong and is also ductile at room temperature and is not embrittled by recrystallization. Tungsten, for instance, is not ductile in the massive state at room temperature.

Since mechanical-property measurements were also made on thoriated rhenium, the following work is recorded under two headings, "Pure Rhenium" and "Thoriated Rhenium".

TABLE 15. LINEAR THERMAL EXPANSION FOR PURE RHENIUM

Temperature Range, C	Coefficient, $(1/C) \times 10^{-6}$
20-100	6.6
20-200	6.6
20-300	6.6
20-400	6.6
20-500	6.7
20-600	6.7
20-700	6.7
20-800	6.8
20-900	6.8
20-1000	6.9
20-500 (Tungsten)	4.45

#### Pure Rhenium

#### Modulus of Elasticity

Young's modulus of elasticity had never been determined for rhenium. Köster<sup>(22)</sup>, however, estimated this modulus to be about  $73 \times 10^6$  psi.

A total of six determinations has been made on three separate test specimens in the present work. Four of these measurements were on one of the specimens. In each case, the material used was 150-mil swaged rod about 5 inches long. A standard 1/8-inch-diameter round tensile section was ground in the center of each rod; the specimens were annealed, and two Type A-7 strain gages applied to measure the elongation. Curves of load versus elongation were plotted from the average strain readings of the two gages as the specimens were loaded and unloaded within the elastic limit. The modulus values were all calculated from the return, or unloading, curve, since any adjustment of the specimen in the grips would have occurred during loading, and any other error could only have made the modulus values lower.

The average of the six determinations, each reported in Table 16, was  $66.7 (\pm 2.9) \times 10^6$  psi. This is lower than Köster's estimation, but is possibly one of the highest modulus determinations ever measured. The value falls between those of tungsten and osmium, as would be expected from the periodic table, and is the third highest among the metals (see Table 17 and Figure 24).

TABLE 16. MODULI OF ELASTICITY FOR THREE ANNEALED RHENIUM SPECIMENS

Specimen	Modulus of Elasticity, psi
25	$72.6 \times 10^6$
28	$65.8 \times 10^6$
27, Determination 1	$64.9 \times 10^6$
27, Determination 2	$66.4 \times 10^6$
27, Determination 3	$64.6 \times 10^6$
27, Determination 4	$67.1 \times 10^6$
Average of six determinations $66.7 (\pm 2.9) \times 10^6$	

TABLE 17. MODULI OF ELASTICITY OF RHENIUM AND SEVERAL OTHER METALS

Metal	Modulus of Elasticity, psi
Osmium (9) (22)	$81 \times 10^6$
Iridium (22)	$76 \times 10^6$
Rhenium	$67 \times 10^6$
Ruthenium (8)	$60 \times 10^6$
Tungsten (1)	$51 \times 10^6$
Molybdenum (23)	$47 \times 10^6$

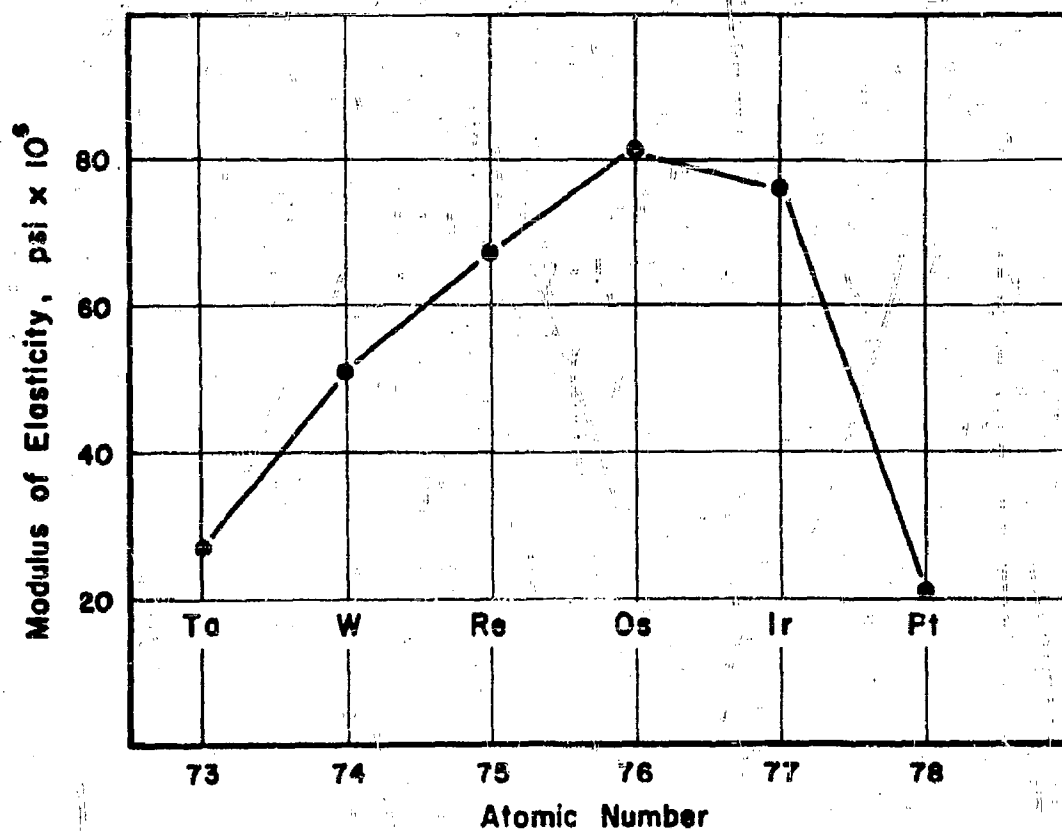


FIGURE 24. RELATIONSHIP BETWEEN THE POSITION OF CERTAIN METALS IN THE PERIODIC SYSTEM AND THEIR TENSION MODULUS OF ELASTICITY

A-9699

## Tensile Strength and Ductility

Room-Temperature Tensile Tests. Very little information on this subject is available from the literature. Agte<sup>(3)</sup> and his co-workers reported on the ultimate tensile strength and elongation of an 0.25-mm-diameter halide-process vapor-deposited rhenium wire with an 0.03-mm tungsten core wire. Their results attributed a tensile strength of about 70,000 psi with an elongation of 24 per cent to this specimen. The present work has borne out Agte's findings in the sense that agreeing values have been found for crystal-bar tensile strength.

A 1/8-inch-diameter reduced section was ground into the center of a length of crystal bar for tension testing. A strength of 75,000 psi was found, but the elongation was only 3 per cent. These results, combined with metallographic work (see Figure 3) and in the light of recent values found for sintered and cold-worked rhenium, indicate that crystal-bar rhenium represents a conglomeration of loosely adherent crystals attached to a tungsten wire more than sound, well-knit metal. The tensile tests on this type of rhenium do not present a true picture of very high tensile strength of annealed rhenium.

Three separate tensile tests have been conducted on round swaged rhenium rod prepared by powder-metallurgy techniques. Each rod was about 150 mils in diameter and 5 inches long; each had a standard 1/8-inch-diameter reduced section ground into the center (these were the same specimens as those on which modulus determinations were made previously). Special grips were constructed to hold the ends of the rods. After measurement of the elasticity modulus, one of the two A-7 strain gages was removed and a specially constructed extensometer for use with small specimens of this type was applied. Strain was recorded by use of the remaining A-7 gage and the extensometer.

Plots of the load versus elongation within the limits of the strain gages were obtained, and, from these, the proportional limit and the 0.1 and 0.2 per cent offset yield strengths were recorded. These values are shown in Table 18, which also includes the measured values of ultimate tensile strength, elongation, and reduction of area.

It can be seen that the annealed rhenium rod possesses a tensile strength of about 165,000 psi, combined with excellent ductility, more than double the values found for crystal bar. The tensile strength of annealed rhenium is much higher than that of annealed molybdenum wire (about 70,000 psi)<sup>(23)</sup> and higher than that of annealed tungsten wire (about 110,000 psi)<sup>(24)</sup>. The yield strengths are rather low, but the large spread between them and the relatively high ultimate tensile strength reflects the very high work-hardening properties of rhenium. Rhenium also possesses an appreciable room-temperature ductility (about 25 per cent), whereas tungsten, for instance, possesses little or none.

TABLE 18. TENSILE AND ELONGATION DATA FOR PURE ANNEALED RHENIUM

Standard ASTM 1/8-Inch-Diameter Reduced Section, 1/2-Inch Gage Length

	Specimen 25	Specimen 27	Specimen 28	Average Value for Specimens 25, 27, and 28
Proportional Limit, psi	35,100	26,800	18,100	26,300
0.1 Per Cent Offset Yield Strength, psi	50,600	44,000	31,500	42,000
0.2 Per Cent Offset Yield Strength, psi	55,200	49,500	35,000	46,000
Ultimate Tensile Strength, psi	168,000	164,000	161,000	164,000
Elongation in 1/2-Inch, per cent	24.6	22.0	25.4(a)	24
Reduction of Area, per cent	24.1	20.1	21.1	21.7
True Stress at Unit Strain, $E$ , psi	360,000	370,000	370,000	367,000
Strain-Hardening Exponent, $n$	0.328	0.360	0.372	0.353

(a) Broke outside punch marks.

The true stress,  $\sigma$ , and true strain,  $\delta$ , were calculated for a number of points from the extensometer and load readings and plotted in Figure 25 for each specimen. These functions are related by the flow equation:

$$\sigma = \beta \delta^n$$

where

$\beta$  = the strain coefficient, the true stress at unit strain

$n$  = the strain-hardening exponent.

These constants are also included in Table 18, and were taken from Figure 25.  $\beta$  was read from the intercept of the true stress-strain curves at  $\delta = 1.0$ , and  $n$  was measured from the limiting slope of the curves.

Figure 26 shows the average of the three rhenium curves of Figure 25 as one plot, and compares it with those for molybdenum<sup>(25)</sup>, nickel<sup>(26)</sup>, and copper<sup>(26)</sup>. It will be noticed that rhenium possesses a strain-hardening exponent similar to those for nickel and copper (as the slopes are similar), but the initial strength of rhenium is of the same order of magnitude as that of molybdenum. The combination of this high initial strength and the high strain-hardening rate produce  $\beta$ -values of nearly 400,000 psi. It is possible that no other metal possesses such a high combination of tensile strength, work-strengthening properties, and ductility as found in rhenium.

In addition to these room-temperature tensile tests on pure massive rhenium, a tensile test has been completed on a 9.5-mil-diameter wire prepared by swaging, Turk's head drawing, and wire drawing of a sintered-type rod. The ultimate tensile strength in the annealed condition was 174,000 psi, which agrees with results reported below for 54-mil wire at room temperature. The elongation was 12 per cent, which is only half the value found for more massive rod, but which agrees with the wire tensile tests reported below.

Elevated-Temperature Tensile Tests. Many of the proposed uses for rhenium are in the elevated-temperature field, particularly from the standpoint of its potentiality as an electronic tube material. Thus, a survey of the high-temperature strength properties of rhenium is essential.

Results to date have been obtained from tensile tests conducted at room temperature and 500, 1000, 1500, and 2000 C on annealed and 9 and 15 per cent cold-worked rhenium wire. The wire ranged in diameter from 48 to about 64 mils; the cold-worked specimens were prepared by wire drawing for the 9 per cent reduced stock and wire drawing combined with swaging for the 15 per cent reduced stock. The specimens were 4 to 5 inches long.

The test apparatus had two basic requirements: (1) the specimens were to be broken in tension at an elevated temperature; and (2) the



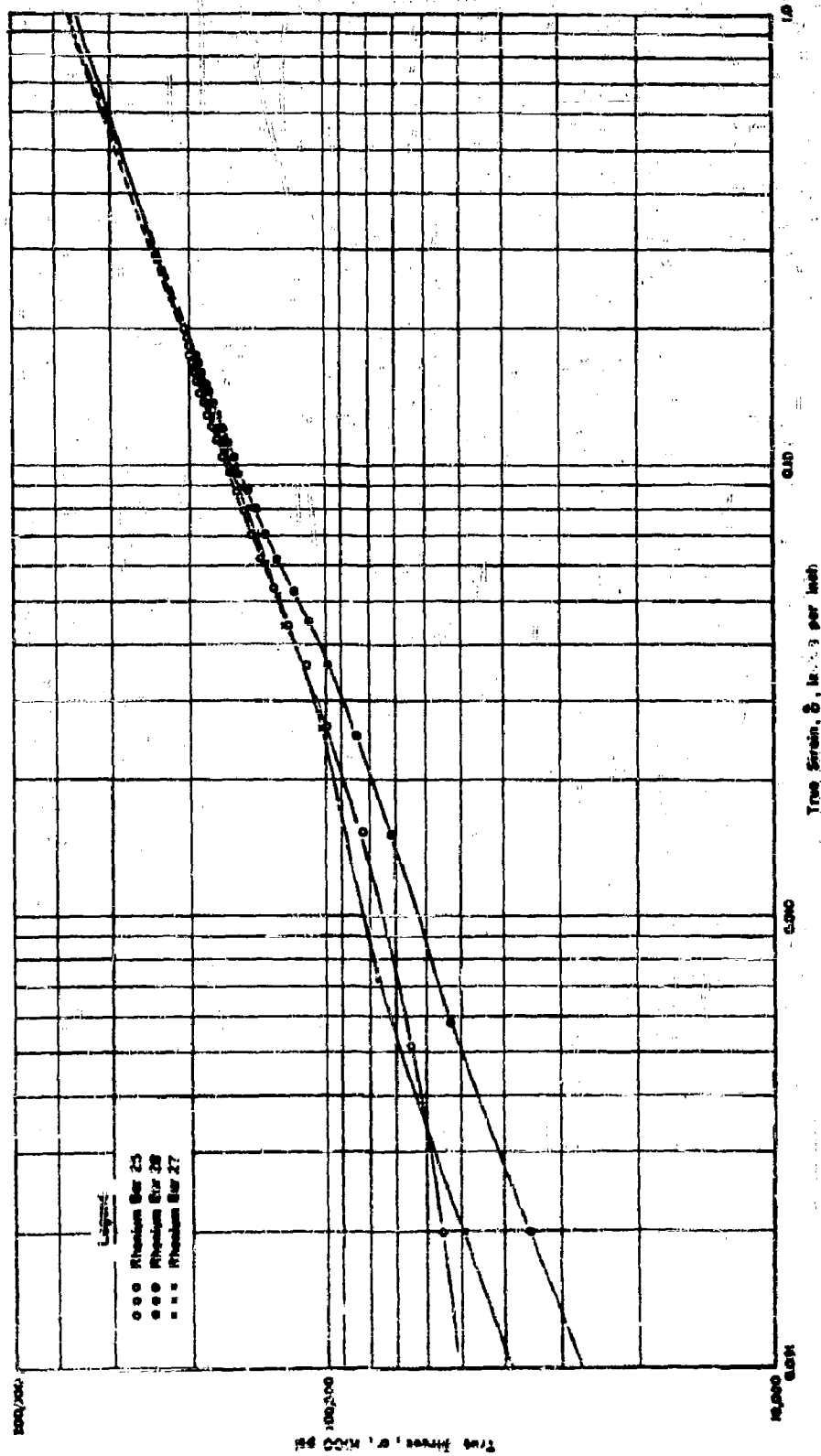


FIGURE 25. TRUE STRESS - STRAIN DIAGRAM FOR THREE PURE RHENIUM SPECIMENS C-3701

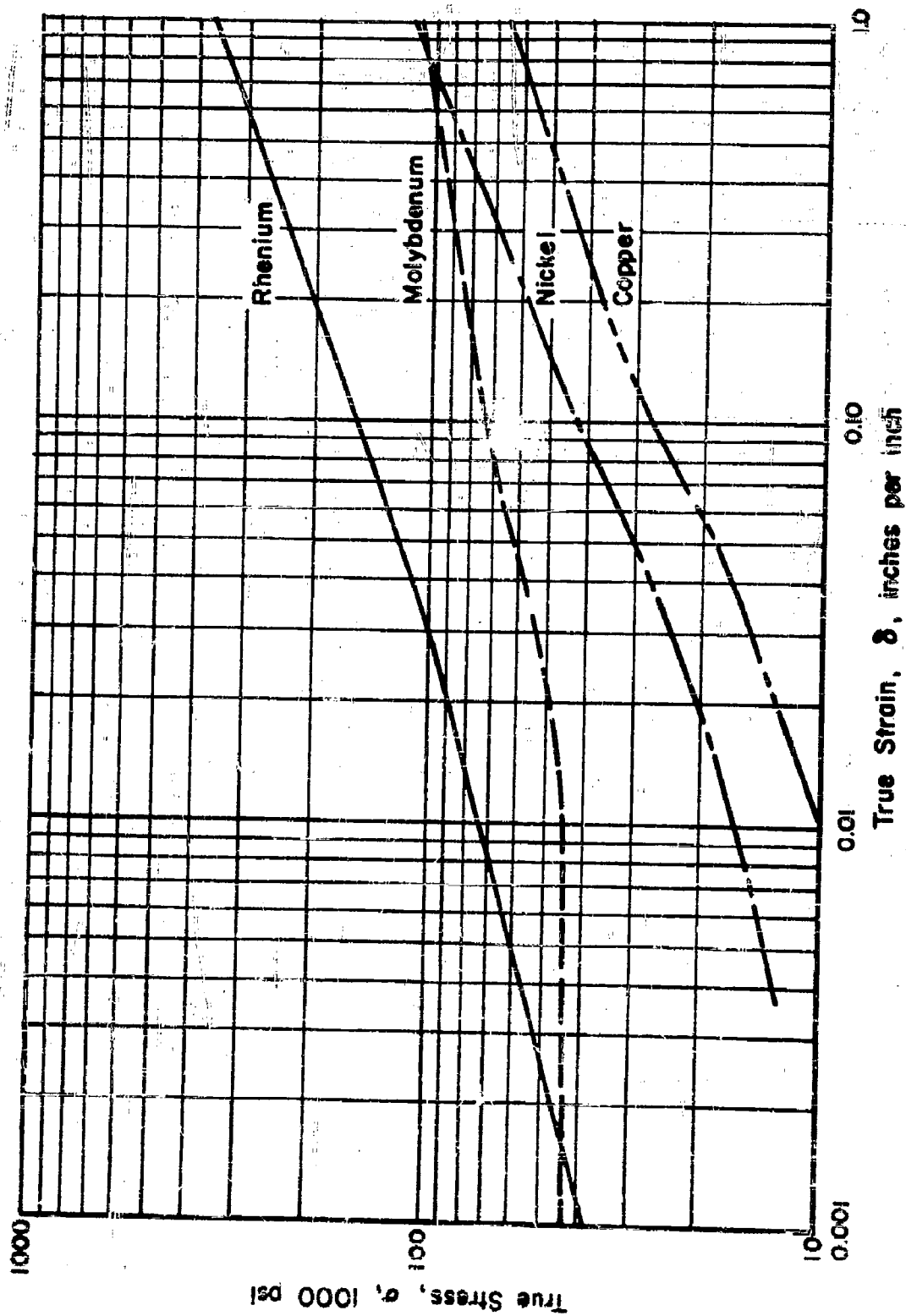


FIGURE 26. AVERAGE TRUE STRESS-STRAIN DIAGRAM FOR RHENIUM AND OTHER METALS (25, 30)

A-10133

specimen has to be protected from air when heated above 600 C to prevent oxidation. To accomplish this, special screw-tightening grips were constructed to grasp the small-diameter wire. These were mounted on rods that were attached to an Amsler 1000-pound universal testing machine; one of the rods was electrically insulated from the Amsler machine. Electrical connections were attached and the entire apparatus enclosed in a gas-tight Pyrex tube mechanism, as illustrated in Figure 27. The apparatus was designed with flexible seals so as not to affect load readings when the wire was stressed. Dry helium was passed through the protection chamber to prevent oxidation. The rhenium wire was heated to test temperature by self-resistance and the temperature read by an optical pyrometer through a hole in an asbestos shield that surrounded the Pyrex tube, thus providing some measure of thermal insulation.

The results are recorded in Table 19 and plotted in Figure 28. The room-temperature ultimate tensile strength of annealed rhenium wire is essentially that reported earlier for stock of more massive cross-sectional area. Increasing amounts of cold work raise the strength significantly; wire reduced only 15 per cent by cold work has a tensile strength of nearly 340,000 psi. With increasing temperature, the tensile strength drops off rather rapidly, as it does for most metals. At 1500 C, recrystallization has proceeded with sufficient rapidity to eliminate any strengthening effect from initial cold work, and all types of wire have a tensile strength of about 40,000 psi.

High-temperature ductility, however, is not good. As can be seen in Table 19, both elongation and reduction of area drop to values of about 1 or 2 per cent above 500 C. The only difference between the present room-temperature test results and earlier ones occurs in the data for annealed rhenium wire; previous elongation averaged about 24 per cent for massive rod specimens, but for wire it is about 10 to 12 per cent.

Figure 29 compares the tensile and elongation data for 15 per cent cold-worked rhenium with data on wrought tungsten and molybdenum, as reported by Kiefer and Hotop(24). Despite the fact that the rhenium is about 54 mils in diameter and the other metals 24 mils, the data are probably quite comparative. The rhenium tested was not fully wrought (15 per cent cold work will not rid rhenium entirely of a recrystallized structure), but, nevertheless, it appeared stronger than tungsten and molybdenum at temperatures below 1300 to 1400 C. In this range, and above, recrystallization tends to equalize the strength characteristics.

In the matter of high-temperature ductility, rhenium is inferior to both tungsten and molybdenum. Although tungsten, particularly, tends to be brittle at room temperature, it becomes quite ductile at elevated temperatures. Conversely, rhenium is ductile at room temperature and becomes brittle at high temperature. This may be caused by the hot shortness observed during hot-working attempts, but it also may be, in part, an effect of the impurity content, which is discussed in detail below. If the latter

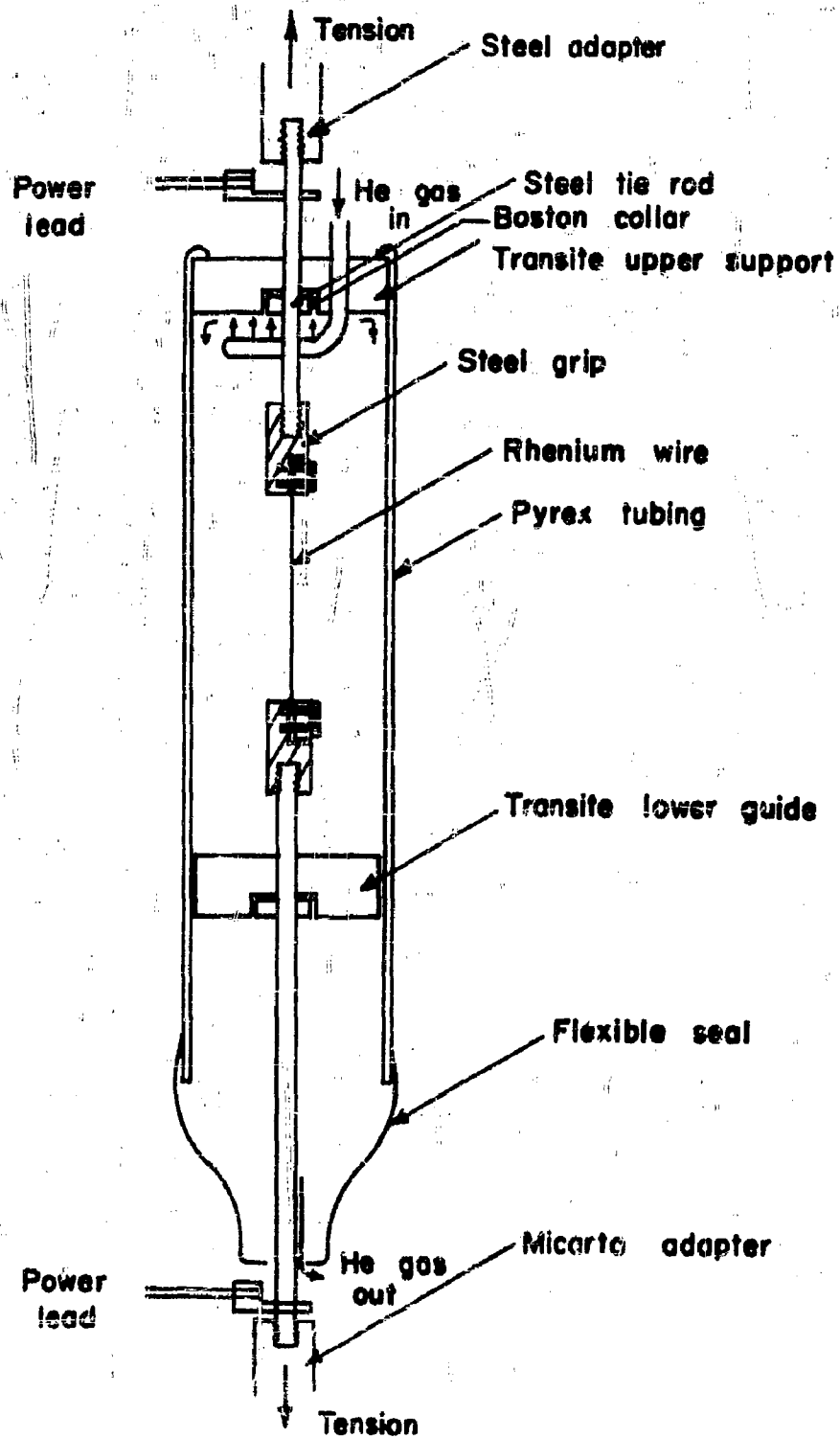


FIGURE 27. APPARATUS FOR ELEVATED-TEMPERATURE TENSILE TESTING OF RHENIUM UNDER CONTROLLED ATMOSPHERE

A-10825

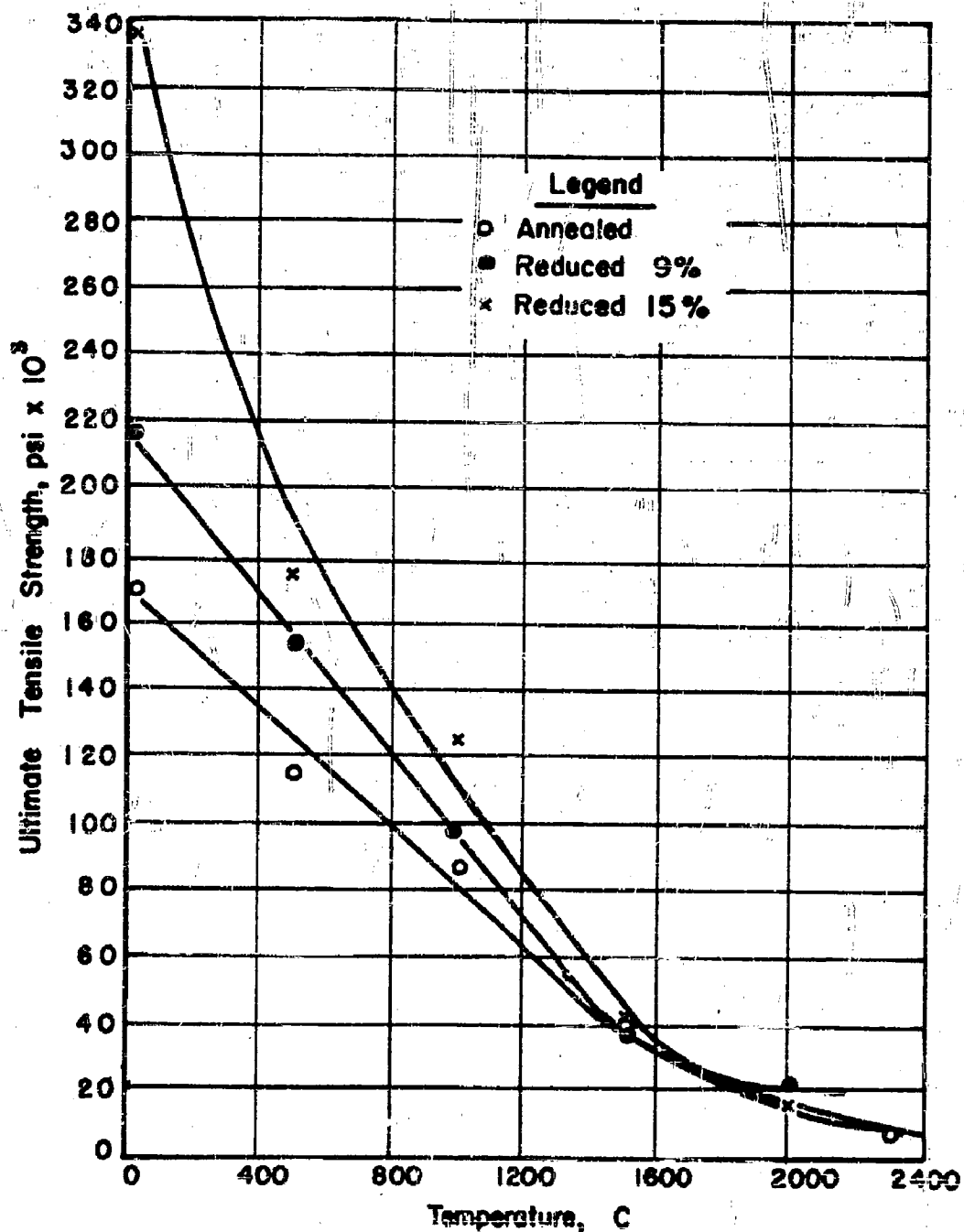


FIGURE 28. ULTIMATE TENSILE STRENGTH OF ANNEALED AND COLD-WORKED 0.050 TO 0.065-INCH-DIAMETER RHENIUM WIRE AT ELEVATED TEMPERATURES

A-10876

TABLE 19. ROOM- AND ELEVATED-TEMPERATURE STRENGTHS OF ANNEALED AND COLD-WORKED RHENIUM WIRE

Testing Temperature, C	Annealed			Reduced 9 Per Cent			Reduced 15 Per Cent		
	Ultimate Tensile Strength, psi x 10 <sup>3</sup>	Elongation, per cent in 3 in.	Reduction of Area, per cent	Ultimate Tensile Strength, psi x 10 <sup>3</sup>	Elongation, per cent in 3 in.	Reduction of Area, per cent	Ultimate Tensile Strength, psi x 10 <sup>3</sup>	Elongation, per cent in 3 in.	Reduction of Area, per cent
Room Temperature	170	9.6	16	216	7.7	6	337	-(a)	1
500	114	10.7	19	152	6.6	9	174	1.0	1
1000	85	1.7	2	98	2.2	2	124	1.0	1
1500	38	1.7	2	37	1.9	2	40	1.2	1
2000	--	--	--	22	2.4	2	16	1.2	1
2300	77	2.0	2	--	--	--	--	--	--

(a) Not available because of grip slippage. Value is estimated to be between 5 and 10 per cent from incomplete data.

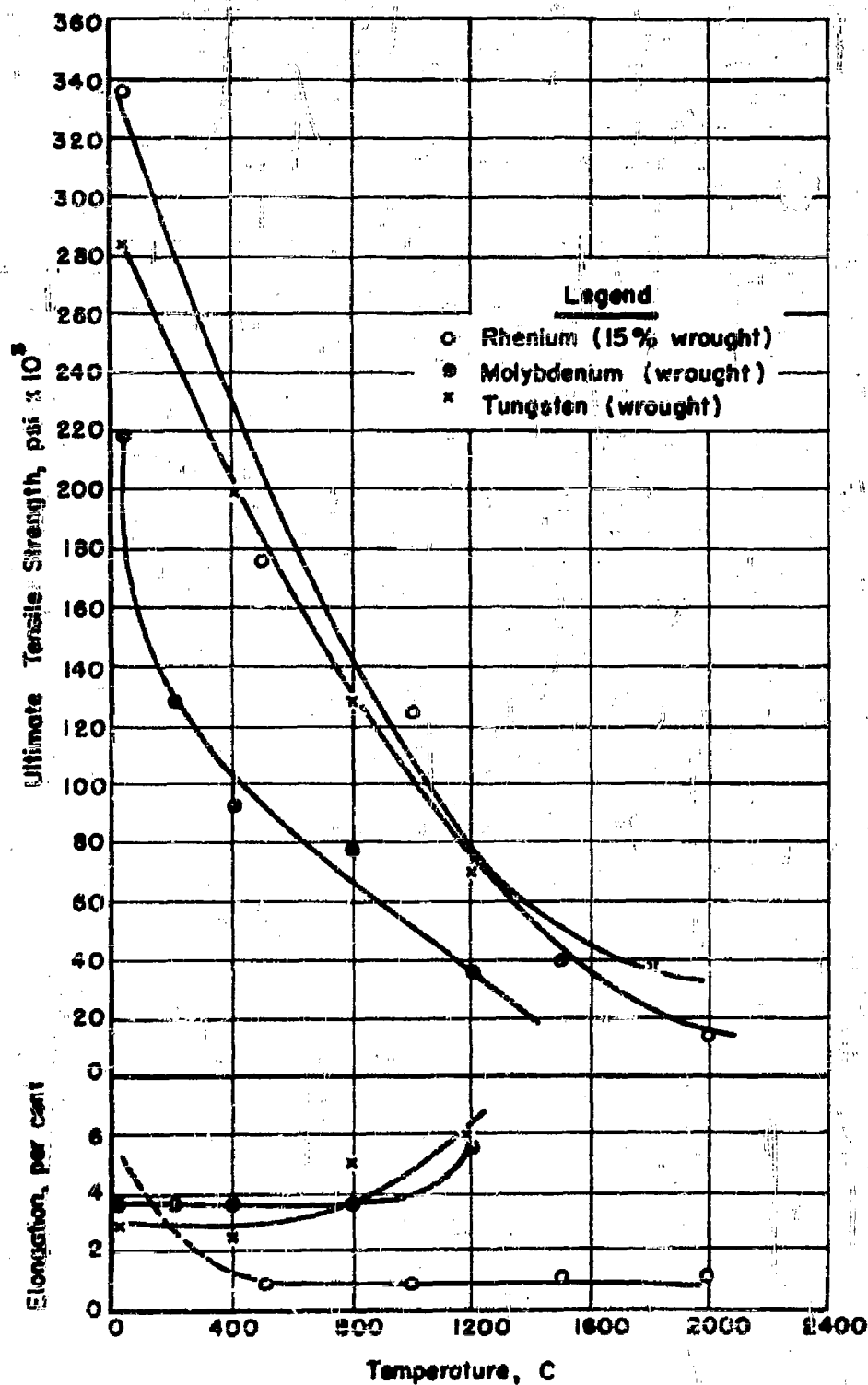


FIGURE 29. COMPARISON OF THE ELEVATED-TEMPERATURE TENSILE PROPERTIES OF WROUGHT RHENIUM (15% REDUCED), MOLYBDENUM<sup>(24)</sup>, AND TUNGSTEN<sup>(24)</sup>

is the case, the very pure rhenium now being prepared may exhibit more favorable high-temperature ductility.

### Annealed Hardnesses

The annealed hardnesses of various types of rhenium vary considerably from one type of metal to another. Figure 30 illustrates the three types of consolidated metal; hot-wire-deposited rhenium, arc-melted rhenium, and sintered rhenium. As can be seen, the hardness of unworked arc-melted metal is lowest, about 135 VHN. Crystal bar is also quite soft, and shows a hardness of 160 VHN. Both of these types of metal are quite large grained, compared with annealed rhenium fabricated from pressed and sintered metal powder, which has a hardness of about 270 VHN. Grain size is probably the controlling factor, as the sintered material has a grain size considerably finer than those of the other materials.

### Work Hardening and Recrystallization

The literature to date has shed little light on the work hardenability of rhenium, except for Winkler's<sup>(27)</sup> statement that annealed rhenium work hardens from 247 VHN to 637 VHN when cold worked. This indication of extensive work hardening has been more than borne out by the current studies.

In general, the experimentation consisted of cold swaging rhenium to various reductions, then heating specimens of each reduction in hydrogen at various temperatures. By taking hardness measurements and photomicrographs at each step, the work-hardening characteristics and recrystallization behavior were readily determined.

Specifically, a specimen of 150-mil swaged rod was annealed a number of hours to make certain it was fully annealed. Its structure is shown in Figure 31a. The rod was then reduced 10 per cent in cross-sectional area by swaging, and a number of small specimens removed. Next, the rod was reduced an additional 10 per cent to a total of 20 per cent reduction, and more specimens removed. This cycle was continued until 40 per cent reduction was reached, at which stage the rod commenced to crack and break. The structure of 40 per cent cold-worked rhenium is shown in Figure 31b. A specimen of each percentage reduction was then heated for an hour under hydrogen at temperatures from 700 to 2100 C, so as to study softening, recrystallization, and grain growth (as reported below).

Cold working of the rhenium produced very high increases in hardness. Figure 32 shows a comparison of rhenium with nickel<sup>(8)</sup>, a metal that also work hardens greatly. It is obvious that nickel is not in the same range as rhenium, the latter metal tripling its annealed value to over 800 VHN with only 30 per cent reduction. In all probability, rhenium work hardens more

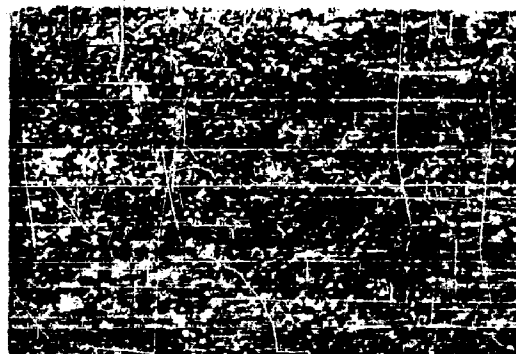




a. Hot-Wire Deposited Rhenium, Near Center of Bar;  
VHN = 166  
(Average grain size = 0.06 mm)

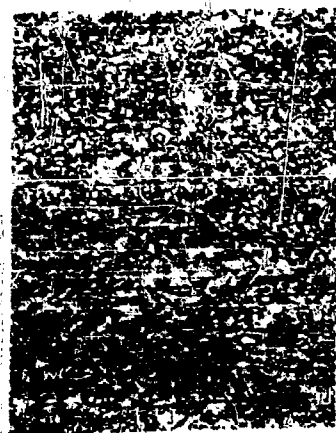


b. Rhenium Arc Melted From Cut Crystal Bar;  
VHN = 135  
(Average grain size = 3 mm)



c. Annealed Rhenium From Compacted, Sintered, and Swaged Metal Powder;  
VHN = 270  
(Average grain size = 0.004 mm)

FIGURE 30. HARDNESS AND GRAIN STRUCTURES OF HOT-WIRE-DEPOSITED, ARC-MELTED, AND POWDER-METALLURGY TYPES OF RHENIUM, ALL IN THE ANNEALED CONDITION



100X

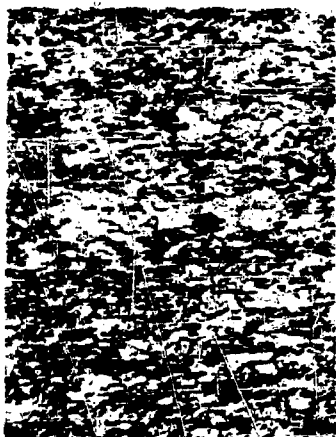
N3847



500X

N3852

a. Microstructure of Pure Annealed Rhenium; VHN = 270



100X

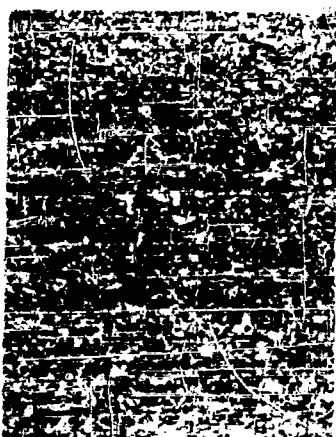
N3851



500X

N3856

b. Rhenium Reduced 40 Per Cent in Cross-Sectional Area by Swaging; VHN = 824



100X

N5316



500X

N5455

c. Specimen of Figure b (Above) After 1 Hour at 1300 C; VHN = 344

FIGURE 31. MICROSTRUCTURES OF ANNEALED, COLD-WORKED, AND RECRYSTALLIZED RHENIUM

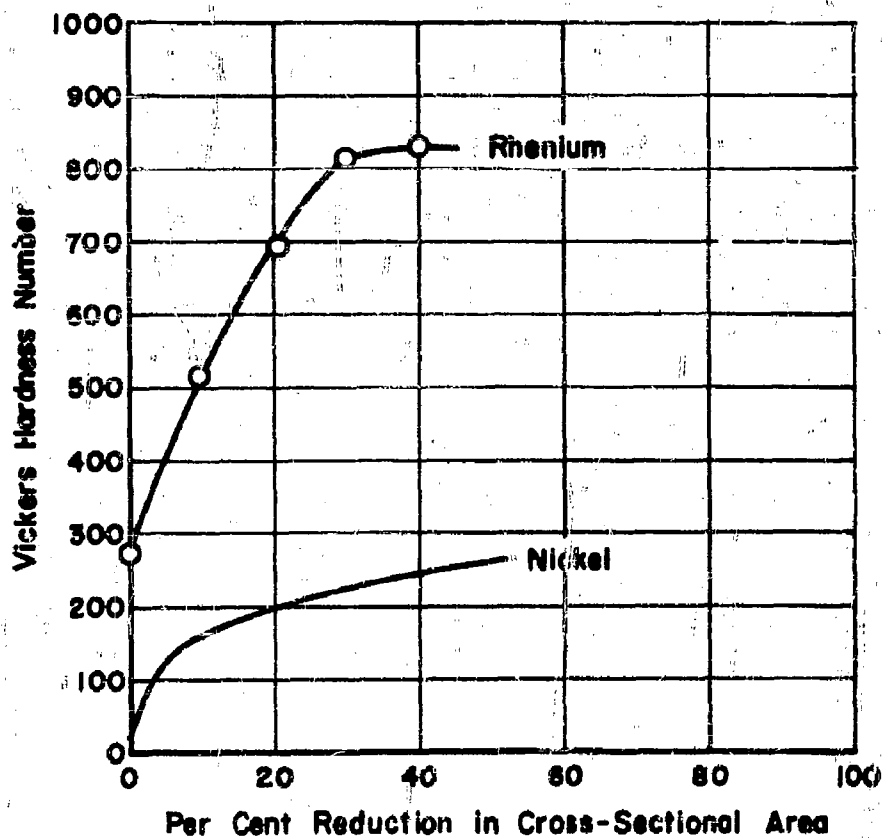


FIGURE 32. COLD-WORK-HARDENING CHARACTERISTICS OF RHENIUM AND NICKEL (8)

A-10136

than any other fabricable pure metal and more than most alloys, and the work-hardened hardness is in the same range as that of many intermetallic compounds.

After study of the hardening characteristics, the effects of annealing at different temperatures on the various worked types of rhenium were studied. The hardness values after 1 hour at various annealing temperatures are given in Table 20 and plotted in Figure 33. The values appear to be rather erratic, particularly above 2000 C, where temperature control was poor. The results, however, clearly show that recrystallization and softening commence about 900 C. Metallographic studies (as illustrated in Figure 32c for 40 per cent reduced metal) and the hardness curves indicate that rhenium reduced 10 per cent has softened and recrystallized after 1 hour at 1500 C, whilst rhenium reduced 20, 30, and 40 per cent requires an hour at about 1300 C to reach a well-softened state. The 10 per cent cold-worked metal requires a higher recrystallization temperature because it contains less available energy from less working, and thus cannot trigger recrystallization so readily as those specimens containing more work.

This information indicates that anneals of about 1 hour in the temperature range 1300 to 1500 C should be sufficient to soften rhenium and allow cold working to proceed as described above in this report. In actual practice, however, it has been found that annealing somewhat above these limits is necessary for successful fabrication; if all annealing is done around 1700 C and for 2 to 4 hours, little trouble results, but annealing according to the recrystallization curves sometimes results in postanneal hardnesses gradually creeping upward to over 400 VHN, a condition which causes cracking and failure of the stock during the cold working.

#### Grain Size and Grain Growth

During the recrystallization study reported above, grain counts were instituted in the temperature ranges above that at which recrystallization commenced for all types of cold work. The Jeffries method for grain-size estimation was used; the results are shown in Figure 34, which compares grain diameters and annealing temperature.

In general, the grain size was very small. Before grain growth commenced, the recrystallized grain diameter was only about 0.004 to 0.006 mm, much finer than unworked hot-wire-deposited and arc-melted rhenium (see Figure 30 for comparisons).

Despite some scatter, the graph clearly shows that increasing amounts of cold work produce successively finer grain sizes upon recrystallization, as would be expected. In addition, reductions up to 20 per cent cause the highest rate of grain-size decrease, corresponding to the greatest rate of work-hardening (Figure 32). Further reduction increases these effects, but at a lower rate.

TABLE 20. HARDNESS VALUES FOR RHENIUM AFTER WORK HARDENING BY SWAGING AND RECRYSTALLIZING BY REHEATING

Reduction, per cent	R. T.	Average VHN After 1-Hour Anneal at Following Temperatures, C												
		700	800	900	1100	1200	1300	1400	1500	1600	1700	1900	2100	2300
9.5	519	496	--	482	457	407	395	381	329	306	340	275	274	--
20.4	690	674	--	608	463	355	313	330	325	300	300	297	315	--
29.8	813	734	--	724	441	360	313	323	319	297	291	328	353	260
40(a)	824	--	815	--	452	348	357	328	315	343	328	330	329	238

(a) Approximately; difficult to measure because of uneven reduction and cracking.

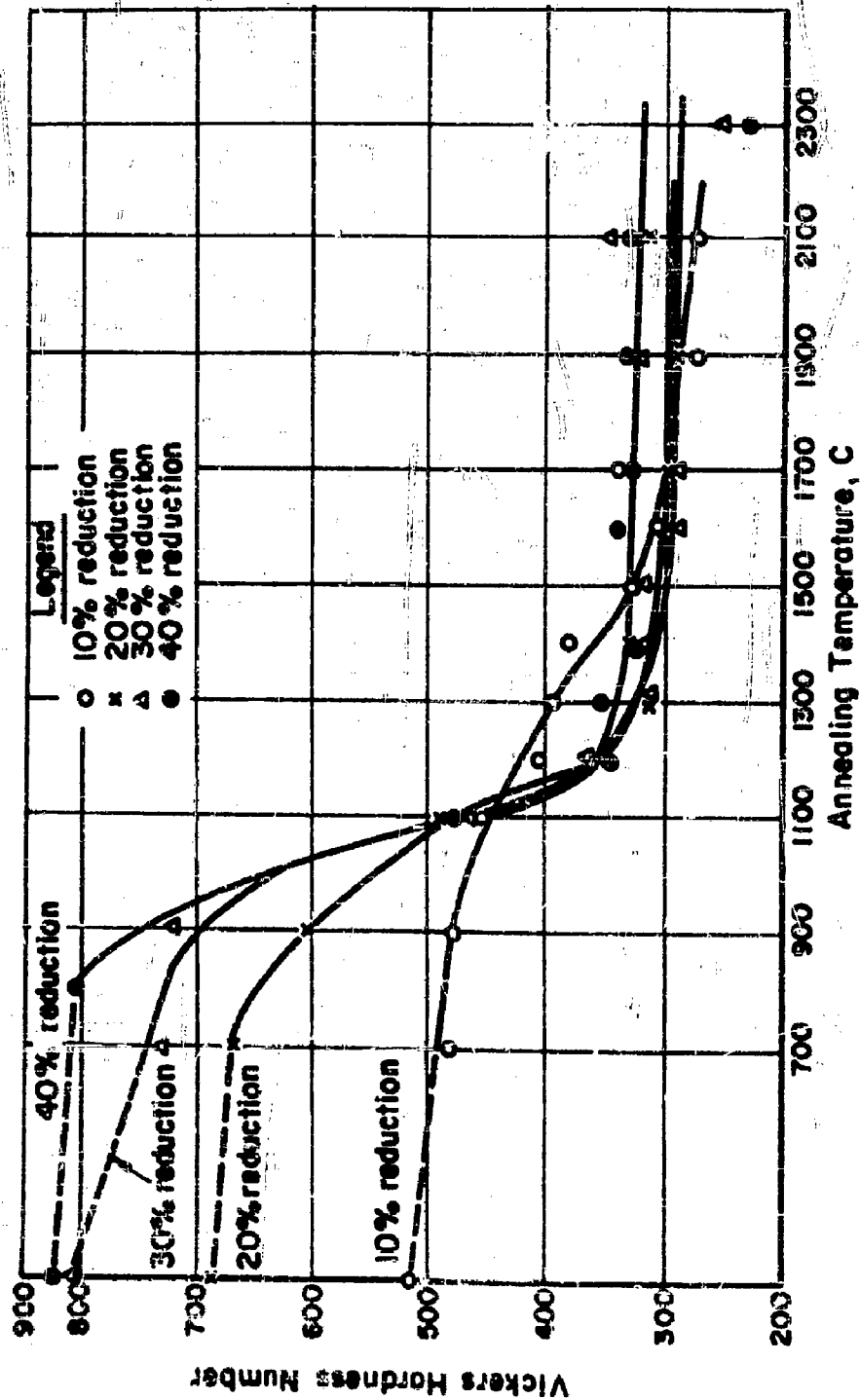


FIGURE 33. THE EFFECT OF 1-HOUR ANNEALING TREATMENTS ON THE HARDNESS OF COLD-WORKED RHODIUM

A-9764

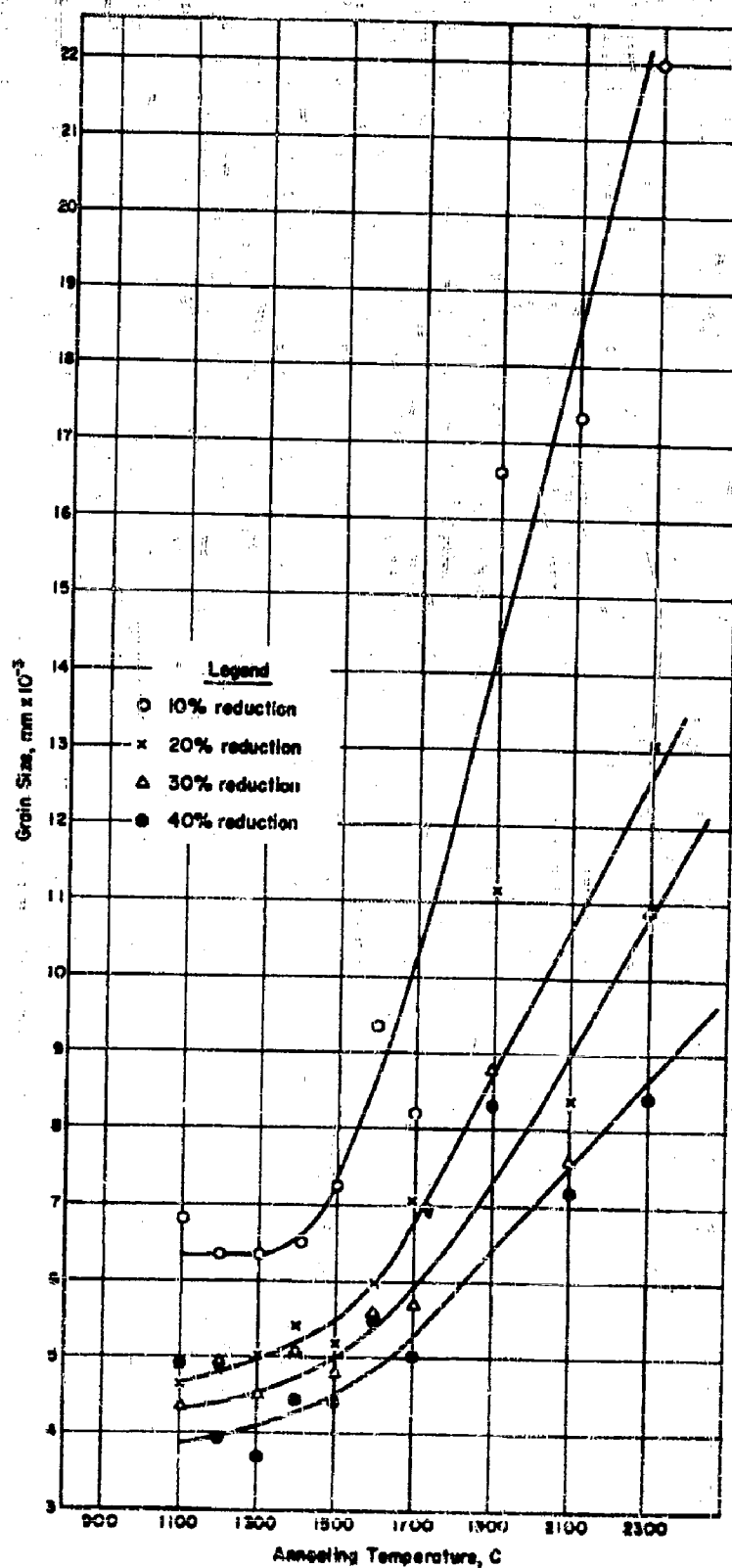


FIGURE 34. THE EFFECT OF 1-HOUR ANNEALING TREATMENTS ON THE GRAIN SIZE OF COLD-WORKED RHENIUM

Figure 33 shows that recrystallization is nearly complete in the temperature range 1300 to 1400 C, and it is in this range that grain growth commences. The single exception is the 10 per cent reduced metal, which lags in recrystallization and correspondingly lags in inception of grain growth to the 1400 to 1500 C range.

### Thoriated Rhenium

Thoriated tungsten is a very commonly used thermionic-emission material, and it has been thought that thoriated rhenium might have an enhanced emission also. Accordingly, some of the basic mechanical properties of thoriated rhenium have been investigated.

#### Tensile Strength and Ductility

Three tensile tests have been completed on thoriated rhenium, one each for 0.5, 1.0, and 2.0 per cent thoria content by weight calculated as thorium metal. A 5.0 per cent alloy was too brittle to be fabricated and tested. All of these tensile tests were conducted on rod containing 1/8-inch standard reduced tensile sections, the tests being carried out in exactly the same manner as has been described for pure rhenium, with the exception that no modulus of elasticity was determined.

The results are summarized in Table 21. Increasing amounts of thoria reduce the ultimate tensile strength in a roughly proportional manner, but do not affect the proportional limit and offset yield strength to any marked degree. Even small amounts of thoria reduce the elongation and reduction of area appreciably, but increased amounts of thoria cause no further decrease.

#### Work Hardening and Recrystallization

Specimens of the 0.5, 1.0, and 2.0 per cent thoriated rhenium rod were annealed; their structures appeared as in Figure 35a. Reductions of 10, 20, 30, and 40 per cent by swaging were given to each bar, as previously reported for pure rhenium. Structures at 40 per cent reduction appeared as in Figure 35b. Anneals at various temperatures up to 1700 C were then conducted in order to study the effect of thoria content on the crystallization behavior.

The hardness values after annealing 1 hour at various temperatures are plotted in Figure 36 and recorded in Table 22. In general, thoria tends to lower the recrystallization temperature, the 0.5 per cent addition being quite effective. There was no marked further lowering of the recrystallization temperature with increasing amounts of thoria.

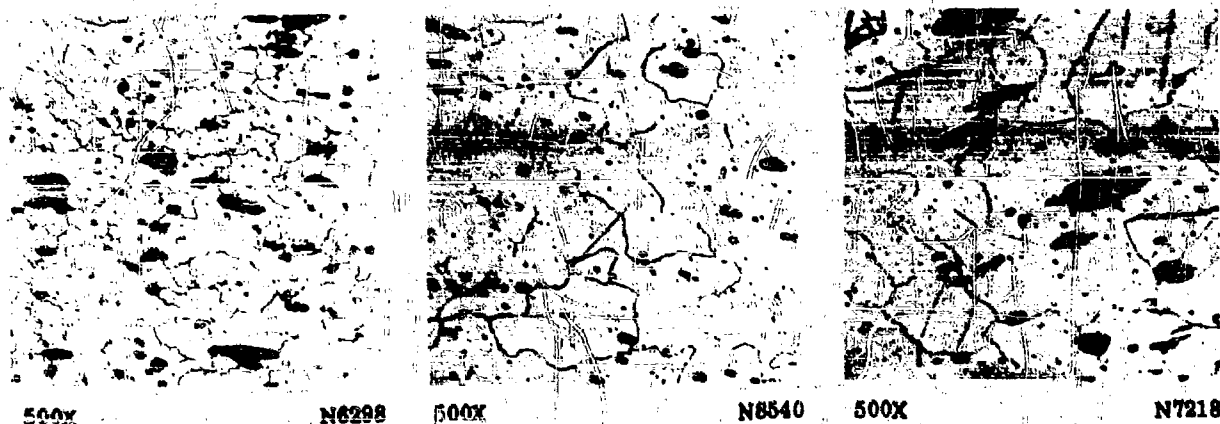


TABLE 21. TENSILE AND ELONGATION DATA FOR ANNEALED THORIATED RHENIUM

Standard ASTM 1/8-Inch-Diameter Reduced Section,  
1/2-Inch Gage Length

Percentage Thorium (as ThO <sub>2</sub> )	0.0	0.5	1.0	2.0
Specimen	--	36	35	37
Proportional Limit, psi	26,300	23,000	27,000	22,900
0.1 Per Cent Offset Yield Strength, psi	42,000	39,600	42,400	42,400
0.2 Per Cent Offset Yield Strength, psi	46,600	44,700	47,600	48,400(a)
Ultimate Tensile Strength, psi	164,000	144,000	135,000	137,00
Elongation in 1/2 Inch, per cent	24	14	11	14
Reduction of Area, per cent	21.7	16	16	16

(a) Estimated.



0.5% thorium

1.0% thorium

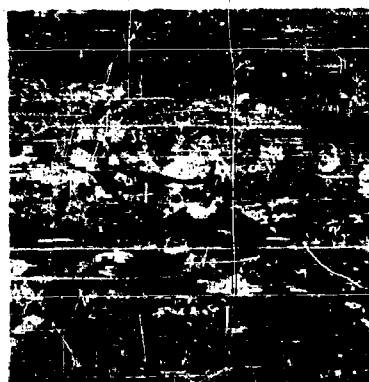
2.0% thorium

a. Microstructure of Swaged and Annealed Thorium-Containing Rhodium



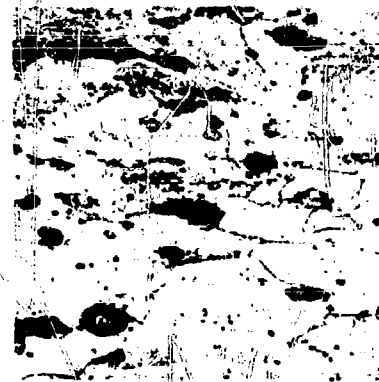
500X

N6302



500X

N8544



500X

N7222

0.5% thorium

1.0% thorium

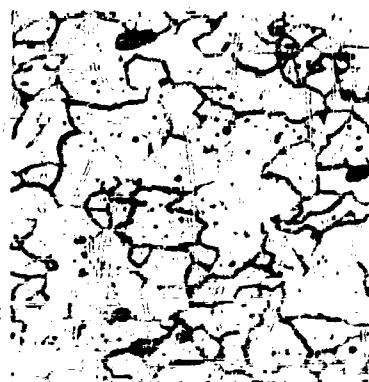
2.0% thorium

b. Thorium-Containing Rhodium Swaged to 40 Per Cent Reduction in Cross-Sectional Area



500X

N7217



500X

N8538



500X

N7250

0.5% thorium

1.0% thorium

2.0% thorium

c. Metal of b (Above) Recrystallized by Annealing 1 Hour at 1700°C

FIGURE 35. MICROSTRUCTURES OF ANNEALED, COLD-WORKED, AND RECRYSTALLIZED THORIATED RHODIUM

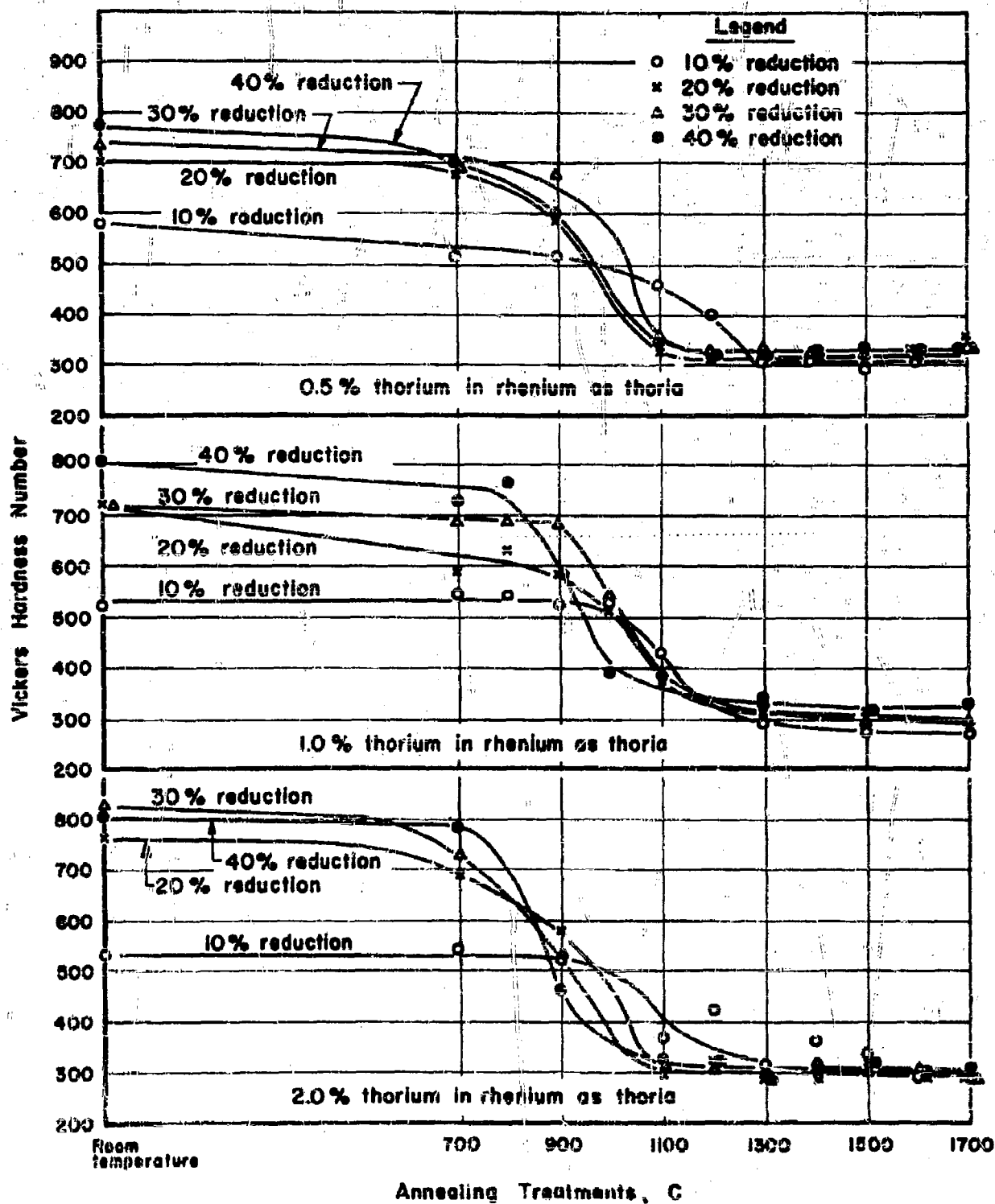


FIGURE 36. THE EFFECT OF 1-HOUR HEAT TREATMENTS AT VARIOUS TEMPERATURES ON THE HARDNESS OF COLD - WORKED THORIATED RHENIUM

A-9703

TABLE 22. HARDNESS VALUES FOR THORIATED RHENIUM AFTER WORK HARDENING BY SWAGING AND RECRYSTALLIZING BY ANNEALING

Thorium Content, per cent		Reduction, per cent	Average VHN After a 1-Hour Anneal at the Following Temperatures, C												
			R. T.	700	800	900	1000	1100	1200	1300	1400	1500	1600	1700	
0.5	10		582	516		518		460		400	309	307	290	306	334
0.5	20		708	680		586		324		316	312	314	308	334	351
0.5	30		743	684		678		357		336	337	319	321	322	337
0.5	40		778	702		600		352		323	309	336	334	333	335
1.0	10		526	551	549	524	523	421			291		274		266
1.0	20		724	699	632	583	515	370			312		313		284
1.0	30		726	690	693	682	546	291			333		299		283
1.0	40		810	731	770	585	391	384			339		316		332
2.0	10		533	545		520		364		427	317	359	336	289	290
2.0	20		759	697		580		285		318	286	291	315	284	288
2.0	30		839	728		528		301		304	304	312	301	291	282
2.0	40		912	789		460		321		214	287	305	315	296	304

The annealed hardnesses seem to be less erratic than those found for pure rhenium; for all types of cold work and for all thoria contents, they level to about the 300 VHN value above the recrystallization temperature and maintain this level. As was the case with pure rhenium, 10 per cent reduced metal does not recrystallize so readily as the more heavily reduced stock. The apparent average recrystallization or softening temperatures, compiled from hardness-temperature plots and visual examination of the microstructures for both pure and thoriated rhenium, are summarized in Table 23.

TABLE 23. TEMPERATURES AT WHICH SOFTENING OCCURS  
IN PURE AND THORIATED RHENIUM

Composition	Softening Temperature, C, for the Following Per Cent Reductions by Swaging			
	10	20	30	40
Pure rhenium	1500	1300	1300	1300
0.5 per cent thoriated rhenium	1300	1200	1200	1200
1.0 per cent thoriated rhenium	1200	1200	1200	1200
2.0 per cent thoriated rhenium	1300	1100	1100	1100

### ELECTRONIC PROPERTIES

E. N. Wyler, D. N. Gideon, and F.C. Todd

#### Thermionic Emission of Pure Rhenium

##### Introduction

A survey of the literature at the beginning of this project disclosed only two sets of emission constants for rhenium, reported by Mellor<sup>(28)</sup> from Alterthum and by Levi and Espersen<sup>(19)</sup>. Alterthum, using a surface of rhenium deposited on tungsten by vapor-phase decomposition of a rhenium halide, obtained a work function of 5.1 electron volts and a Richardson

constant of 200 amp/cm<sup>2</sup>/K<sup>2</sup>. Levi and Espersen obtained a work function of 4.74 electron volts and a Richardson constant of 720 amp/cm<sup>2</sup>/K<sup>2</sup> for rhenium electroplated on a tungsten wire. These values were calculated from measurements by using the relation  $J = AT^2 e^{-\frac{\phi}{kT}}$ , where J is the emission current in amp/cm<sup>2</sup>, A is the Richardson constant, T is the absolute temperature K,  $\phi$  is the work function, and k is the Boltzmann constant.

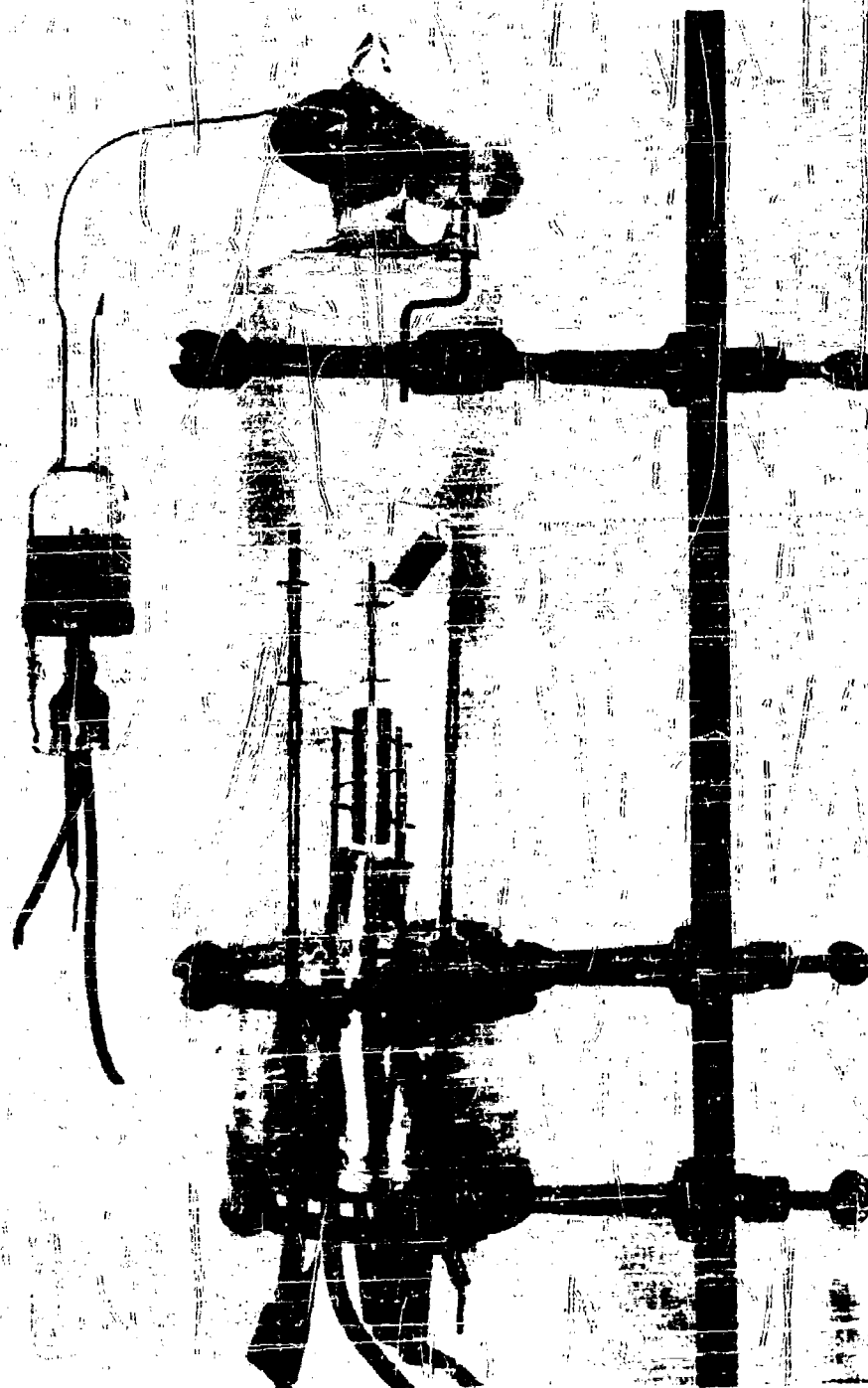
Because the reported Richardson constants exceed the theoretical value of 120 amp/cm<sup>2</sup>/K<sup>2</sup> by wide margins, it is believed that the samples of rhenium were not pure. Another point of interest is that one set of constants indicates that rhenium has considerably poorer emission than tungsten, whereas the other set indicates that rhenium has much better emission than does tungsten. For these reasons, experimental work was initiated on the measurement of the emission constants of pure rhenium.

#### Design of the Guard-Ring Diode

Initial experiments with a guard-ring diode and a dynamic vacuum system indicated the need for a guard-ring diode sealed off from the vacuum pumps. The emission constants obtained for a cathode in a tube with a dynamic vacuum varied over a period of time, indicating an impurity on the rhenium. Since carburization of the hot rhenium surface by the diffusion-pump oil was suspected, the next experiments were conducted with a guard-ring diode that could be sealed off after being outgassed in an oven and pumped to a pressure of about 10<sup>-7</sup> mm of mercury before sealing. A photograph of the guard-ring diode used in the later measurements is shown in Figure 37. The anodes in this structure have an internal diameter of 0.400 inch, and the central anode has an axial length of 0.294 inch. The over-all axial length of the three anodes is great enough that the entire length of the cathode was surrounded. To reduce the possibility of contamination of the emission specimen by evaporation of material from the anodes, they were constructed of molybdenum. Also, to reduce the possibility of contamination of the specimens by evaporated materials from the getters, the getters were mounted in a side tubulation on the glass envelope. An ionization-gage tube was also attached to the main glass envelope, so that the pressure in the test chamber could be monitored during the emission measurements. The ionization gage was operated continuously to clean up trace gases.

#### Preparation of the Rhenium Cathodes

The cathode used in the first set of experiments was a wire drawn to a final diameter of 0.020 inch. The ends of a 1.75-inch length of this wire were forced into holes in the ends of 1/8-inch-diameter molybdenum rods. These molybdenum rods served as mechanical supports and as current leads in the diode structure.



N11359

FIGURE 37. GUARD-RING DIODE USED FOR THERMIONIC-EMISSION MEASUREMENTS ON PURE RHENIUM

For the second set of experiments, a cathode was prepared by grinding. The ends of a rod that had been drawn to a diameter of 0.064 inch were mounted in holes in the ends of molybdenum rods. The rhenium, in its molybdenum-rod supports, was ground in a lathe with an alumina abrasive wheel to a final diameter of 0.0235 inch. An alumina wheel is not the best one for rapid grinding, but it was used because particles of alumina are easy to remove from the surface of rhenium by electropolishing.

Both cathodes described above were electropolished with precautions against removal of excessive amounts of rhenium.

#### Processing of the Guard-Ring Diode

Prior to assembly of the guard-ring diode, all parts of the tube were cleaned very thoroughly. After assembly, the tube was attached to a vacuum system and the exhaust schedule initiated. The vacuum pumps were a Distillation Products three-stage oil-diffusion pump backed by a Welch Duo-Seal mechanical pump. After the diffusion pumps had operated for about an hour, the tube was baked at a temperature of 450 C for 16 to 24 hours. Then the tube was cooled to room temperature and hydrogen was introduced. A hydrogen glow was operated between the several metal parts to reduce oxides and to remove adsorbed gases. Some parts, particularly the anodes, were also outgassed by induction heating. After this, the pumps were started again. When a good vacuum had been obtained, the filament was outgassed by electrically heating to 1500 C. The getters were also outgassed by induction heating. Finally, the diode was baked out at 450 C for 24 to 48 hours. The diode was then cooled to room temperature, the filament again outgassed at 1500 C, and the tube sealed off. The getters were then fired, giving an ionization-gage reading of 3 to 6 x 10<sup>-8</sup> mm of mercury. The diode was then ready for experimentation.

#### Determination of the Thermionic-Emission Constants

The emission constants of the drawn rhenium wire were determined for three ranges of operating temperature. The first series of measurements was made with a maximum cathode brightness of 1600 C. The second and third series were made with maximum cathode brightness of 1800 C and 2000 C, respectively. Several determinations of the emission constants of the rhenium cathode were made over each temperature range. The emission constants were determined from Richardson plots, which involve the use of saturation currents from the cathode at various temperatures. For each Richardson plot, the emission currents were measured first for the highest temperature for that series, and then the measurements were repeated as the temperature was decreased in steps. It has been found from previous experience with this type of measurement that the cathode remains in a reasonably constant state of activation, and, consequently, less change in the work function is noted, when the measurements are started at the



highest temperature and at the highest anode potential that is to be used for a given sequence. The brightness temperatures were determined with an optical pyrometer. From the known value of the spectral emissivity, discussed elsewhere in this report, the true temperatures were calculated and then were used in determining the emission constants.

The emission characteristics for the drawn-wire rhenium in the test diode are shown in a plot of the logarithm of current against the square root of the electric-field intensity. When the data are plotted in this manner, the Schottky portions of the curves are linear and the saturation current at a given temperature is determined by extrapolating the Schottky line to zero electric field. A typical set of Schottky plots for the drawn-wire rhenium cathode is shown in Figure 38. The saturation currents determined from Schottky plots were inserted in Richardson plots, where the work function is found from the slope, and the A value (or Richardson constant) is found by substitution of the work function in the Richardson equation.

The emission constants of the rhenium cathode, which was ground to size, were determined in a similar manner. Measurements on this cathode were initiated at approximately 1800 C brightness as the highest temperature on a Richardson plot, and a set of typical Schottky plots of the data collected for the ground rhenium-wire cathode is shown in Figure 39.

In order that the best data obtained might be reduced to a single work function and a single Richardson constant, a Richardson plot was made of the data from two sets of measurements on the drawn wire and one set of measurements on the ground-down wire as shown in Figure 40. The straight line was fitted to the points by the method of least squares. The work function determined from this plot is 4.80 electron volts, and the Richardson constant is 52 amp/cm<sup>2</sup>/K<sup>2</sup>.

#### The Effects of Impurities on Thermionic Emission

Data from each of the two wires were collected over an extended period of time. These data indicated that changes occurred in the emission constants during the period of the measurements. It was established as reasonably certain that the change in emission constants was the result of the presence of small amounts of impurities in the wires, known to be about 0.2 per cent for the ground wire. The impurity content of the drawn wire is not known accurately, but the proportions of the impurities are believed to be very similar to those for the wire that was ground to size. A typical spectrographic analysis of the impurities is presented in Table 1 as Sample 12. Depending on the type, the amount, and the distribution of the impurity on the surface, the emission current at a given temperature may be either raised or lowered. This change in the emission is also shown, of course, by a change in the measured values of the Richardson constants.

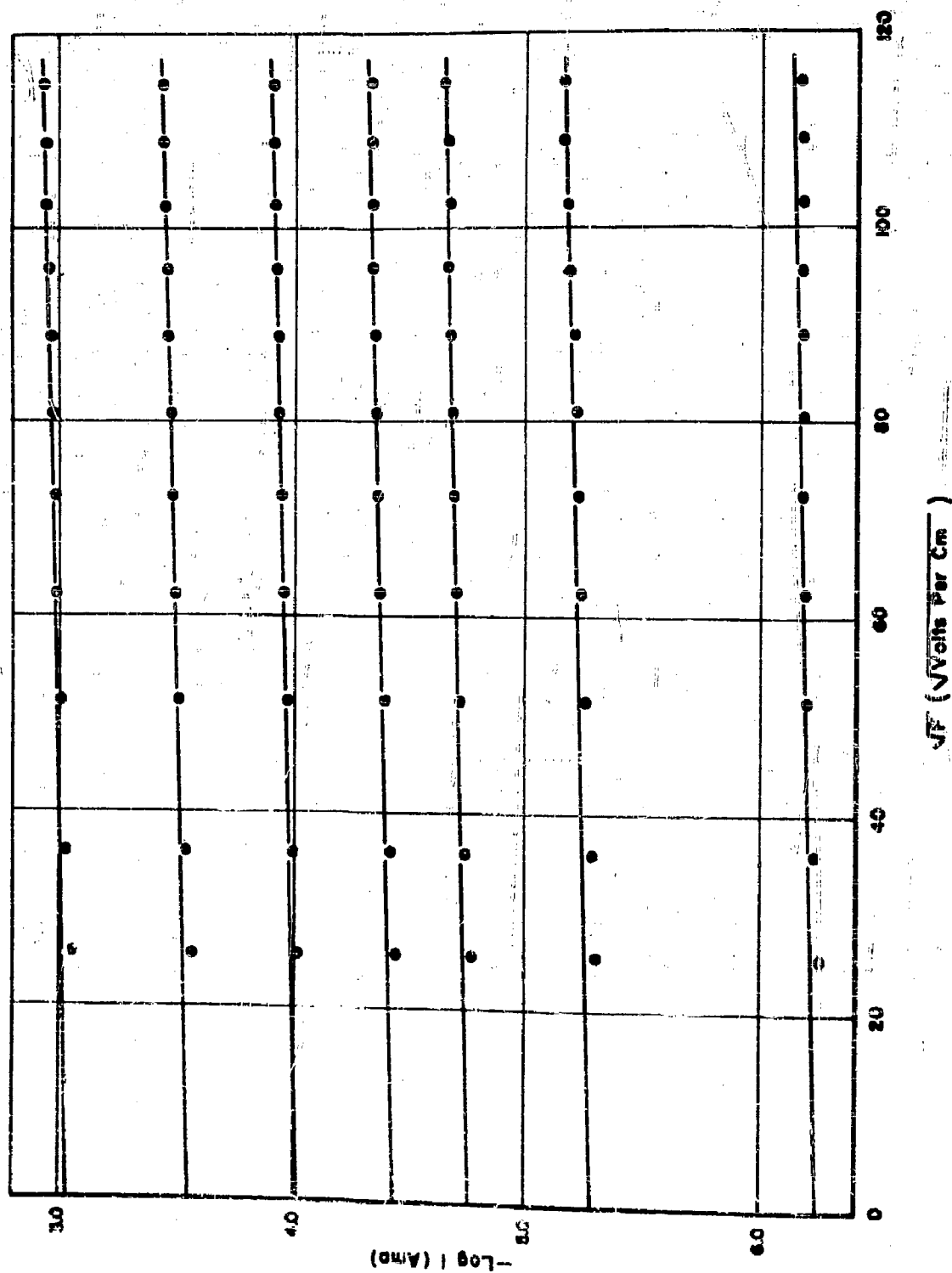


FIGURE 38. SCHOTTKY PLOT FOR DRAWN-WIRE RHENIUM CATHODE

A-9705

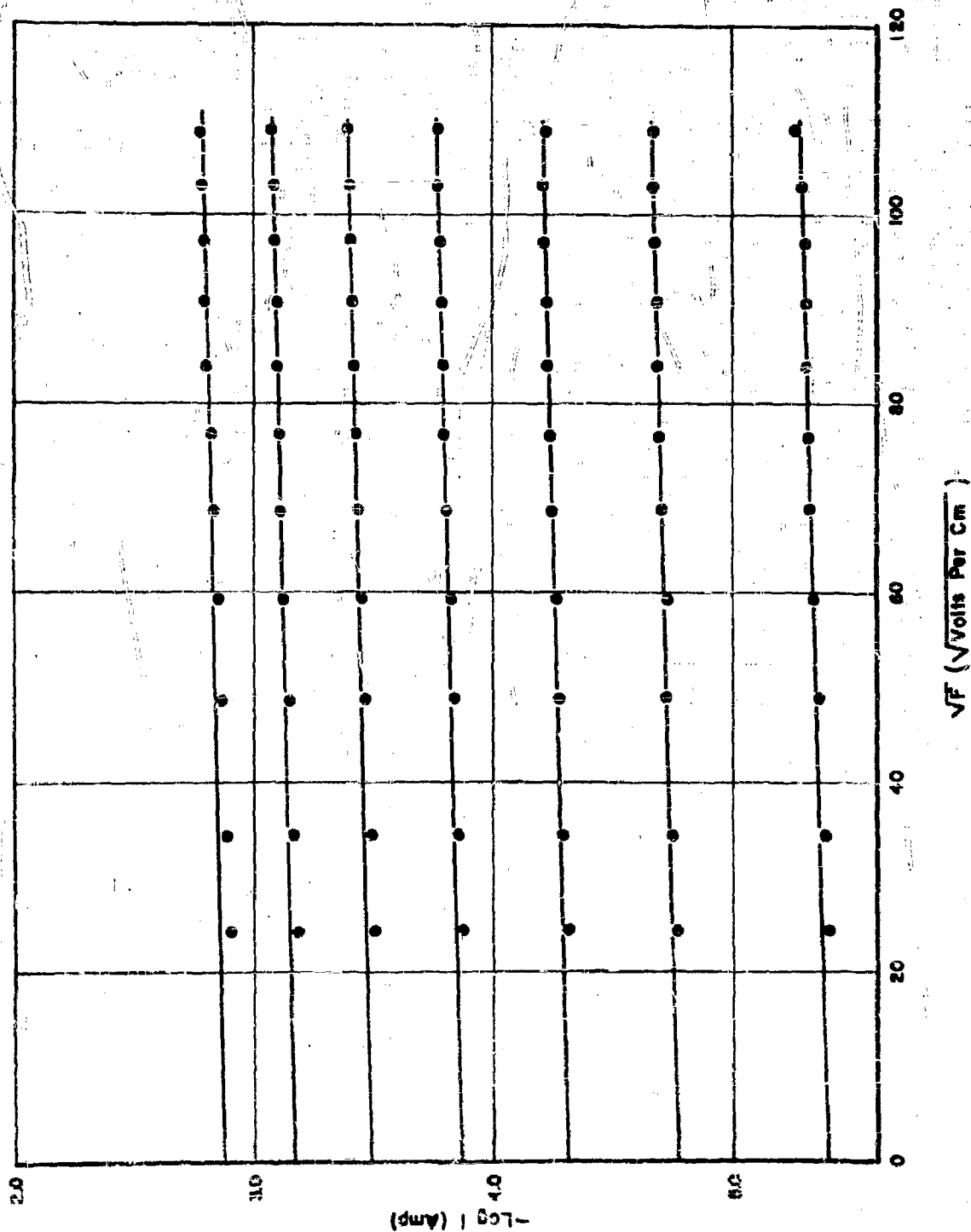


FIGURE 39. SCHOTTKY PLOT FOR GROUND - WIRE RHENIUM CATHODE A-9708



It has been noted by this laboratory and by other investigators (29) that a plot of the work function versus the log of  $A$  for various degrees of surface contamination will yield a straight line. Schottky and Zwikker have advanced theories for this relation which are summarized by DeBoer (30). In general, the relation is attributable to adsorbed ions which form a dipole layer and this dipole layer changes the reflection coefficient for electrons that approach the surface from the interior of the material. Adsorbed electronegative ions such as O and N result in an increase in the work function while adsorbed electropositive ions such as Ba and Cs result in a decrease in the work function. A plot (Figure 41) of the work function versus  $\log A$  was made with the data obtained from the two rhenium wires. The Richardson constants for the average curves through the data from both wires are indicated by the point with the descriptive note. The measurements for these points were made very early in the series of tests before the rhenium was held at elevated temperature long enough for much diffusion of impurities to the surface. With continued operation of the wire at an elevated temperature, the work functions of both wires first decreased to values lower than average, and then increased slowly to the higher values. Measurements known to be in error were omitted from the plot. The decrease and then increase in the work function would be expected if there were at least two impurities in the body of the material, and if these two materials diffused to the surface at different rates while the rhenium wire was held at a high temperature.

It may also be observed from the curve that the emission current is readily reproducible from one cathode to another, and the fact that the data from both cathodes are on the same straight line indicates that both cathodes may have the same impurities. Furthermore, the times at each temperature were quite different for the two wires, so that the check is remarkable. Since the measurements near the start of the heating check each other, it is our opinion that these readings most closely approximate the true work function of rhenium.

### Thermionic Emission of Thoriated Rhenium

#### Introduction

Because of the possibility that thoriated rhenium might be a better thermionic emitter than thoriated tungsten, experiments were initiated to determine the emission constants of thoriated rhenium. The greater emission of thoriated tungsten as compared with pure tungsten is due to the presence of thorium metal on the emitting surface. The thorium, which is incorporated in the bulk of the tungsten as thorium oxide, is produced by reduction of the oxide at temperatures in the range of 2200 to 2500 C. Thoriated tungsten filaments are always carbonized so that the thorium oxide is reduced by the carbon at operating temperatures. At the operating temperature of the emitter, 1600 to 1800 C, an equilibrium exists between the rate of evaporation of thorium from the surface and the rate of diffusion of thorium oxide to the surface.

Since the rate of diffusion of thorium and the effect of thorium on the emission characteristics almost certainly differ in magnitude for rhenium and tungsten, a considerable number of experiments would be necessary to

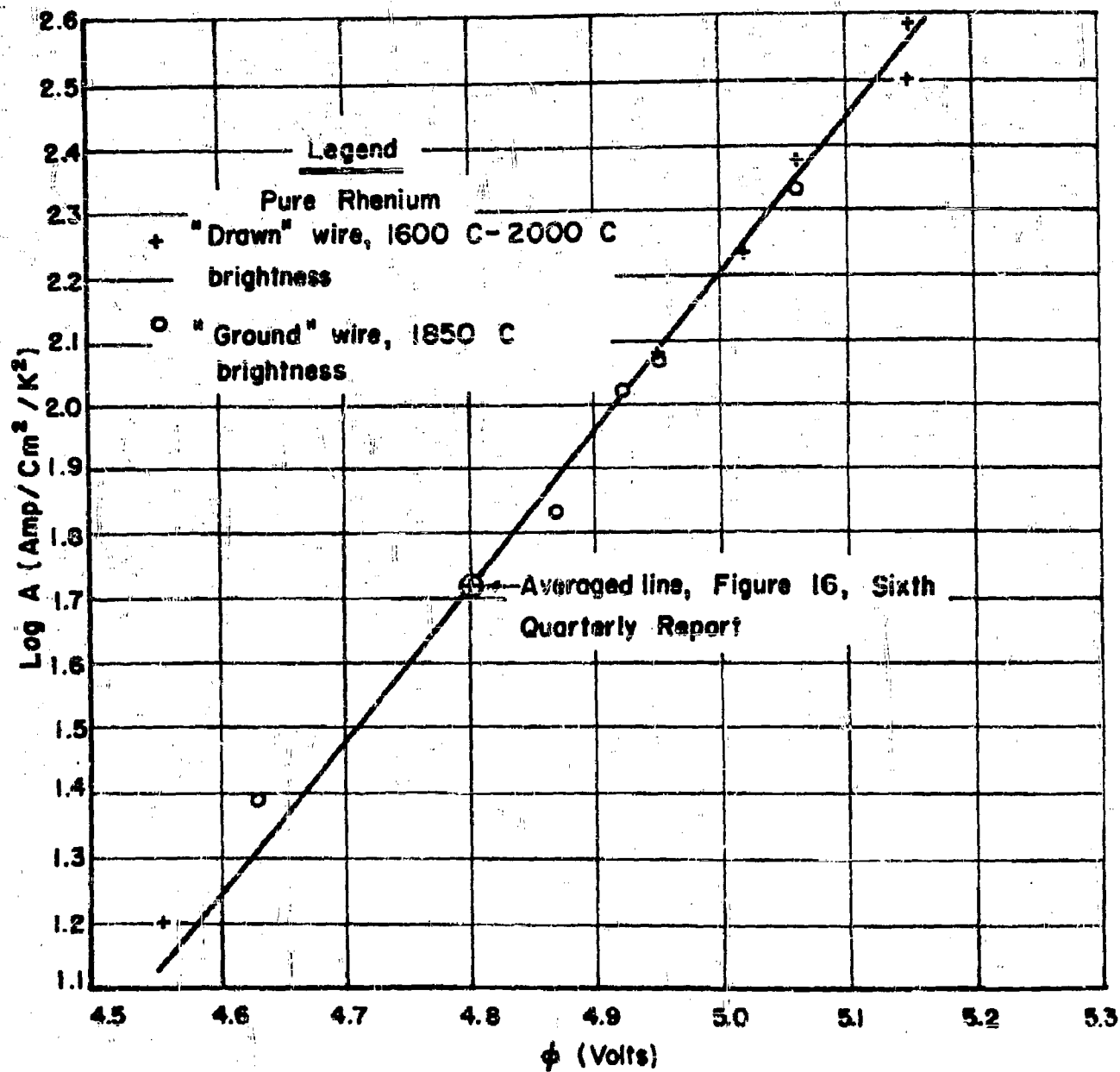


FIGURE 41. ACTIVATION PLOT FOR PURE RHENIUM FILAMENTS

A-10624

determine the optimum conditions of preparation and of operation of thoriated rhenium cathodes. A set of preliminary experiments was carried out with a thoriated rhenium cathode that originally contained 1 per cent thorium as thorium oxide.

#### Fabrication of Cathode for Guard-Ring Diode

The thoriated rhenium cathode employed for the measurements to be described was ground to the desired dimensions with an aluminum oxide abrasive wheel. After grinding to size, the cathode was electropolished to remove impurities left by the abrasive wheel. The final dimensions of the cathode were a diameter of 0.023 inch and a length of 0.6 inch. The cathode was mounted in a guard-ring diode similar to that shown in Figure 37, but which did not have an ionization-gage tube attached.

#### Processing of Guard-Ring Diode

The guard-ring diode with the thoriated rhenium cathode was attached to the same vacuum system and processed in essentially the same way as described for the pure rhenium cathode. Just before the tube was sealed off from the vacuum system, the pressure indicated by the ion gage in the pumping system was near  $10^{-7}$  mm of mercury. After the tube was sealed off, the getters were fired.

#### Determination of the Thermionic-Emission Constants

The emission constants of the thoriated rhenium cathode were measured in essentially the same way as they were for pure rhenium. That is, readings of temperature and saturation emission current were obtained first for a certain temperature that had been maintained for several hours. The saturation current at each temperature was determined by measuring emission currents as the anode voltage was decreased from its highest value to low values, and by plotting these quantities on a Schottky plot. This process was repeated as the temperature was decreased stepwise. The work function and the Richardson constant were calculated from a Richardson plot of the saturation currents and the temperatures.

The temperature-time schedule followed in the experiments was similar to the schedule appropriate for a thoriated tungsten cathode. After activation at a high temperature and aging at an intermediate temperature, a Richardson plot was made, beginning at a true temperature of 1575 C. Richardson plots were made for higher temperatures later, as the maximum temperature was increased in steps from 1575 C to 2350 C. Throughout the series of experiments, the emission of the thoriated rhenium cathode did not exceed  $0.003 \text{ amp/cm}^2$  at 1625 C, compared with about  $1.5 \text{ amp/cm}^2$  at 1625 C to be expected from a thoriated tungsten cathode (31). The carbonization of the surface for the reduction of the thorium oxide was obtained from the cracking of the oil from the diffusion pump on the surface of the hot wire.

These values may be compared with 0.000036 amp/cm<sup>2</sup> for pure rhenium and 0.00022 amp/cm<sup>2</sup> for pure tungsten at a temperature of 1625 C. These data indicate a hundredfold increase in the emission current of rhenium upon the addition of 1 per cent thorium. The increase in emission current of thoriated tungsten over that of pure tungsten is approximately 70,000. Although exhaustive tests of thoriated rhenium have not been made, the present data tend to indicate that the degree of emission enhancement will not be nearly so great for the addition of thorium to rhenium as for the addition of thorium to tungsten. It is expected that an increase in the emission of thoriated rhenium would be produced by increasing the thorium content of the rhenium, but whether the emission of thoriated rhenium under any condition would surpass the emission of thoriated tungsten is problematical.

### Thermionic Emission of Impregnated Cathodes

Impregnated-type cathodes have become industrially important in recent years. The Philips impregnated cathode consists of a mixture of powdered tungsten and powdered barium aluminate pressed into the desired form and sintered. Since impregnated cathodes are widely used in various types of vacuum tubes, especially in military magnetrons, it appeared desirable to determine whether a cathode that employs rhenium powder instead of tungsten has comparable characteristics. Therefore, a test program to determine the properties of rhenium-barium aluminate-impregnated cathodes was initiated at Battelle.

### Cathodes Impregnated With Barium-Strontium Carbonates

A study of impregnated rhenium cathodes was initiated with mixtures of powdered barium and strontium carbonates as the emitter impregnating material. Several sleeve shapes were pressed from a mixture of 90 per cent rhenium powder with 10 per cent of a barium-strontium carbonate mixture. The carbonate mixture contained 60 mole per cent barium carbonate and 40 mole per cent strontium carbonate. The sleeves were presintered at temperatures up to 1300 C. After the presintering treatment, the sleeves were placed in a compression-type mount, so that current could be passed through them for additional sintering and activation in the test diode. It was necessary to keep the presintering temperature low to prevent decomposition of the barium and strontium carbonates. Had the sleeves been heated to a temperature high enough to decompose the carbonates, the cathodes would have been poisoned by water vapor before they could have been placed in the test diode. It was found by experiment that the presintering treatment did not yield a body of sufficient mechanical strength to withstand the sintering operation in the test diode. After unsuccessful attempts



to produce an impregnated cathode of rhenium and barium-strontium carbonates, work was directed toward producing a cathode of rhenium impregnated with barium aluminate.

#### Cathodes Impregnated With Barium Aluminate

A sample of normal barium aluminate was prepared by the Analytical Chemistry Division of Battelle. The aluminate was prepared by mixing water solutions of barium hydroxide and aluminum nitrate in stoichiometric quantities. The solution was dried and the salt was pulverized in an agate mortar, and then placed in a platinum crucible and heated to a temperature of about 750 C for 1/2 hour. The final product was normal barium aluminate.

Impregnated cathodes were formed by thoroughly mixing the barium aluminate and rhenium powder and pressing a sleeve in a three-segment die of the type usually used for the formation of molybdenum-thoria compacts for cermet-type cathodes. Mixtures of two compositions were compressed for the initial tests. One mixture was 20 per cent barium aluminate with 60 per cent rhenium powder. The resulting compacts were fired in a vacuum furnace for 1/2 hour at a brightness temperature of 1800 C. Both mixtures produced mechanically strong sleeve-type cathodes that could be heated by passing current through them. These sleeve-type cathodes were supported for test in a special mount that maintained the cathode under compression during operation.

Testing occurred in a water-cooled diode provided with two platinum anodes. One of these anodes is movable and surrounds the cathode during the early stages of activation. It is then removed to expose the clean surface of the main platinum anode for the thermionic-emission measurements. Past experience has shown that reproducible measurements of the emission constants of various materials can be obtained in a dynamic vacuum system with these diodes.

After the cathode was placed in the diode and the system exhausted to a pressure of approximately  $10^{-6}$  mm of mercury, the cathode temperature was raised slowly to 1100 C brightness while the cathode was surrounded by the movable platinum anode. When the pressure became constant at this temperature, d-c voltage was applied across the diode and raised slowly. When the emission current reached a value corresponding to the maximum safe power dissipation for the movable platinum anode, the anode was raised to expose the clean platinum surface of the main anode. The anode potential was then raised slowly, while a pressure of about  $10^{-6}$  mm of mercury was maintained, until saturation of the emission current was obtained. The saturation currents were measured for various temperatures by decreasing the voltage and temperature in steps. The emission was measured alternately under pulse and then under d-c conditions. The data from these

measurements were placed in Richardson plots for the purpose of determining the emission constants. After one Richardson plot was obtained, the maximum temperature of measurements was then raised about 50 C and another Richardson plot obtained. Several sets of data were obtained in this manner, up to a maximum cathode temperature of 1350 C brightness.

A Richardson plot for the pulse-emission data from a cathode of 20 per cent barium aluminate and 80 per cent rhenium at a maximum brightness temperature of 1350 C is shown in Figure 42. The pulse work function under these conditions of operation was 2.5 electron volts, and the A value was  $6.8 \text{ amp/cm}^2/\text{K}^2$ . The pulse emission current at a temperature of 1350 C was  $50 \text{ ma/cm}^2$ .

A Richardson plot for the d-c emission data from a cathode of 20 per cent barium aluminate and 80 per cent rhenium for a maximum cathode temperature of 1350 C brightness is shown in Figure 43. The d-c work function under these conditions of operation was 1.96 electron volts, and the A value was  $0.09 \text{ amp/cm}^2/\text{K}^2$ . The d-c emission current at a temperature of 1350 C brightness was  $230 \text{ ma/cm}^2$ . Both of the Richardson plots for d-c and pulse emission include two sets of observations.

The emission currents that were obtained are suspected of being low for this type of cathode, as it may be more susceptible to poisoning by water vapor before insertion in the diode than was expected originally. Determination of the emission constants of an impregnated rhenium cathode in a sealed-off tube now appear necessary. Arrangements are being made to place a rhenium-impregnated cathode in a nonoscillating magnetron so that both the thermionic-emission constants and the behavior of the cathode in a magnetron may be determined in the same sealed-off tube.

### Secondary-Electron-Emission Coefficient

The secondary-electron-emission coefficient of rhenium metal was measured in order to determine the possibility of employing rhenium as an electron-tube grid material or as a magnetron cathode emitting surface. These measurements were performed with equipment that had been set up previously and employed for the same type of measurement on another project. This equipment was properly reconditioned and tested prior to the rhenium secondary-emission determinations. The essential circuit components and the arrangement of some of the electrodes in the electron-gun assembly are illustrated by the sketch in Figure 44. The measurements are obtained in a vacuum of the order of  $10^{-6}$  mm of mercury maintained by a dynamic system. The system is evacuated through a liquid-nitrogen cold trap by a three-stage, oil diffusion pump with the usual mechanical fore-pump. A pulse technique is employed for the measurements, so that the equipment can be employed for either metals or dielectrics.

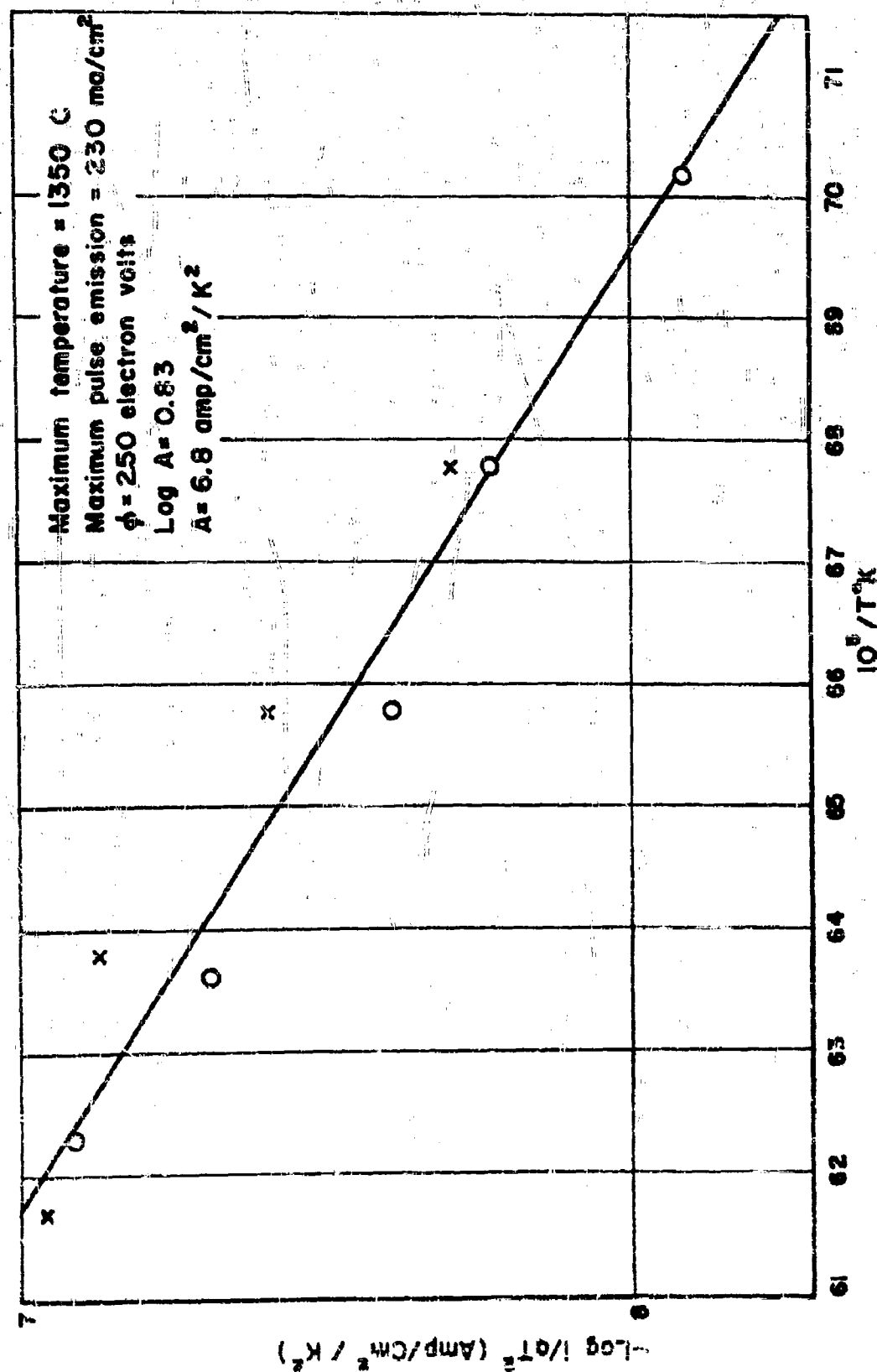


FIGURE 42. RICHARDSON PLOT OF PULSE EMISSION DATA FOR IMPREGNATED CATHODE: 20 PER CENT BARIUM ALUMINATE, 80 PER CENT RHENIUM

A-10622

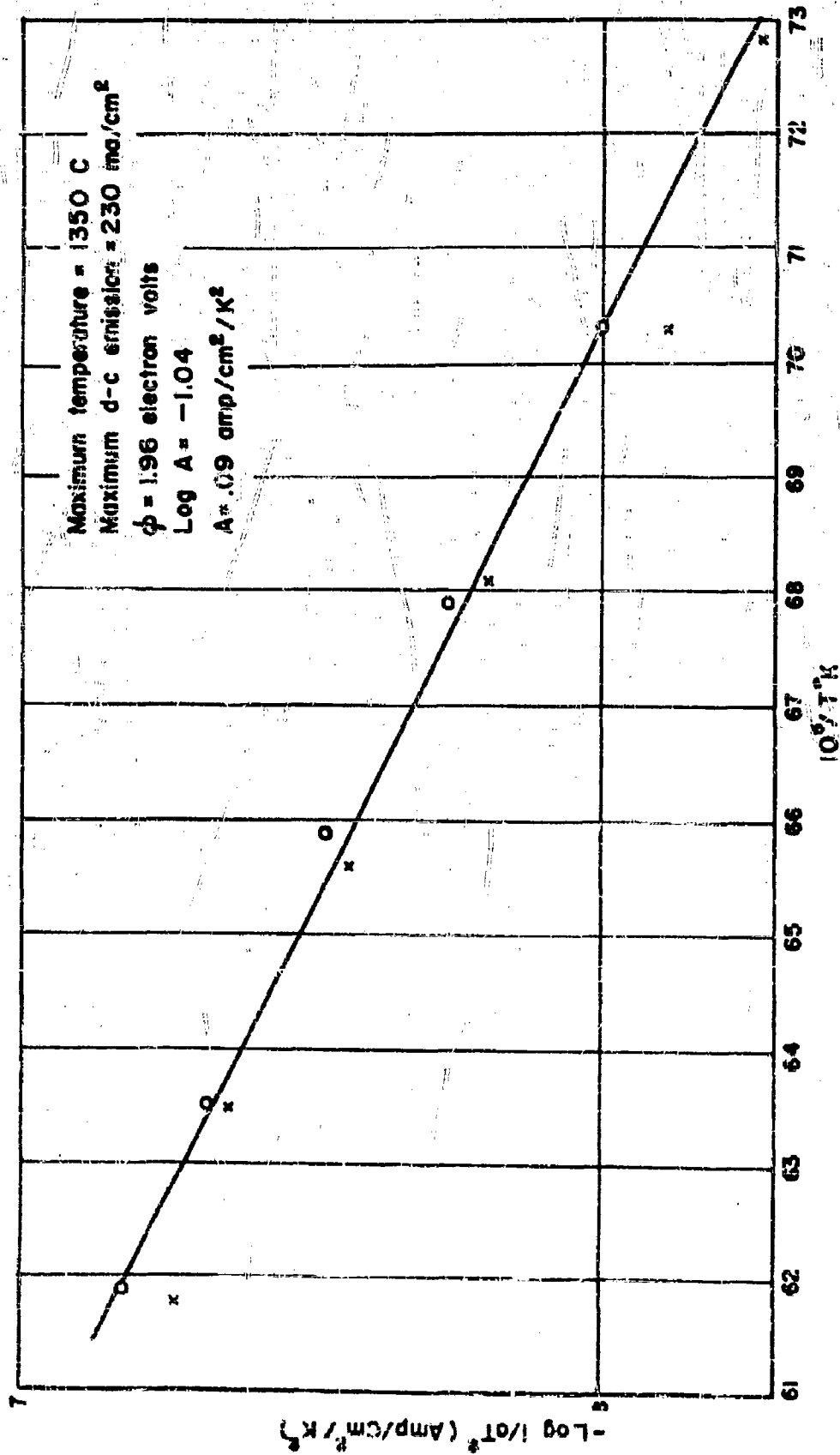


FIGURE 43. RICHARDSON PLOT OF D-C EMISSION DATA FOR IMPREGNATED CATHODE: 20 PER CENT BARIUM ALUMINATE, 80 PER CENT RHENIUM

A-10623

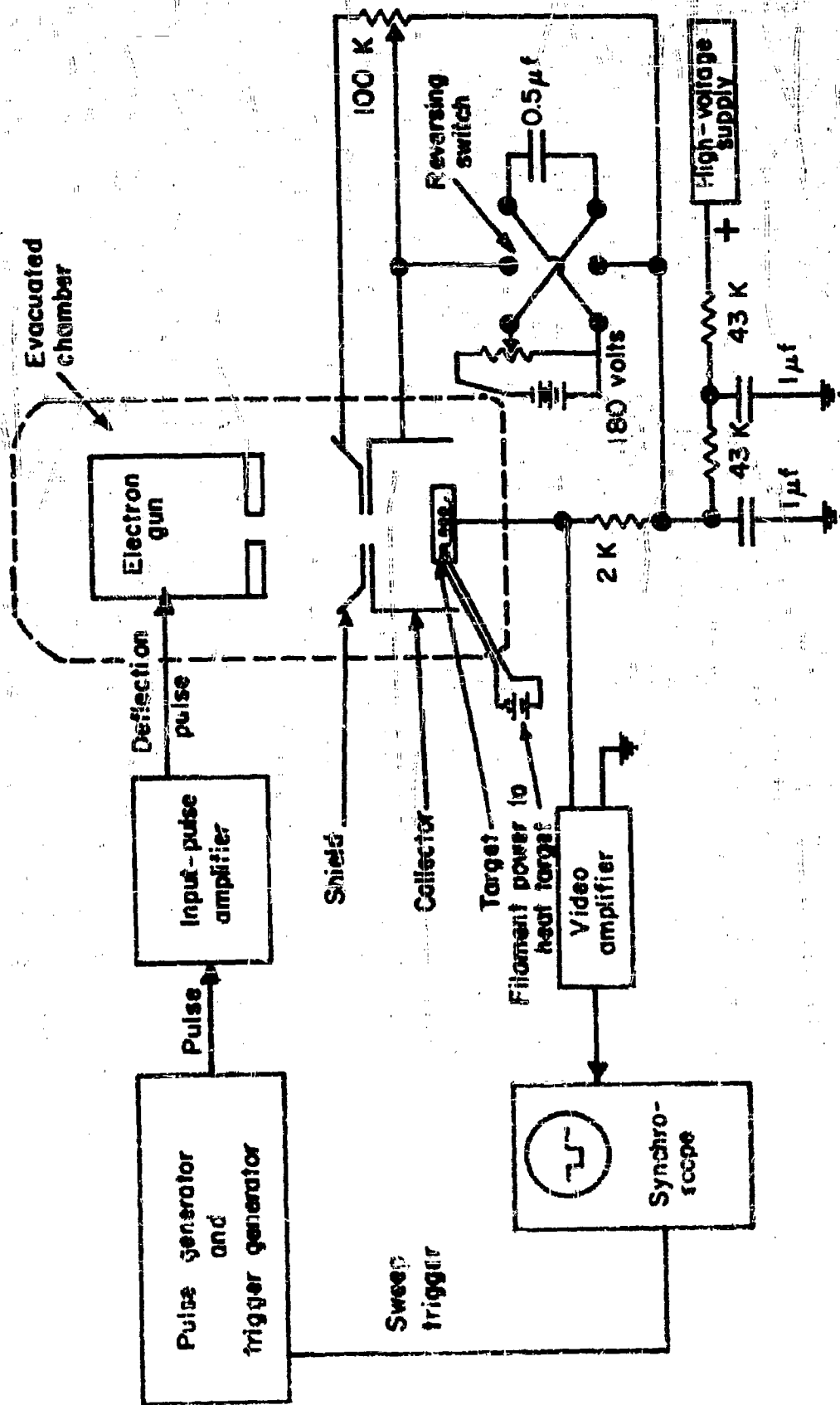


FIGURE 44. BLOCK DIAGRAM OF SECONDARY-EMISSION APPARATUS

A-10629

A pulse of voltage and a trigger are produced in a pulse generator. The trigger may be adjusted to occur at any desired time before the pulse, and operates a synchroscope on which the amplitude of the pulse is observed. The voltage pulse is amplified from 40 to 150 volts, and then is applied to the electron gun to turn on a beam of electrons for the duration of the pulse. The electron beam from the gun is directed to the target. With the reversing switch, the collector around the target is made negative with respect to the target by a potential that can be increased to 180 volts. The current through the 2000-ohm resistor, designated 2K in the sketch, produces a voltage pulse with an amplitude that is proportional to the current in the primary beam of electrons. The reversing switch is then thrown to make the collector positive with respect to the target by an adjustable potential so that it collects secondary electrons, but does not collect any electrons from the primary beam. The current through the 2000-ohm resistor is then the difference between the secondary-electron-emission current and the primary beam current. For a negative collector voltage, the current incident on the target surface is the total current in the incident electron beam, and all secondary electrons are driven back into the target. For the positive collector voltage, all secondary electrons are drawn to the collector and the current crossing the target surface is the beam current minus the secondary-electron current. If the current for a positive collector voltage is designated as  $I_p$  and the current for the negative collector voltage is  $I_n$ , then

$$\text{Secondary Current} = I_n - I_p,$$

$$\text{Primary Current} = I_n.$$

The coefficient of secondary emission is

$$\delta = \frac{I_n - I_p}{I_n}.$$

Since the filament in the electron gun is at ground potential, the target is at a positive potential with respect to ground. This positive potential is equal to the energy of the electrons in the primary beam that is incident on the target. As a consequence, the video amplifier must measure a small pulse voltage that may be from 100 to 5000 volts positive with respect to ground. The double-mesh, RC-filter that is indicated in the sketch is to permit this measurement at this high potential with respect to ground. The steady, thermionic-emission current from the heated target does not affect the video amplifier and, therefore, does not affect the measurement of the secondary-emission current.

Several determinations of the secondary-emission coefficient of rhenium were made under various conditions of temperature. Two different samples were employed for the measurements. One of these samples consisted of a section of an arc-melted button that had been ground to a thickness of 10 mils. After the initial measurements, this specimen was

removed from the system and polished and then replaced for additional determinations of the secondary-emission coefficient. The second sample consisted of a 1-cm-square piece of 5-mil-thick foil that had been rolled from a sintered bar of pure rhenium metal. A curve showing the secondary-emission coefficients for both samples at an optical temperature of 1000 C is shown in Figure 45. From this curve, it may be observed that the maximum coefficient occurs over a rather broad range of primary-beam energies. A maximum of 1.4 is indicated, and occurs at a primary energy of approximately 650 volts. The data were fairly reproducible and independent of target temperature.

The impurity contents of the samples were not known, although it is highly possible that small amounts of aluminum, magnesium, calcium, and silicon were present in the samples. These impurities are believed to represent not over 0.2 per cent of the total. It is known that impurities do affect the value of the secondary-emission coefficient but sufficient data are not available to ascertain the effect in the above measurements.

### The Water-Cycle Effect

Hot tungsten filaments in practical vacua fail partly because of an oxidation-reduction reaction involving water vapor. This reaction is called "the water-cycle", because of its cyclic nature. The filament first reacts with water vapor to form tungsten oxide and atomic hydrogen. Then the volatile tungsten oxide vaporizes from the filament and condenses on the cooler parts of the bulb. Here it is reduced by atomic hydrogen to metallic tungsten, with the re-formation of water.

Langmuir<sup>(32)</sup> indicated the importance of the water-cycle effect, in contrast to evaporation, in the failure of tungsten filaments. In order to compare the merits of tungsten and rhenium as filaments, it is important to know their relative losses by the water-cycle effect.

### Qualitative Observation

For the first comparative test of the water-cycle effect on rhenium and tungsten, hairpin filaments of each of the metals were placed in opposite ends of a glass U-tube. Both filaments were made from approximately 0.015-inch wire and were 2 inches long. The tube was exhausted and sealed so that the water-vapor pressure was about  $10^{-4}$  mm of mercury. Both filaments were heated to a temperature of 1400 C brightness for 20 hours. The results are apparent in the photograph shown in Figure 46, where the darkest portion of the tube is the area surrounding the tungsten filament. Most of the deposit on the glass walls near the rhenium filament accumulated during the first 2 hours.

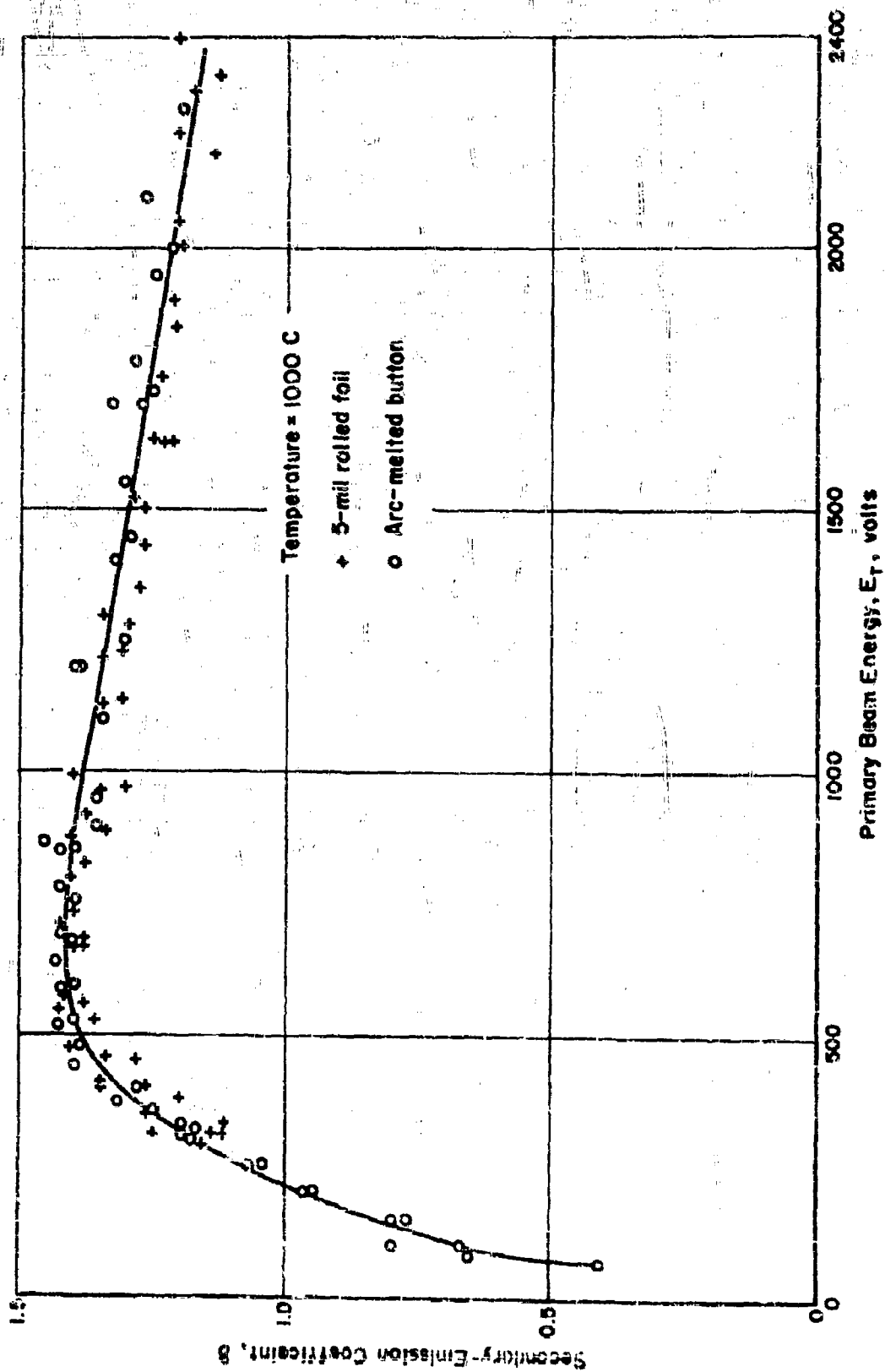


FIGURE 45. SECONDARY-EMISSION COEFFICIENT FOR RHENIUM METAL  
A-11723



### Relative Water-Cycle Losses of Rhenium and Tungsten

A U-tube similar to that shown in Figure 46 has been used to measure, by weighing, the relative losses from rhenium and tungsten filaments. In these experiments, coiled filaments made from wires of approximately the same diameter and length were surrounded by molybdenum cylinders. These cylinders could be inserted and removed easily, and were weighed on a microbalance before and after exposure to the hot filaments.

In the first experiment of this type, the tube was evacuated and sealed to give a water-vapor pressure of about  $10^{-4}$  mm of mercury. Both filaments were heated at a temperature of 1400 C brightness for 22 hours, 1600 C brightness for 168 hours, and 1800 C brightness for 4-1/2 hours. The weights of rhenium and tungsten collected were 0.17 milligram and 29.96 milligrams, respectively. This indicates that the tungsten filament erodes at a rate approximately 176 times greater than the rhenium filament does under the conditions of this experiment.

In a second test, the filaments were prepared in the same way as in the first test, but the U-tube was evacuated with an oil diffusion pump and liquid-nitrogen trap. The tube was sealed off when the ionization-gage reading was  $8 \times 10^{-7}$  mm of mercury. The amounts of tungsten and rhenium collected after 370 hours' operation at 1600 C brightness gave a ratio of loss of tungsten to rhenium of 120.

In a third test, using the same rhenium filament as before but a new tungsten filament, the U-tube was evacuated and baked at 450 C for about 4 hours. The filaments were then outgassed at 1600 C brightness. The U-tube was again baked at 450 C for about 2 hours, a liquid-nitrogen trap inserted, and the tube cooled to room temperature. The filaments were again outgassed. When the ionization-gage reading showed a pressure of  $8 \times 10^{-7}$  mm of mercury, the tube was sealed. After operation of the filaments at 1600 C brightness for 220 hours, the ratio of losses of tungsten to rhenium was 14.

The results of the three tests are summarized in Table 24. The evaporation rates of tungsten and rhenium are of the same order. In the second run, the rate of loss of tungsten is about  $2 \times 10^6$  times greater than the evaporation rate, whereas for rhenium the rate of loss is about  $10^4$  times greater than the evaporation rate. In the third run, where the water-vapor pressure was lowest, the corresponding ratios for tungsten and rhenium are  $6 \times 10^4$  and  $3 \times 10^3$ , respectively.



N5689

FIGURE 46. RELATIVE WATER-CYCLE-RESISTANCE TUBE

TABLE 24. COMPARISON OF WATER-CYCLE LOSSES OF RHENIUM AND TUNGSTEN

Run	Temperature, C	Time, hr	Metal Collected, mg		Loss by Water Cycle, g/cm <sup>2</sup> /sec		Rate of Evaporation, g/cm <sup>2</sup> /sec at 1600 C	
			Tungsten	Rhenium	Tungsten	Rhenium	Tungsten	Rhenium
1	1600	22						
	1700	168						
	1800	4	28.96	0.17				
2	1600	370	76.08	0.64	$0.42 \times 10^{-7}(a)$	$0.35 \times 10^{-9}$	$2 \times 10^{-14}(b)$	$2.9 \times 10^{-14}(c)$
3	1600	220	1.28	0.082	$1.2 \times 10^{-9}$	$0.085 \times 10^{-9}$	$2 \times 10^{-14}(b)$	$2.9 \times 10^{-14}(c)$

(a) At 2000 ft.  $75 \times 10^{-13}$  g/cm<sup>2</sup>/sec is the accepted value for true evaporation of tungsten, according to Smithells<sup>(1)</sup>.

(b) Estimated from data in Reference 32.

(c) Calculated from vapor-pressure value in this report.

### The Water-Cycle Effect on Rhenium at High Water-Vapor Pressures

The relative loss of rhenium by the water-cycle reaction was measured as a function of the pressure of water vapor at partial pressures above  $10^{-4}$  mm of mercury. The principle of this experiment depended on controlling the partial pressure of water vapor over ice by the temperature of the ice and the surrounding vessel. The vessel was a tube with a rhenium filament attached to leads through one end. The filament was surrounded by a platinum cylinder. A fraction of a milliliter of water was introduced into the tube which was evacuated while held at liquid nitrogen temperature in order to avoid pumping out the water. The vapor pressure of water vapor in the tube was determined by the freezing temperature of the bath in which the tube was inserted. The liquids and their freezing temperatures were: carbon tetrachloride at  $-22.8^{\circ}\text{C}$ ; 70 per cent nitric acid at  $-42^{\circ}\text{C}$ ; chloroform at  $-63.5^{\circ}\text{C}$ . These temperatures were taken from the Handbook of Chemistry and Physics. The filament was operated at a temperature of  $1600^{\circ}\text{C}$  brightness for a sufficient length of time to collect an accurately weighable deposit of rhenium on the platinum cylinder which surrounds the filament. The results of these measurements are shown graphically in Figure 47. The graph indicates that the rate of loss of rhenium by the water-cycle reaction increases by about 50,000 times as the pressure of water-vapor increases from  $10^{-4}$  to  $4 \times 10^{-3}$ .

In most commercial applications for such items as electron tubes and electric lamps, filaments are operated in evacuated vessels at pressures of the order of  $10^{-7}$  to  $10^{-4}$  mm of mercury. This study covers a range of slightly higher pressures, but indicates from Figure 47 that the loss of the material drops off very rapidly as the pressure decreases toward the normal commercial-practice range. Comparisons of the water-cycle effect between tungsten and rhenium have indicated that, within the range of pressures normally used in practice, rhenium is considerably more resistant to attack by water vapor than is tungsten.

### Rhenium Contacts for Relay Service

Several experiments were conducted to determine the relative merits of rhenium and other commonly used materials as contacts in electrical relays. The experiments included observations of electrical resistance, weight loss, and welding of the contacts.

For two of the experiments, a modified Allen-Bradley four-pole Type BX44 relay was used. A set of contacts of each of the metals (rhenium, tungsten, and platinum-ruthenium) was mounted on the same relay to assure

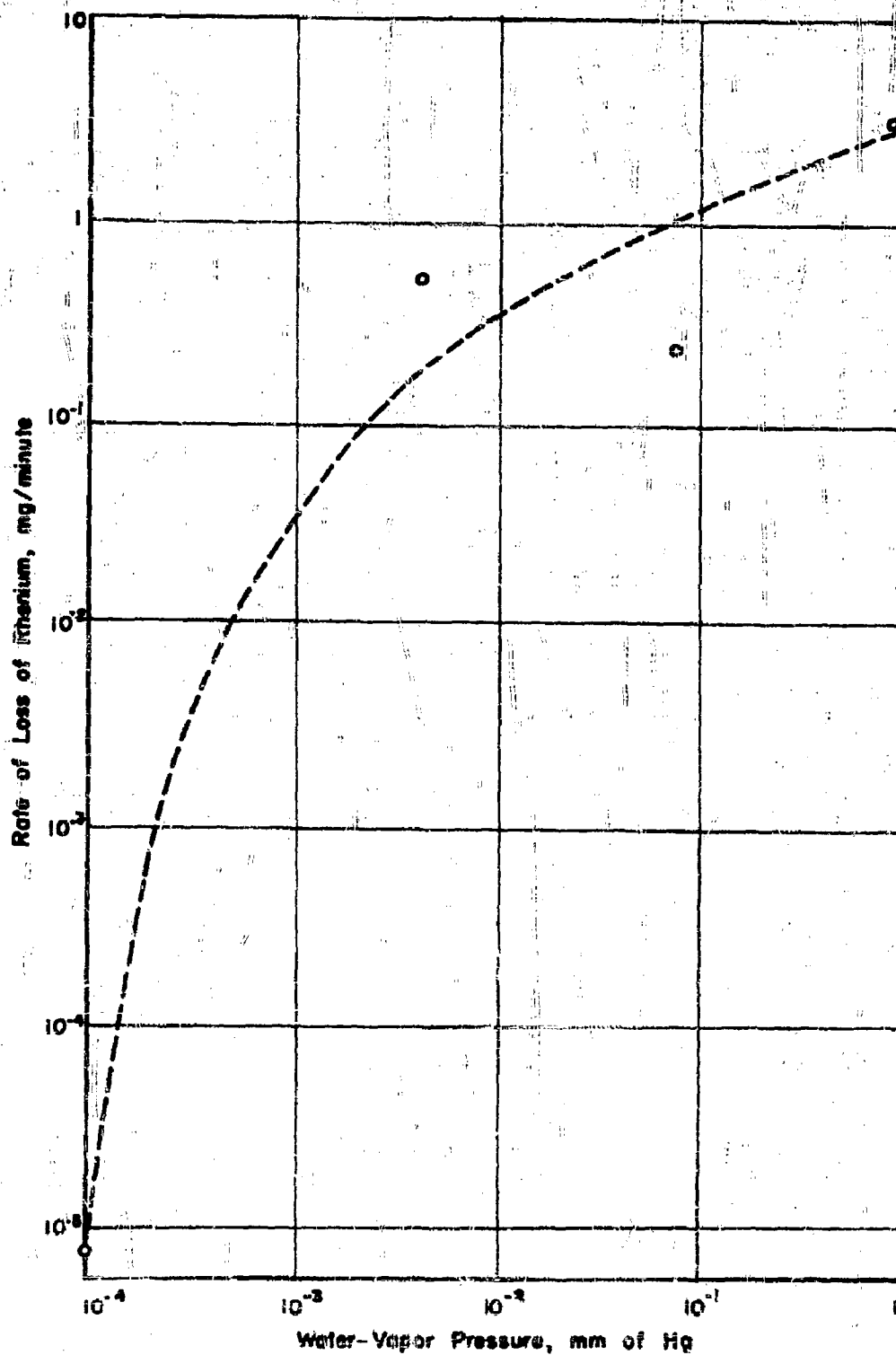


FIGURE 47. RATE OF WEIGHT LOSS BY WATER-CYCLE MECHANISM FROM RHENIUM FILAMENT AT 1600 C BRIGHTNESS TEMPERATURE

A-10420

identical cycling for the three materials and to approach similarity of conditions of bounce. The test contacts were closed once per second and remained closed for  $1/3$  second. Each break of the circuit consists of two arcs in series between four contact tips of the material which is under test.

In the first experiment to determine the relative merits of these contact materials, each set of contacts was wired to break a 115-volt, 60-cycle-per-second circuit that supplied a load of 11.7 ohms and 1.5 millihenrys. The steady-state current in each load was 8.0 amperes. Before and during the run, the contact resistance of each set of contacts was measured with a Wheatstone bridge on which the applied voltage was 1.5 volts. A summary of these measurements is given in Table 25. Each recorded value is the mean of ten measurements. The contacts were opened and closed for each measurement. These data indicate that the resistance of the rhenium contacts was consistently low, in contrast to the resistances of the two other contact materials.

The contacts ran a total time of about 125 hours, or 450,000 openings. At the end of this time, the rhenium contacts were eroded only slightly, and were still usable. In contrast, the tungsten was badly chipped from mechanical bouncing and the platinum-ruthenium contacts were badly pitted and burned by arcing as shown in Figures 48, 49, and 50.

During the operation of the contacts, red and black powders formed on the rhenium, the quantity of black powder appearing greater than that of the red powder. X-ray diffraction patterns were taken of the black powder and of the predominantly red powder. Both patterns showed that the major phase in each sample was  $\text{ReO}_3$ . The amount of  $\text{ReO}_3$  in the red powder appeared to be only a little greater than in the black powder. Other components could not be identified, because their lines in the diffraction pattern were very faint.

The presence of  $\text{ReO}_3$  on the rhenium contacts explains their very low contact resistance. The resistivity of rhenium trioxide is  $200 \times 10^{-6}$  ohm-centimeter, according to Meyer<sup>(33)</sup> and according to Biltz<sup>(34)</sup>. For comparison, the resistivity of carbon is about  $3500 \times 10^{-6}$  ohm-centimeter; that of mercury,  $98 \times 10^{-6}$  ohm-centimeter at 50 C; and that of copper,  $1.7 \times 10^{-6}$  ohm-centimeter. In the Literature Survey Report on this project, page 60, it is stated that oxidation of any of the lower oxides produces rhenium heptoxide,  $\text{Re}_2\text{O}_7$ , that heating rhenium heptoxide and rhenium at 300 C results in the formation of rhenium trioxide, and that the heptoxide melts at 297 C and vaporizes at 363 C. These statements are consistent with the results obtained in the contact experiments.

The second experiment differed from the first only in the load circuits. The load current in each circuit was 8 amperes and the line voltage was 115 volts. There was an inductance of 38 millihenrys in the load circuit.

TABLE 25. RESISTANCE OF CONTACTS, EXPERIMENT 1

Time, hours	Resistance, ohms		
	Rhenium	Tungsten	Platinum-Ruthenium Alloy
0	0.17	0.11	0.66
1	0.038	1.5	3.7
2	0.040	1.7	1.8
3	0.035	2.5	2.9
4	0.039	1.6	3.1
5.8	0.042	2.4	1.8
7	0.039	2.6	1.9
9.5	0.043	2.3	1.6
14	0.042	1.6	2.5
29	0.040	2.0	2.3
47	0.040	1.5	2.5
71	0.055	1.6	3.9
101	0.044	1.5	4.4

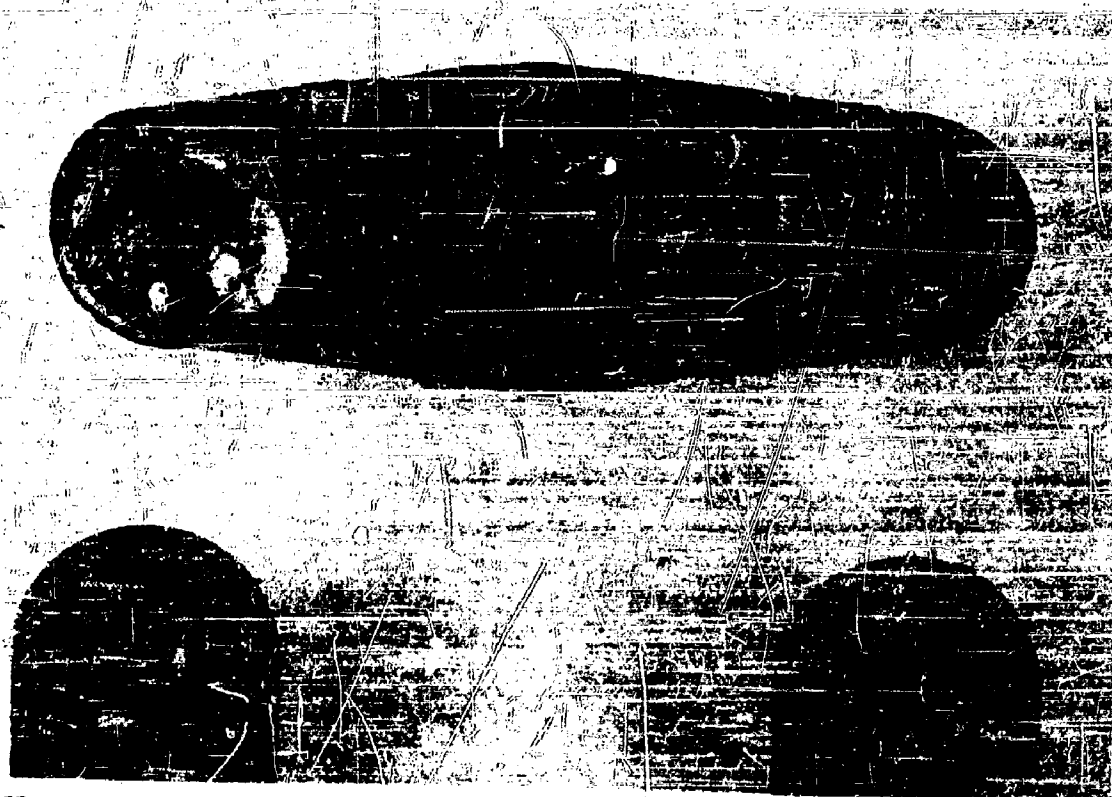


10X

N7940

**FIGURE 48. CONDITION OF RHENIUM CONTACTS FOLLOWING  
BREAKER-POINT TESTS**

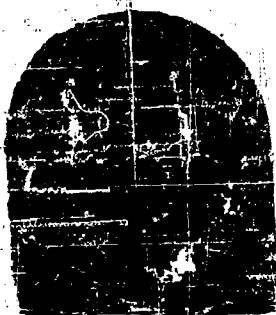
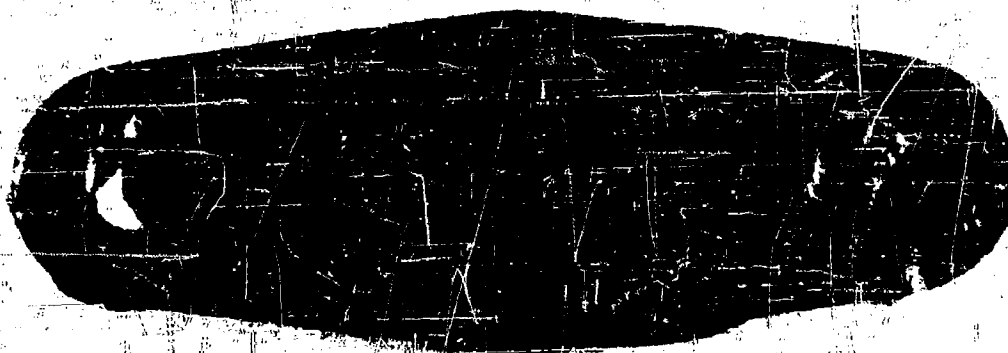




10X

N7939

**FIGURE 49. CONDITION OF TUNGSTEN CONTACTS FOLLOWING  
BREAKER-POINT TESTS**



10X



N7938

**FIGURE 50. CONDITION OF PLATINUM-RUTHENIUM CONTACTS  
FOLLOWING BREAKER-POINT TESTS**

The contact resistances, which were measured in the same way as for the first experiment, are shown in Table 26.

TABLE 26. RESISTANCE OF CONTACTS, EXPERIMENT 2

Time, hours	Resistance, ohms		
	Rhenium	Tungsten	Platinum-Ruthenium Alloy
0	0.031	0.026	0.3
5.2	0.042	0.7	2.1
7	0.042	0.85	1.8
13	0.038	0.95	1.6
17	0.041	1.0	2.0
22	0.048	0.9	1.5
29	--	1.1	1.8
45	0.038	--(a)	--(a)

(a) Contacts were not meeting properly.

The loss of weight of each set of contacts was measured after 45 hours of operation. These losses, in milligrams, were 40, 338, and 443, for rhenium, tungsten, and platinum-ruthenium, respectively. As in the first run, described above, the rhenium contacts had accumulated some rhenium trioxide powder.

Because the multicontact relay used in the experiments just described did not permit observation of welding or sticking of contacts, rhenium and tungsten were each tested, one at a time, on one pole of a Struthern-Dunn two-pole relay, Model AD3T8. The single arc was drawn between contact tips of metal under test. The contacts were closed once per second and were held closed for  $1/3$  second. An auxiliary timing circuit was arranged to turn off the power whenever the contacts remained closed longer than about 0.4 second.

It was found that rhenium contacts, while opening a 115-volt, 60-cycle-per-second, resistance load of 8.0 amperes, did not weld in a period of 20 hours. However, when a variable inductor with d-c resistance of only a few tenths of an ohm was used as a load, it was found that both tungsten and rhenium contacts welded objectionably for currents as small as 1 ampere. The rhenium contacts generally welded tightly, so that they had to be opened manually, whereas the tungsten contacts usually opened upon normal action of the relay.

The above tests have indicated that, for a number of applications, where the load is mainly resistive, rhenium contacts are superior to tungsten and a platinum-ruthenium alloy. Rhenium contacts should find widespread use in applications where a minimum of contact resistance is a necessity and where a very hard material is desirable.

### MISCELLANEOUS PROPERTIES

Several important properties were investigated that cannot logically be included in the major divisions of this report. A report on these investigations follows.

#### Maximum Theoretical Oxygen Solubility<sup>(35)</sup>

A recent publication<sup>(36)</sup> discusses the limiting solid solubility of oxygen in transition metals. The oxygen solubility is plotted against a parameter for a number of metals so that a straight line is formed; the equation for this is:

$$\log S = -0.909 \left( \frac{E}{V} \right) + 2.33, \quad (1)$$

where

S = solubility of oxygen, atom per cent

E = modulus of elasticity

V = octahedral volume.

E is taken as 67,000,000 psi, and V is calculated from the equation:

$$V = \frac{4}{3} \pi \sqrt{\left[ (0.577a)^2 + \frac{c^2}{16} - \frac{a^2}{4} \right] \left[ (0.577a)^2 + \frac{c^2}{16} \right]}, \quad (2)$$

where  $a$  and  $c$  are the lattice constants, taken as 2.760 Å and 4.458 Å, respectively. This gives  $V = 9.77 \text{ Å}^3$ . If the  $c/a$  ratio is assumed to be ideal ( $c/a = 1.633$ ), then

$$V' = \frac{c^3 \sqrt{2}}{3} \quad (3)$$

and  $V' = 9.89$ , a good check.

Substituting for  $E$  and  $V$  in equation 1 gives a solubility of 0.000138 atomic per cent, which, if multiplied by the ratio between the atomic weights of oxygen and rhenium, gives

$S' = 0.000012$  weight per cent, or maximum solubility of oxygen in rhenium.

Vacuum fusion analysis has indicated the soluble oxygen in arc-melted, crystal-bar, and sintered rhenium to be around 0.0001 per cent, approximately ten times the theoretical value. This is fairly good experimental agreement.

### Oxidation Resistance

The literature contains no specific data on the oxidation of pure rhenium metal, although Agte and co-workers<sup>(3)</sup> stated that rhenium oxidized at the same rate as tungsten at 1900 C, but only one third as fast above 1600 C. Rhenium, of course, would be expected to possess a volatile oxide, as its position in the periodic system between tungsten and osmium would indicate. This fact has been observed qualitatively many times.

In order to place the oxidation characteristics on a more firm basis, air oxidation tests were conducted on quarter sections of arc-melted buttons. Despite variations in the grain size and purity of arc-melted, hot-wire deposited, and sintered rhenium, it is felt that the present results are probably broadly correct for all types of rhenium; only minor variations due to grain size and purity are apt to occur.

Each quarter button weighed about 3 grams, and was exposed to slowly moving air in a muffle furnace. The test temperatures were 300, 600, 900, 1200, and 1500 C. The results are recorded in Table 27 and Figure 11.

In general, a catastrophic oxidation rate commences above 1000 C, with the evolution of white fumes similar to those evolved by osmium. These fumes are the highest oxide of rhenium,  $\text{Re}_2\text{O}_7$ , a volatile oxide which melts at 297 C and boils at 363 C. Inspection of the oxidation products metallographically showed that the attack was of a general nature, and did not take place preferentially at grain faces or interfaces.

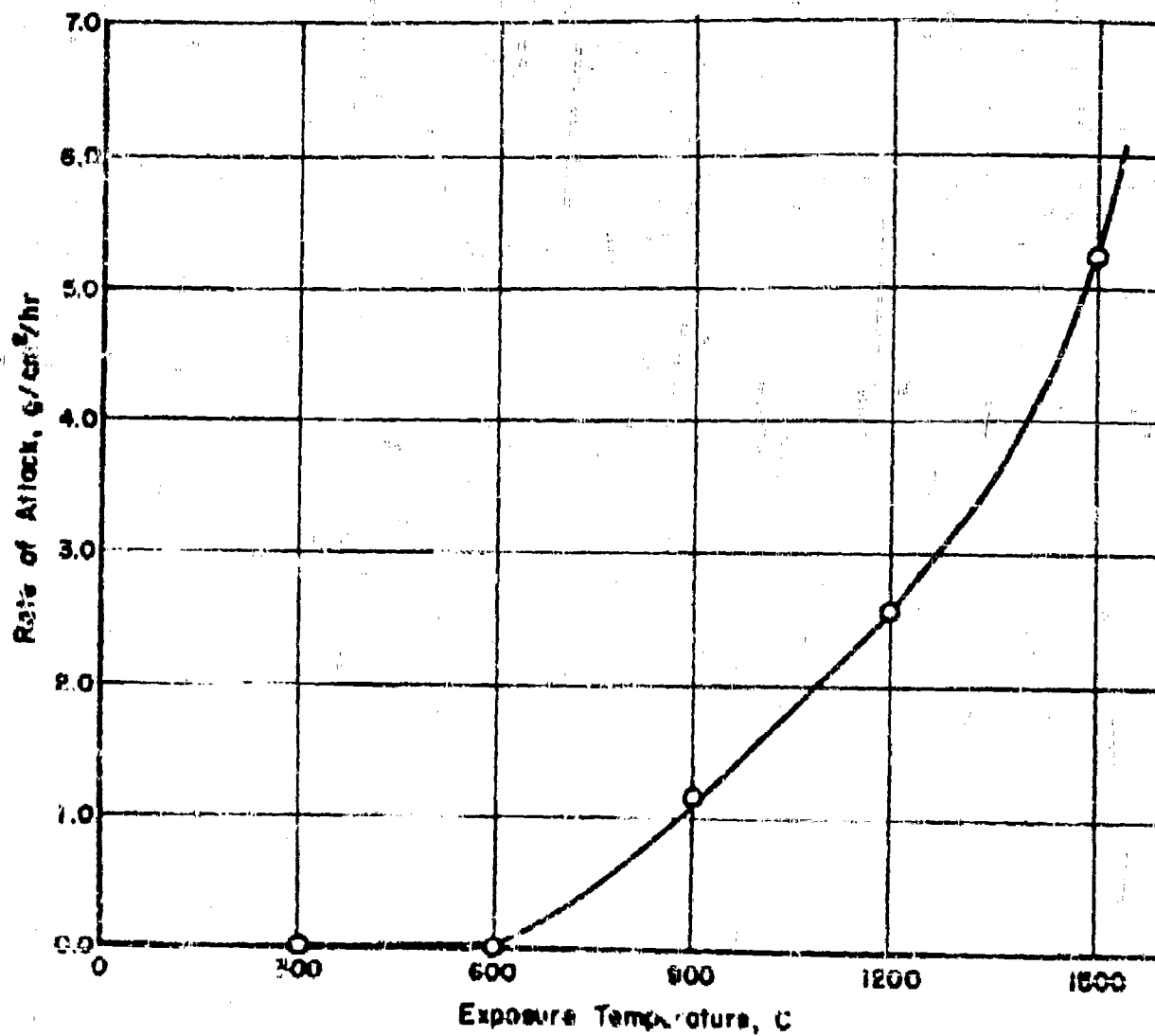


FIGURE 51. THE INFLUENCE OF TEMPERATURE ON THE AIR OXIDATION OF ARC-MELTED RHENIUM

A-10137

TABLE 27. OXIDATION OF RHENIUM IN AIR

Note: Specimens prepared by quartering arc-melted buttons weighing about 15 grams.

Exposure Temperature, C	Exposure Time, hour	Specimen Weight, grams	Specimen Area, cm <sup>2</sup>	Weight Change, grams	Rate of Attack, g/cm <sup>2</sup> /hr
300	1	2.3988	1.29	+0.0007	-0.0005
600	1	2.3833	1.47	-0.0172	0.0117
900	1	2.1973	1.29	-1.5015	1.17
1200	0.5	3.5961	1.78	-2.2724	2.56
1500	0.25	3.0609	1.74	-2.2684	5.24

The room-temperature oxidation of rhenium has been assumed to be zero in Figure 51. As nearly as can be ascertained, massive rhenium retained in the open in this laboratory does not oxidize and does not lose its surface finish if kept clean. This is over a 2-year observation period. Electroplated metal alone, however, shows a definite tarnishing tendency, which can be eliminated if the plated metal is fired in hydrogen following a given electrodeposition run.

#### Rhenium Coatings

A study of the literature (see First Quarterly Progress Report "A Survey of the Literature" for this contract) indicates that, in all previous electroplating studies, potassium perrhenate has been used as the source of rhenium. The increased solubility (about 5 times greater) of ammonium perrhenate over that of potassium perrhenate might be advantageous in securing electrodeposits of improved quality. Therefore, a series of electroplating tests was performed using the relatively soluble ammonium perrhenate. The plating bath was a cylindrical Pyrex vessel with a capacity of about 500 ml. The anodes were a pair of 4 x 2 x 0.005-inch platinum sheets.

Tests were performed employing plating baths of different compositions. The first bath was prepared by dissolving 50 grams of ammonium perrhenate in 1 liter of dilute sulfuric acid (pH range 0.8 to 1.0).

Plates of rhenium on copper up to 0.0008 inch in thickness were produced at an optimum current density of 18 amp/dm<sup>2</sup>. These plates, however, were rather porous, and oxidized upon standing in air.

The next plating bath tried was a modified sulfuric acid bath. This bath was prepared by dissolving 25 grams of ammonium perrhenate, 54 grams of sulfuric acid (specific gravity 1.86), and 60 cc of 28 per cent ammonium hydroxide in sufficient distilled water to make 600 ml of solution. The pH of this solution was maintained in the range of 1.0 to 1.3 by the addition of sulfuric acid.

Plating tests were performed at room temperature and at 124 F for periods of from 3 to 24 minutes. At room temperature, a current density of 10.8 amp/dm<sup>2</sup> was found to produce bright adherent plates. An increase in the current density to 12 amp/dm<sup>2</sup> produced comparable plates at a temperature of 124 F.

The best plates were obtained by plating the specimens for 6 minutes at room temperature and at a current density of 10.8 amp/dm<sup>2</sup>. The specimens were then hydrogen fired at 900 to 950 C for 15 minutes to make certain that no rhenium oxides were present in the plate. This plating-firing cycle could be repeated as often as desired. Two cycles produced a plate about 0.001 inch in thickness.

Specimens plated as described above have remained bright after standing in air for 10 months.

Tungsten wire from 0.003 to 0.020 inch in diameter also has been plated successfully using the plating-firing technique.

### Purity, Porosity, and Temperature Relationships

Following its successful fabrication, rhenium wire of various dimensions was utilized for experimental work. Among the properties determined on wire stock were the thermionic-emission characteristics and the vapor pressure of solid rhenium, both types of testing being conducted at temperatures above 1800 C; some of the tests reached 2700 C.

During these experiments, a disturbing phenomenon was noted, particularly in connection with the vapor-pressure work. The 50-mil wire specimens appeared to be fracturing or failing at the hottest part of their 6-inch lengths after one or two tests had been made (see the section on vapor pressure). The actual break occurred during cooling of the specimen. Some small tensile or compressive stresses were present during the testing, but were considered too low to be of any significance. A thermionic-emission specimen failed in a similar manner, but after a long (700-hour) test. In general, no failures were observed when the specimen had not been heated over 2200 C. The fractures appeared as shown in Figure 52.

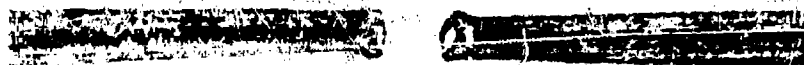




20X

N8652

a. Fracture of Vapor-Pressure Specimen



20X

N8649



20X

N8648

b. Fracture (Above) and Surface Protrusions (Below)  
of Thermionic-Emission Specimen

FIGURE 52. MACROGRAPHS OF THE EXTERNAL APPEARANCE OF  
RHENIUM SPECIMENS FAILED IN HIGH-TEMPERATURE  
TESTS

This was an alarming phenomenon, since the high-temperature mechanical and physical properties of rhenium have indicated that it might have elevated-temperature usefulness. As a result, much effort was directed toward uncovering the source of the trouble.

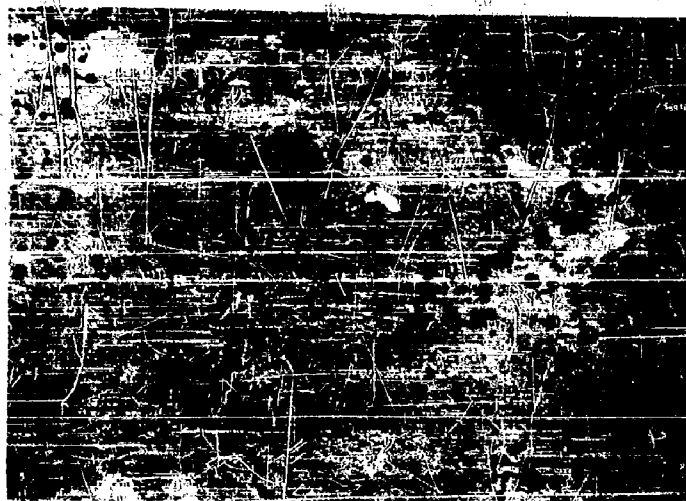
Inspection of the fractures alone told little except that the breakage was brittle in each case. Metallographic studies told the story illustrated in Figure 53. Figure 53 consists of micrographs taken (a) at the fracture end, (b) at a position halfway from the fracture to the cold electrical clamp end, and (c) at the cold clamp end. The fracture actually occurred during cooling of the 50-mil wire when the electrical power had been turned off. Thus, no arcing occurred to cause extensive melting. The fractured end shows many small voids, which extend back along the hot portion of the wire at least to a point halfway to the cold end. The cold end shows a perfectly normal rhenium structure. It was immediately obvious that exposure to elevated temperatures was necessary to cause the porosity, and quite probably the porosity was connected with fracturing. Inspection of the thermionic-emission specimen of Figure 52 showed a like history.

#### Controlled Porosity and Fracture Tests

A series of control tests was instituted then to determine more exactly the conditions surrounding these fractures or "burn-outs". Several rhenium specimens were cut from 60-mil wire and ground to the shape of small dumbbells. The reduced center portion was designated as the test section and had been ground to 25-mil diameter in each case. The specimens were then mounted on nickel supports in evacuated ( $10^{-6}$  to  $10^{-7}$  mm of mercury) and hydrogen-filled ( $1/2$  to  $2/3$  atmosphere) glass tubes. Current was passed through the specimens, one at a time, each being heated to a different temperature. They were held at temperature for 1 hour if no failure occurred. Table 28 lists the results of these tests.

As had been estimated previously, the porosity and burn-outs both commenced in the 2200 to 2300 C temperature range for the vacuum tests. The ambient atmosphere of hydrogen raised the effective operating temperature of the rhenium about 200 degrees centigrade to 2500 C. The porosity and fracturing then occurred exactly as had been the case in vacuum. The increase in fracture temperature under hydrogen may have been due only to the increase in ambient pressure, or to the positive reduction effect of hydrogen.

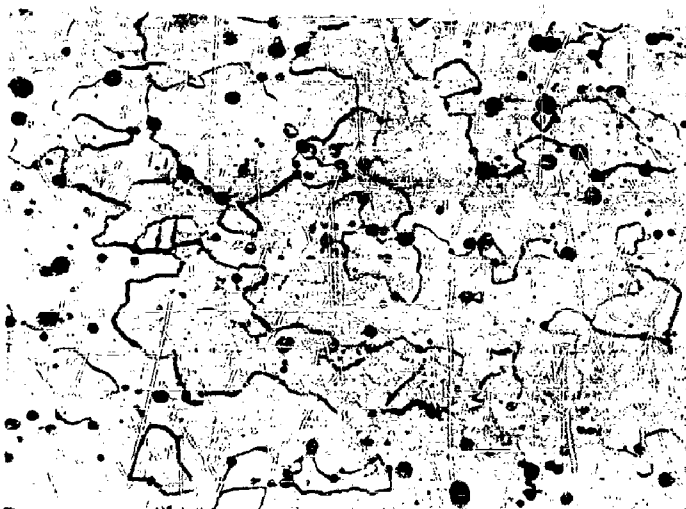
The appearance of these specimens was somewhat different at the fracture (or, more specifically, "burn-out", in these cases) than was found for the vapor-pressure specimens of Figure 53. Figure 54 illustrates the condition existing in the controlled tests; the difference in appearance was due to the specimens' still being heated by an applied current during the occurrence of the burn-out, which caused arcing and melting to occur



250X

N8773

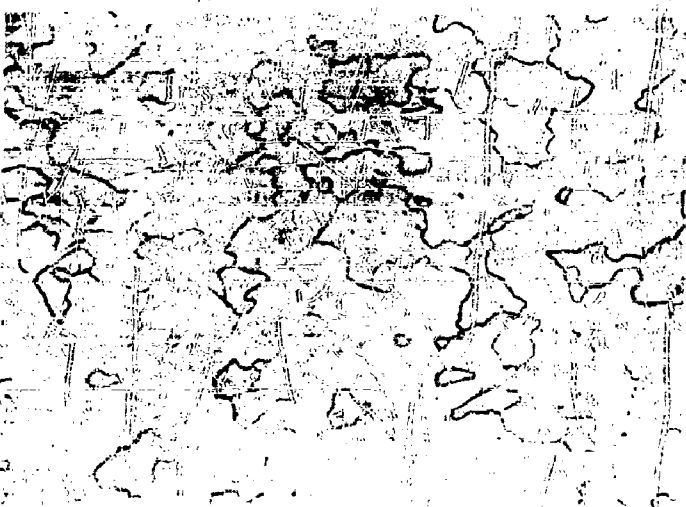
- a. Porosity at Fracture of  
Rhenium Vapor-Pressure  
Specimen



250X

N8774

- b. Porosity Halfway From  
Fracture to Clamp End



250X

N8775

- c. Absence of Porosity  
in Relatively Cold  
Clamp End

FIGURE 53. POROSITY IN RHENIUM VAPOR-PRESSURE  
SPECIMEN WHICH FAILED IN TEST

**TABLE 28. THE EFFECT OF HEATING RHENIUM IN  
HIGH VACUUM AND HYDROGEN**

<b>Ambient Condition</b>	<b>Temperature, C</b>	<b>Test Time, minutes</b>	<b>Occurrence of Burn-Out</b>	<b>Occurrence of Porosity</b>
Vacuum	1700	60	No	No
Vacuum	1900	60	No	No
Vacuum	2100	60	No	No
Vacuum	2200	60	No	Slight
Vacuum	2300	17	Yes	Yes
Vacuum	2400	4	Yes	Yes
Hydrogen	2200	60	No	No
Hydrogen	2400	60	No	No
Hydrogen	2500	48	Yes	Yes
Hydrogen	2600	None <sup>(a)</sup>	Yes	Yes

(a) Burned out at about 2650 C while heating to temperature.



100X

N11842

a. Vacuum Heated at 2400 C



100X

N11888

b. Heated Under Hydrogen to 2550 C

FIGURE 54. POROSITY AND BURN-OUT ENDS OF RHENIUM  
HEATED IN VACUUM AND HYDROGEN

at the moment of failure. Figure 54a shows that porosity existed near the fracture in the unmelted metal. The pores evidently increased in size until the resistance increased, causing a temperature increase, which caused more porosity and finally a burn-out. Arcing occurred at the moment of burn-out, leaving a ball of molten metal on the burn-out ends. Pores continued to form in the molten metal until it cooled and solidified. Figure 54b shows an exceptionally large pore trapped by freezing like a balloon about to burst.

These series of experiments resulted in two obvious conclusions.

- (1) 2300 C was the critical temperature above which porosity and burn-outs would occur in vacuum.
- (2) Porosity was the cause of the burn-outs.

#### The Effects of Purity on Porosity and Burn-Outs

Upon observing the porosity and the attendant filament failures, one of the first items to be brought under surveillance was the impurity content of the metal. It was thought that vaporizing impurities might have caused the pores; as the experimentation progressed and more analytical data were gathered, it became increasingly obvious that this view was correct.

Gaseous Impurities. A check of the possible gaseous impurities, oxygen, hydrogen, and nitrogen, showed no significant difference between crystal-bar rhenium, sintered-type rhenium in which pores had been formed, and rhenium from the same lot that had not been treated at high temperature and thus contained no pores. The crystal-bar material generally is considered to be an extremely pure type of metal insofar as gaseous impurities are concerned. Table 29 shows the results of the vacuum-fusion-type analysis conducted; that there is no significant difference between the three specimens is obvious. Thus, the porosity could not be the result of included gases.

Nongaseous Impurities. The sections of this report on metal preparation and consolidation record how it was found necessary to prepare finely divided ammonium persulfate in order to produce metal powder sufficiently finely divided to be sinterable. The ammonium persulfate usually was prepared only as relatively coarse crystals, which were then comminuted to a fine powder by ball milling in a rubber-lined ball mill. The balls were made of Burundum, a ceramic composed of aluminum, magnesium, and calcium oxides. The ball-milling step caused an increase in impurities (see Table 30) but this did not appear to harm the fabrication techniques or the various physical\* and mechanical properties. The total

---

\*With the exception of the melting point; see the section on this subject above.

TABLE 29. GAS CONTENT OF RHENIUM AS DETERMINED BY VACUUM-FUSION ANALYSIS

Material	Gas Content, parts per million by weight		
	O <sub>2</sub>	H <sub>2</sub>	N <sub>2</sub>
Porous rhenium (a)	8	1.3	< 6
Nonporous rhenium (b)	6	0.6	< 5
Crystal-bar rhenium	9	1.4	< 8

(a) Prepared by powder-metallurgy methods; porosity resulted from failure during vapor-pressure test at 2250 C.

(b) From same stock as porous rhenium, but not exposed to test.

TABLE 30. METALLIC IMPURITIES PRESENT DURING THE PROCESSING OF RHENIUM

Impurity	Impurity Content, per cent <sup>a</sup>			
	Ammonium Perrhenate (a)	Rhenium Metal (b)	Rhenium Metal (c)	Rhenium Metal (d)
Copper	0.0003	0.0002	0.0021	0.0015
Iron	0.0030	0.030	0.024	0.015
Aluminum	0.004	0.025	0.024	0.005
Manganese	N. F. (e)	N. F.	0.0020	0.005
Silicon	0.005	0.018	0.028	0.039
Magnesium	0.005	0.025	0.038	0.012
Calcium	N. F.	0.010	0.017	0.005
Molybdenum	N. F.	0.0025	N. F.	N. F.
Total impurity content	0.017	0.111	0.205	0.083
Total aluminum, calcium, and magnesium content	0.014	0.060	0.153	0.022

(a) Prior to ball milling.

(b) Prepared from an early batch of ball-milled ammonium perrhenate.

(c) Prepared from a recent batch of ball-milled ammonium perrhenate.

(d) Prepared from non-ball-milled (hand ground in agate) ammonium perrhenate.

(e) Not found.

impurity content of the reduced powder was about 0.111 per cent, compared with 0.017 per cent impurity in the ammonium perrhenate prior to ball milling.

More recent analyses (see Table 30) have uncovered a substantial increase in impurities; a total of around 0.205 is now reportable. Table 30 shows that this is entirely due to aluminum, magnesium, and calcium. It is obvious that the Burundum balls alone were responsible for this additional pickup; furthermore, the aluminum, magnesium, and calcium were present in the rhenium powder in the same ratio to each other as they were in the Burundum.

Table 31 gives the approximate boiling points of the major metallic impurities and of the oxides of aluminum, calcium, and magnesium; it is not known positively whether all of these materials were present in the reduced state or not. However, if the oxides were present and unreduced, their vapor pressure from the liquid state might be sufficient to cause the porosity experienced. If they were reduced by the many hydrogen treatments that the metal had undergone in fabrication, the presence of pure unalloyed metals as impurities, many of which boil below 2300 C, certainly would be sufficient to cause the porosity. Of these impurities, magnesium or magnesia, having the lowest boiling points and appearing in appreciable quantities, might be expected to cause the most trouble. In any case, removal of the impurities placed in the rhenium powder by ball milling certainly would be expected to be a large step toward solution of the porosity problem.

This was done simply by hand grinding the ammonium perrhenate crystals in a small agate mortar, instead of ball milling them. This is a very laborious, impractical operation, but it sufficed to produce fine sinterable rhenium metal powder upon reduction. The analysis is repeated in Table 30 (d), and shows a total impurity content of only 0.083 per cent, the total aluminum, calcium, and magnesium content having been cut to one-seventh its former high value.

Two observations immediately indicated that success had been achieved. First, upon sintering the metal, it assumed a much finer, smoother surface finish, indicating that the tendency toward gasification at the high sintering temperature of 2700 C was very slight. Second, a determination of the melting point (see Table 9) on this new high-purity material gave results that checked closely with the literature and with each other, indicating that earlier results probably were invalid due to low melting caused by the presence of the much-discussed impurities.

Final proof that these impurities were the cause of porosity was obtained when a dumbbell-like test specimen was fabricated from the new high-purity metal exactly as described previously. It was heated under a pressure of  $10^{-7}$  mm of mercury for 1 hour at 2500 C; not only did it not fracture or "burn-out" as the other material had done at 2300 C, but it exhibited no visible deposition because of vapor pressure or water cycle on

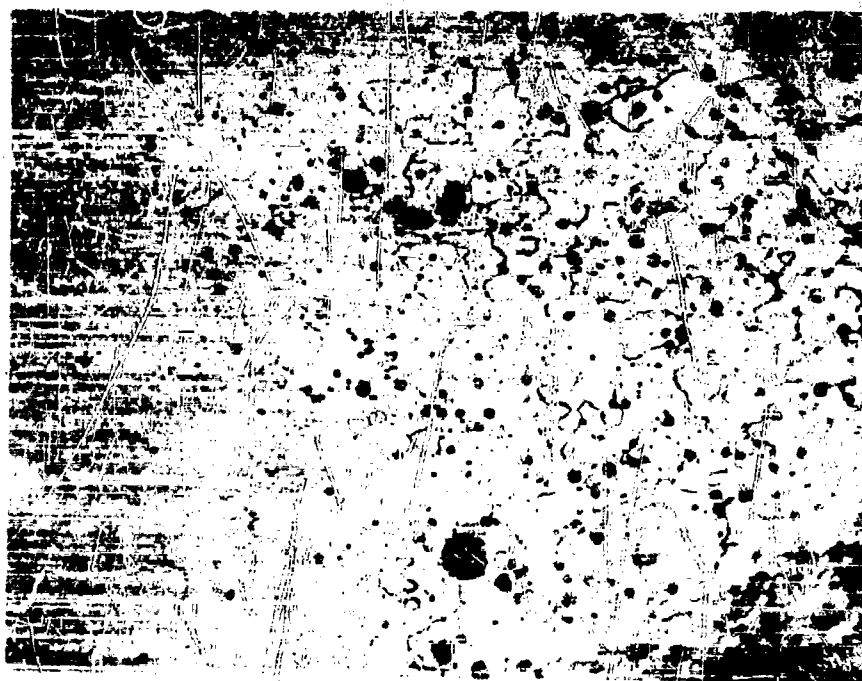


Reproduced From  
Best Available Copy

TABLE 31. BOILING POINTS OF METALLIC IMPURITIES  
AND OF CERTAIN OF THEIR OXIDES

Impurity	Boiling Point, °C (37, 38)
Copper	2300
Iron	3000
Aluminum	2300
Manganese	1900
Silicon	2200
Magnesium	1110
Calcium	1240
Molybdenum	3700
$Al_2O_3$	2980
$CaO$	2850
$MgO$	> 2500

the walls of the sealed tube. One hour at 2700 C gave essentially the same results. At 2900 C, the specimen burned out after 37 minutes; later, the burn-out was determined to have been caused by porosity, and not by vapor-pressure failure, even though considerable blackening of the tube wall occurred at this temperature. The porosity, occurring at 2900 C in the new material as opposed to 2300 C in the rhenium with high impurity content, appeared as in Figure 55. This has essentially the same appearance as the porosity that occurs in tungsten projection lamp filaments when operated at about 3000 C<sup>(39)</sup>. Thus, by increasing the purity of rhenium by the process of avoiding ball milling, the practical operating temperature of rhenium filaments has been raised from about 2200 C to around 2800 C. It is entirely possible that further improvement could be effected by further increasing the purity. There is little doubt that the worst porosity promoter is either aluminum, calcium, or magnesium.



500X

N14903

FIGURE 55. POROSITY IN RHENIUM METAL HEATED TO 2900 C

#### Metallographic Techniques

Rhenium work hardens greatly, and thus exhibits a strong tendency toward excessive twin development during grinding and polishing. Repeated etching and polishing is often necessary to alleviate the situation. The

most successful etchant has been found to be an electrolytic oxalic acid solution. The current density recommended is about 3 to 10 amp/in.<sup>2</sup> at 7 to 8 volts.

### DISTRIBUTION OF INFORMATION AND MATERIALS

Since the direct object of these researches on rhenium has been to discover new uses for the metal through a more thorough evaluation of its properties, it was obvious at the onset of the work that close contact would have to be established with industrial organizations concerned with the use of such a metal as rhenium. Ideally, the situation would be for this Governmental research to do the primary digging work, and then allow interested industrial (or educational) parties to continue with more detailed research on rhenium, and, if possible, to carry their research to its ultimate goal, production of a commercial item containing rhenium. Thus, the potential of rhenium would commence to be realized. In at least one case, this policy has been followed almost to the letter, and commercial use of rhenium for the specific application involved appears to be very close.

Accordingly, a policy of cooperation with interested organizations was established in the early stages of this work. The cooperation usually took the form of at least one of the following:

- (1) Arrangements with the Air Force to place an interested organization on the distribution list for these reports
- (2) Arrangements to satisfy requests for small experimental quantities of rhenium (in these instances, we requested that the user inform us of his "over-all" experimental findings)
- (3) Supplying of information in response to a request for same.

In all cases where a desire was expressed directly to us to be placed on the distribution list, the request was referred to the Sponsor. Whenever rhenium metal was shipped out in answer to a request, the Sponsor was informed of this activity by a carbon of the covering letter.

### Organizations Contacted

By many different mechanisms, including referrals to us by the Sponsor, we have contacted and cooperated with the following parties pursuant to the desire to expand the field of rhenium knowledge:

- (1) AC Spark Plug Division, General Motors Corporation
- (2) Armour Research Foundation
- (3) Bell Telephone Laboratories
- (4) Bendix Aviation Corporation
- (5) B. G. Corporation
- (6) Bomac Laboratories, Inc.
- (7) Champion Spark Plug Company
- (8) Chase Brass & Copper Co.
- (9) Climax Molybdenum Company
- (10) Cornell University
- (11) Dentist's Supply Company of New York
- (12) Department of the Air Force
  - Air Research and Development Command
  - Cambridge Research Center
  - Rome Air Development Center
- (13) Department of the Army
  - Evans Signal Laboratory
- (14) Department of the Navy
  - Office of Naval Research
  - Bureau of Ships
- (15) Fansteel Metallurgical Corporation
- (16) Federal Telephone and Radio Corporation
- (17) General Electric Company
  - Cleveland Wire Works

Lamp Development Laboratory

Research Laboratory

Knolls Atomic Power Laboratory

~~Aeronautical~~ and Ordnance Systems Division

- (18) General Laboratories, Associates
- (19) Horizons, Incorporated
- (20) Johns Hopkins University
- (21) Kennicott Copper Corporation
- (22) Linfield College
- (23) L. H. Marshall Company
- (24) Massachusetts Institute of Technology
- (25) Miami Copper Company
- (26) Murex, Limited
- (27) National Bureau of Standards
- (28) National Research Corporation
- (29) National Union Radio Corporation
- (30) North American Philips Company
- (31) Oak Ridge National Laboratory
- (32) Permo, Incorporated
- (33) P. R. Mallory & Co., Inc.
- (34) Raytheon Manufacturing Company
- (35) Sylvania Electric Products, Inc.

Electronic Division

Metallurgical Laboratories

- (36) University of Chicago

- (37) University of Illinois
- (38) University of Tennessee
- (39) Vacuum Specialties Company
- (40) Westinghouse Electric Corporation

Small samples of rhenium in one or more of several forms have been given to about 20 of those on the above list. In cases of this sort, the average sample is probably about 5 grams in weight. Upon mailing the rhenium, the request has always been made that the scrap metal be returned to us for reprocessing; also, the rhenium has been given only with the stipulation that the "over-all" results of the experiments be made known to us.

With few exceptions, return of information to us from the users of rhenium samples has been gratifying. In order that this information may be reported, it will be found below classified according to subject. In order to provide a certain measure of security to the organizations who have reported this information, the information is not identified as to source.

#### Research on Rhenium by Various Industrial and Educational Organizations

##### Electrical-Contact Tests

The Contact Division of the P. R. Mallory and Company has confirmed the results of the electrical contact tests recorded herein, and they and their British associates have evaluated rhenium and its alloys on electrical contact materials.

##### Electronic Properties

Another industrial organization has determined the work function and A value. One run gave  $\phi = 4.6(5)$  and  $A = 24$ ; the other run gave  $\phi = 4.7(0)$  and  $A = 24.5$ . This is fair agreement with the results of  $\phi = 4.80$  and  $A = 52$  found in our work.

##### Metallizing Applications

Certain work has indicated that rhenium metal has high resistance to molten nickel and that it performs satisfactorily as a heater wire in deposition or metallizing operations with nickel.

Other results from rhenium samples sent out are expected. Cooperation of this type with educational, Governmental, and industrial organizations will continue.

### SUMMARY

This investigation has shown that it is possible to produce ductile rhenium metal by a process that requires minus 325-mesh rhenium metal powder as a starting material. The chemical processes required to prepare this metal starting powder from potassium perxenate have been developed also. The powder is then pressed, presintered, and sintered into a dense mass that is workable cold if proper care is taken; it has been found important to build up a fine-grained skin on the sintered billet by light cold working prior to applying heavy cold reductions. Using these techniques, rhenium can be reduced (with proper intermediate anneals) by rolling, forging, swaging, wire drawing, Turk's-head drawing, and form rolling. The most difficult of these operations is wire drawing, which has not yet been made entirely successful. Arc-melted rhenium and crystal-bar-type rhenium have been evolved also, but their fabricability and general usage are more limited than those of the metal prepared by powder-metallurgy methods.

Metal in the various consolidated and fabricated forms has been utilized to determine certain physical, electronic, and mechanical properties. The results of some of these experiments are presented below in a semitabular form for simplicity.

Melting point	3180 C
Boiling point (estimated)	5900 C
Density	21.04 g/cm <sup>3</sup>
Lattice constants	a = 2.760 A, c = 4.458 A
Vapor pressure, solid, at 2250 C	$2.61 \times 10^{-9}$ atm
Vapor pressure, solid, at 2725 C	$7.37 \times 10^{-7}$ atm
Electrical resistivity	19.1 to 21.6 microhm-cm
Spectral emissivity, at 1000 C	0.42
Thermal-expansion coefficient	$6.8/C \times 10^{-6}$ (20 to 1000 C)
Modulus of elasticity	$67 \times 10^6$ psi

Annealed tensile strength (rod)	164,000 psi
Wrought tensile strength (wire)	340,000 psi
Annealed elongation (rod)	24 per cent
Wrought elongation (wire)	1 per cent
Vickers hardness, annealed	270
Vickers hardness, wrought 40 per cent	825
Recrystallization range	1100 to 1500 C
Thermionic Emission:	
Richardson constant	52 amp/cm <sup>2</sup> /K <sup>2</sup>
Work function	4.80 ev
Maximum secondary-electron-emission coefficient	1.4 maximum

In addition, other important properties not reportable in such a finite manner were uncovered. For instance, attempts to use rhenium as a component in impregnated cathodes have been partially successful. Rhenium-barium aluminate compacts appear to have promise, but rhenium compacts with impregnation by carbonates could not be sintered without reduction of the carbonate.

One of rhenium's more valuable characteristics is its high resistance to the so-called "water cycle", a phenomenon involving a reaction between residual water vapor and some metals in evacuated tubes. Tungsten is attacked rapidly by even small amounts of water vapor, but rhenium appears to be from 10 to 200 times as resistant as tungsten to this deleterious phenomenon in the water vapor partial pressure range common for electron tubes. This property, combined with rhenium's high elevated-temperature strength, indicates rhenium might be an excellent filament material for electron tubes.

A series of tests has been completed on the utility of rhenium as an electrical-contact material. The tests, which were conducted under conditions approximating those encountered in light duty industrial contactors, showed rhenium to be much superior to both tungsten and platinum-ruthenium.

The oxidation resistance of rhenium has been checked; as expected, rhenium forms a volatile oxide above 600 C, so that, in air or oxygen, the weight loss of rhenium becomes catastrophic above this temperature. The theoretical solubility of oxygen in rhenium has been calculated to be about 0.000012 per cent by weight.



Rhenium has been electrodeposited successfully, using baths based on ammonium perrhenate which is considerably more soluble than is potassium perrhenate. Hence the plating bath is less rapidly depleted of rhenium than those previously recommended in the literature. For satisfactory electrodeposited coatings hydrogen firing immediately after deposition is required.

Porosity has been encountered in the operation of rhenium filaments at temperatures above 2200 C; it has been established that this was caused by impurities, consisting mainly of aluminum, calcium, and magnesium (or their oxides), acquired by the rhenium during ball milling of ammonium perrhenate prior to reduction. Temporary elimination of the ball-milling step has resulted in much improved behavior, with no porosity occurring up to about 2900 C, approximately the same temperature as that at which it occurs in tungsten.

In addition to the work reported above, extensive efforts have been made to cooperate to the fullest with industrial, educational, and Governmental organizations interested in rhenium. This has resulted in communications with over 40 such organizations, and also has resulted in free gifts of experimental quantities of rhenium to about half of these in exchange for information. This program has netted some valuable information to date.

In general, the results of these basic-property determinations, combined with the results of the various application tests, indicate that rhenium will have a very useful future.

#### FUTURE WORK

Continuation of the research work on rhenium will embrace almost all of the fields covered in this technical report; basic studies still will be considered paramount.

Specifically, fabrication studies will be renewed with the objective of shortening the current procedures for preparation of rod, wire, and sheet by more efficient cold-working procedures or by the introduction of hot-working procedures.

In addition, certain basic metallurgical characteristics will be investigated, such as the effects obtained by alloying rhenium with platinum-group metals, tungsten, and others. Wherever rhenium exhibits superior surface properties and unit cost is important, the utilization of rhenium in vapor-deposited or electrodeposited form will be investigated.

Physical properties, such as a more accurate electrical-resistivity constant, will also be investigated or amplified where warranted.

Continuation of electronic studies will be emphasized. This will include a study of rhenium-barium aluminate-impregnated cathodes,

investigations of the water-cycle effect, and studies of the use of rhenium in filaments, plates, and grids in lamp and vacuum-tube applications.

Certain miscellaneous studies, such as study of the resistance of rhenium to mercury at room and elevated temperatures and the resistance of rhenium to other molten metals, will be conducted also.

The encouragement that has been given to interested industrial, educational, and Governmental organizations in the past in connection with their small-scale testing of rhenium will be continued and expanded if possible. In addition, continued close liaison with the organizations concerned with the potential mining and processing of rhenium will be maintained, so that a prompt commercial supply of rhenium will be available if demand so warrants.

#### REFERENCES

- (1) Smithells, C., Tungsten, Chapman and Hall, London (1952).
- (2) Stenzel, W., and Weertz, J., "Precision Determination of Lattice Constants of Non-Cubic Substances", Z. Krist., 84, 20-44 (1933).
- (3) Agte, C., Alterthum, H., Becker, K., Heyne, G., and Moers, K., "Physical and Chemical Properties of Rhenium", Z. anorg. u. allgem. Chem., 196, 129-159 (1931).
- (4) Goldschmidt, V., "The Crystal Structure of Rhenium", Naturwissenschaften, 17, 134 (1929).
- (5) Moeller, K., "Lattice Constants of Rhenium", Naturwissenschaften, 19, 574 (1931).
- (6) Goldschmidt, V., "The Crystal Structure, Lattice Constants, and Density of Rhenium", Z. physik. Chem., B, 2, 244-252 (1929).
- (7) Wood, E., "X-Ray Wave-Length Standards", Phys. Rev., 72, 437 (1947).
- (8) Jaeger, F., and Rosenbohm, E., "Exact Measurements of the Specific Heats of Metals at Higher Temperatures: XII. Specific Heat of Metallic Rhenium", Proc. Acad. Sci. Amsterdam, 36, 786-788 (1933).
- (9) Metals Handbook, The American Society for Metals, Cleveland, Ohio (1948).
- (10) Blocher, J. M., Jr., and Campbell, I. E., J. Am. Chem. Soc., 71, 4040 (1949).

- (11) Langmuir, I., Phys. Rev., 2, 329 (1913).
- (12) Johnston, H. L., and Marshall, A. L., J. Am. Chem. Soc., 62, 1382 (1940).
- (13) Giaque, W. F., J. Amer. Chem. Soc., 52, 4808 (1930).
- (14) Brewer, L., The Chemistry and Metallurgy of Miscellaneous Materials - Thermodynamics, edited by L. L. Quill, McGraw-Hill Book Company, Inc., New York (1950), p 29.
- (15) Meissner, W., and Voigt, B., "Measurements With the Aid of Volatile Helium: XI. Resistance of Rhine Metal at Low Temperatures", Ann. Physik, 7, 916 (1930).
- (16) Prescott, C. H., Jr., "The Pyrometry of Oxide-Coated Cathodes", Temperature: Its Measurement and Control in Science and Industry, The American Institute of Physics, Reinhold Publishing Corporation (1941), pp 1199-1205.
- (17) Worthing, A. G., "Temperature Radiation Emissivities and Emittances", Temperature: Its Measurement and Control in Science and Industry, The American Institute of Physics, Reinhold Publishing Corporation (1941), p 1171.
- (18) Wood, W., and Cork, J., Pyrometry, McGraw-Hill Book Co., New York (1941), pp 127-130.
- (19) Levi, R., and Espersen, G., "Preparation of Rhenium Emitters and Measurements of Their Thermionic Properties", Phys. Rev., 78, 231-234 (1950).
- (20) Becker, K., and Moers, K., "On the Melting Point of the System Tungsten-Rhenium", Metallwirtschaft, 9, 1063 (1930).
- (21) Stephens, R. E., J. Optical Society Amer., 29, 158 (1939).
- (22) Köster, W., "Poisson's Ratio in the Periodic System", Z. Elektrochem., 49, 233 (1943).
- (23) La Chance, M. H., Bruckart, W. L., Craighead, C. M., and Jaffee, R. I., "Recrystallization of Wrought Hydrogen-Sintered Molybdenum and Its Alloy", Trans. ASM, 45, 321 (1953).
- (24) Kiefer, R., and Hotop, W., Pulvermetallurgie und Sinterwerkstoffe, Springer-Verlag, Berlin (1943).
- (25) Unpublished data supplied by W. L. Bruckart, Battelle Memorial Institute.

- (26) Geil, G., and Carwile, N., "Tensile Properties of Copper, Nickel, and Some Copper-Nickel Alloys at Low Temperatures", Natl. Standards (U. S.), Circ. 520, 67-96 (1942).
- (27) Winkler, O., "The Frictional Strength of Noble Metals and of Metals Having High Melting Points", Elektrochem., 49, 221 (1943).
- (28) Mellor, J., "The Physical Properties of Manganese and Rhenium, A Comprehensive Treatise on Inorganic Chemistry, Longmans & Co., London, Vol 12, p 469.
- (29) Blewett, J. P., "The Properties of Carbon-Treated Cathodes", Appl. Phys., 10, 840 (1939).
- (30) De Boer, J. H., Electron Emission and Adsorption Phenomena Macmillan Company, New York (1935) 152.
- (31) Wright, D. A., "A Survey of Present Knowledge of Thermionic Emitters", Proc. Inst. Elec. Engrs. (London), 100, 128 (May, 1952).
- (32) Langmuir, I., "Atomic Hydrogen as an Aid to Industrial Research", Ind. Eng. Chem., 20, 332 (1928).
- (33) Meyer, W., "Electron Emission in Stripping Chemical Bonds", Electrochem., 50, 274-290 (1944).
- (34) Biltz, W., "Rhenium Trioxide and Rhenium Dioxide", Z. anorg. allgem. Chem., 214, 225 (1933).
- (35) Calculations by W. D. Klopp and J. M. Reynolds, Battelle Memorial Institute.
- (36) Seybolt, A. U., and Fullman, R. L., "A Rationalization of the Oxygen Solid Solubility in Some Transition Metals", J. Metals, (5), 548-549 (1954).
- (37) Handbook of Chemistry and Physics, Chemical Rubber Publishing Company, Cleveland, Ohio (1943).
- (38) "Data on Chemicals for Ceramic Use" Natl. Research Council (U. S.), Bull. 107.
- (39) Private communication, C. H. Toensin.
- (40) Work performed by G. H. Wheeler and J. D. Buckleit of Battelle Memorial Institute.

This Document  
Reproduced From  
Best Available Copy